UNIVERSITÉ DU QUÉBEC À MONTRÉAL

BIOSPHERE-CLIMATE INTERACTIONS IN CURRENT AND FUTURE CLIMATE OVER NORTH AMERICA

THESIS

PRESENTED

AS PARTIAL REQUIREMENT

FOR PHD DEGREE IN EARTH AND ATMOSPHERIC SCIENCES

BY

CAMILLE GARNAUD

SEPTEMBER 2014

UNIVERSITÉ DU QUÉBEC À MONTRÉAL

INTERACTIONS BIOSPHÈRE-CLIMAT DANS LE CLIMAT RÉCENT ET FUTUR EN AMÉRIQUE DU NORD

THÈSE

PRÉSENTÉE

COMME EXIGENCE PARTIELLE

DU DOCTORAT EN SCIENCES DE LA TERRE ET DE L'ATMOSPHÈRE

PAR

CAMILLE GARNAUD

SEPTEMBRE 2014

REMERCIEMENTS

J'exprime mes profonds remerciements à ma directrice de thèse, Laxmi Sushama, pour l'aide compétente qu'elle m'a apportée, pour sa patience et son encouragement. Je remercie également Katja Winger et Luis Duarte sans qui je n'aurais pu accomplir cette thèse. Merci aussi à Vivek Arora pour m'avoir fournis CTEM, ainsi que l'aide nécessaire pour comprendre ce modèle.

Je remercie enfin tous ceux du Centre ESCER et de l'UQAM qui, d'une manière ou d'une autre, ont contribué à la réussite de ce travail et qui ne sont pas cités ici.

Enfin, faire une thèse, c'est aussi soutenir et être soutenue par la tribu des doctorants et autres chercheurs : Danahé, Fred, Jacinthe, Guillaume, Jean-Philippe et les autres membres de cette communauté que j'oublie de citer. Merci pour ces heures de diner à discuter de tout et de rien, pour votre soutien depuis mon arrivée au Québec et tout particulièrement pour votre soutien dans cette période éprouvante qu'est la dernière ligne droite.

Une thèse est impossible sans un soutien affectif; la famille en constitue la meilleure source. Sans elle, je n'aurais certainement pas tenu durant toutes ces années. Je tiens donc à remercier chaudement mes parents qui m'ont permis de faire les études que je voulais, où je voulais. Un bel héritage que j'espère transmettre à mes 2 filles ! Mes filles, Juliette et Emma, qui m'ont soutenues sans le savoir durant ce doctorat lorsqu'elles dansaient la samba dans ma bedaine. Merci les filles, vous êtes mes bulles d'oxygène, mon équilibre, surtout en cette fin de doctorat ! And last but certainly not least, des remerciements émus à mon conjoint, Sébastien, pour son amour et son soutien infaillible tout au long de mes études. Sans ma famille, je n'en serais pas là et je leur dédie cette thèse.

Quoique l'UQAM soit une institution de langue française, cette thèse est présentée en anglais afin d'élargir le bassin de lecteurs et de réviseurs externes. Je présente mes sincères excuses aux lecteurs de cet ouvrage pour qui ce pourrait être problématique.

TABLE OF CONTENT

LIST OF FIGURES

LIST OF TABLES

LIST OF ACRONYMS

CanESM2	Canadian Earth System Model, 2nd generation
CGCM	Coupled Global Climate Model
CLASS	Canadian LAnd Surface Scheme
CRCM5	Canadian Regional Climate Model, 5th generation
CTEM	Canadian Terrestrial Ecosystem Model
CUE	Carbon Use Efficiency
DVM	Dynamic Vegetation Model
GHG	GreenHouse Gases
GPP	Gross Primary Productivity
LAI	Leaf Area Index
LHF	Latent Heat Flux
NA	North America
NPP	Net Primary Productivity
PFT	Plant Functional Type
RCM	Regional Climate Model
RCP	Representative Concentration Pathway
SHF	Sensible Heat Flux
SST	Sea Surface Temperature
WUE	Water Use Efficiency

RÉSUMÉ

Alors que le climat contrôle la distribution spatiale des principaux types de végétation sur la terre, la végétation affecte le climat à travers la modification des caractéristiques physiques de la surface de la terre. La plupart de nos connaissances sur ces interactions bi-directionnelles sont basées sur des modèles climatiques en raison d'un manque d'observations. Cependant, du fait de leur faible résolution, les modèles climatiques globaux peuvent négliger un certain nombre d'interactions biosphère-atmosphère à l'échelle régionale et locale. L'objectif principal de cette thèse est donc d'étudier la variabilité spatio-temporelle des interactions et rétroactions biosphère-atmosphère à l'échelle régionale, plus particulièrement en Amérique du Nord, en utilisant la cinquième génération du Modèle Régional Canadien du Climat (MRCC5), qui comprend le modèle de végétation dynamique CTEM (Canadian Terrestrial Ecosystem Model).

La première partie de la thèse porte sur la validation du modèle de végétation dynamique CTEM couplé au Canadian Land Surface Scheme (CLASS) à travers des simulations découplées du modèle climatique sur l'Amérique du Nord. Sachant bien que des biais dans les données de forçage pourraient avoir une incidence sur la biosphère simulée par CTEM/CLASS, deux réanalyses différentes sont utilisées pour forcer le modèle. Les deux variables les plus importantes vis-à-vis de leur influence sur la végétation sont les précipitations et la température. Ainsi, leurs différences entre les deux ensembles de données de forçage ont un impact bien marqué sur les différents réservoirs et des flux de carbone simulés, en particulier sur l'est de l'Amérique du Nord. Cependant, malgré des flux bruts très différents, le modèle produit des estimations similaires de flux net de CO_2 entre la terre et l'atmosphère avec les deux ensembles de données de forçage. L'analyse de la distribution spatiale de l'évolution des stocks et des flux de carbone simulés montre que le puits de carbone simulé en Amérique du Nord est principalement attribuable aux augmentations de la productivité nette dans l'est des États-Unis, également rapporté par d'autres études, renforçant ainsi la confiance dans le modèle.

La deuxième partie de la thèse porte sur l'évaluation de l'impact de la végétation dynamique, soit CTEM, sur le climat simulé par le MRCC5 en Amérique du Nord pour la période 1971–2010. Deux simulations du MRCC5, avec et sans CTEM, sont analysées en accordant une attention particulière aux interactions biosphère-atmosphère et sa variabilité spatio-temporelle. L'analyse montre que la végétation dynamique améliore les interactions à l'interface terre-atmosphère, ce qui se reflète dans les fortes corrélations entre la biosphère et les variables atmosphériques. De même, le MRCC5 incluant la végétation dynamique démontre une mémoire à long terme, mise en évidence par des corrélations en décalage, et une amélioration de la variabilité interannuelle, reflétée dans

les états de la biosphère et l'atmosphère durant les années anormalement sèches ou humides.

Enfin, la troisième partie de la thèse porte sur les modification prévues dans les interactions biosphère-climat, et explore la contribution de la végétation dynamique aux changements climatiques. Cette étude utilise des simulations de l'évolution climatique, avec et sans CTEM, couvrant la période 1971–2100 et forcées aux frontières par le Canadian Earth System Model (CanESM2), et qui correspondent à deux scénarios d'émissions futures - RCP4.5 et RCP8.5. L'augmentation du CO_2 et des températures conduisent à une augmantation de la productivité et de la biomasse de la végétation, et à renforcer l'efficacité d'utilisation de l'eau de la végétation dans le climat futur. De plus, la végétation dynamique permet à la biosphère simulée de répondre aux modifications du climat par une série de rétroactions qui, à leur tour, contribuent de manière significative au changement climatique.

La recherche ci-dessus contribue ainsi à une compréhension systématique de la valeur ajoutée de la végétation dynamique dans le MRCC5 ainsi que la nature et la variabilité des interactions biosphère-atmosphère sur l'Amérique du Nord dans le climat récent et futur.

Mots-clés : végétation dynamique, modélisation climatique régionale, interactions biosphère-climat

ABSTRACT

While climate controls the spatial distribution of major vegetation types over land, vegetation affects climate through alteration of the physical characteristics of the land surface. Most of our current understanding of these bi-directional interactions is based on climate models, due to lack of observations. There is again the limitation that most of the global climate models used to study these bi-directional interactions are of coarse resolution and thus can overlook regional to local interactions. The main aim of this thesis therefore is to study spatio-temporal variability of biosphere-atmosphere interactions and feedbacks at regional scale, more specifically over North America, using the fifth generation of the Canadian Regional Climate Model (CRCM5), which includes the dynamic vegetation model CTEM (Canadian Terrestrial Ecosystem Model).

The first part of the thesis focuses on validating the dynamic vegetation model CTEM coupled to the Canadian Land Surface Scheme (CLASS) through offline simulations over North America. Knowing well that biases in the driving data could impact CLASS/CTEM simulated biosphere, two different reanalysis products are used to drive the model. The differences in precipitation and temperature, the two most important climate variables that impact vegetation, in these two driving datasets are reflected in most of the simulated carbon pools and fluxes, particularly over eastern North America. However, despite very different gross fluxes, the model yields fairly similar estimates of the net atmosphere-land CO_2 flux when driven with the two forcing datasets. The analysis of the spatial distribution of trends in simulated carbon pools and fluxes shows that the simulated carbon sink over North America is driven primarily by net productivity enhancements over eastern United States, as reported by other studies, once again giving confidence in the model.

The second part of the thesis focuses on assessing the impact of dynamic vegetation, i.e. CTEM, on the CRCM5 simulated climate over North America for the 1971–2010 period. This is achieved by comparing two CRCM5 simulations, with and without CTEM, paying special attention to biosphere-atmosphere interactions and its spatio-temporal variability. Analysis shows that dynamic vegetation improves interactions at the land-atmosphere interface, which is reflected in the high correlations between biospheric and atmospheric variables. Similarly, CRCM5 with dynamic vegetation demonstrates long-term memory, estimated through lag correlations, and improved interannual variability, reflected in the biosphere and atmosphere states for anomalously dry and wet years.

Finally, the third part of the thesis studies projected changes to biosphere-climate interactions, and explores the contribution of vegetation dynamics to climate change. Transient climate change experiments, spanning the 1971–2100 period, driven by the

Canadian Earth System Model at the lateral boundaries, corresponding to two future emission scenarios - RCP4.5 and RCP8.5, with and without CTEM, are employed. Results show that increased CO_2 and temperatures lead to increased vegetation productivity and biomass, and enhanced vegetation water use efficiency in future climate. Furthermore, as dynamic vegetation allows biosphere to respond to climate change, it significantly modulates future climate, and therefore climate change, through thermal and hydrological feedbacks.

The above research thus contributes to a systematic understanding of the added value of dynamic vegetation in CRCM5 as well as the nature and variability of biosphere-atmosphere interactions over North America in current and future climates.

Keywords : dynamic vegetation, regional climate modelling, biosphere-climate interactions

INTRODUCTION

Global Climate Models (GCMs) coupling atmospheric, terrestrial, ocean and sea-ice components of the Earth System constitute the most comprehensive tools to study climate change and variability. However, because of the high complexity of the climate system and because the physical processes occurring within each of its components cover a wide range of temporal and spatial scales, GCM simulations are very demanding in computational resources and are thus performed at coarse horizontal resolution. Low resolution precludes GCMs from resolving adequately key regional and local climate processes. Hence, Regional Climate Models (RCMs) have been increasingly employed to dynamically downscale CGCM simulations to finer scales over a region of interest, allowing for high resolution without an increase in computational cost (Laprise, 2008; Rummukainen, 2010). At the resolution of the RCMs, regional water bodies and land-surface heterogeneities begin to be explicitly resolved, thus allowing realistic feedback processes that will increase the realism of climate simulations.

Several studies have demonstrated the importance of the land surface, and particularly the biosphere, in the climate system (Betts *et al.*, 1996; Pielke *et al.*, 1998; Bonan, 2008). Land surface controls the energy and water partitioning at the surface (Brovkin, 2002; Notaro *et al.*, 2006) and is also important from the point of view of carbon exchanges and thus plays an important role in the terrestrial carbon storage evolution. It can therefore influence the climate on time scales ranging from seconds to thousands of years, particularly in transient climate conditions.

Land Surface Models (LSMs) have therefore been developed to include key processes of exchanges of energy, water, momentum and carbon between the surface and the atmosphere in climate models (Pitman, 2003; Bonan, 2008). The first generation of LSMs used simple aerodynamic bulk transfer equations and simple prescriptions of albedo,

surface roughness, and soil water without explicitly representing vegetation or the hydrological cycle (Manabe, 1969). They have since evolved to simulate the hydrological and biogeochemical cycles and vegetation realistically (e.g. Friedlingstein *et al.*, 1995; Cox *et al.*, 1999). Climate models with LSMs of varying complexities have been used to understand the impact of changes in land surface characteristics and processes on climate. For instance, climate models with physically based LSMs have been employed to study impacts of deforestation on climate (e.g., Nobre *et al.*, 1991; Snyder *et al.*, 2004; Garcia-Carreras and Parker, 2011). However, such studies were performed with prescribed changes in vegetation cover because land surface models do not simulate long-term changes in the variability and the characteristics of the biosphere, which are crucial, particularly in the context of a changing climate.

Dynamic Vegetation Models (DVMs) have therefore been developed (e.g., Friend *et al.*, 1995; Foley *et al.*, 1996; Bonan *et al.*, 2003; Hughes *et al.*, 2006) in order to enable the simulation of large-scale structural vegetation changes in response to variations in climate and atmospheric CO_2 concentrations, and to incorporate the relevant biosphere-atmosphere feedback mechanisms in Earth System Models (Denman and et al., 2007). DVMs represent vegetation in terms of plant functional types (PFTs). This approach broadly classifies vegetation according to its form and function into functionally similar types (Box, 1996) such as broadleaf and needleleaf trees and their deciduous and evergreen types; crops and grasses are separated into C_3 and C_4 types according to their photosynthetic pathways. This classification does not take into account species level differences that become important at local scales but is considered sufficient to capture continental scale variability in terrestrial carbon pools and fluxes. A DVM simulates different carbon pools, such as stems, roots, and leaves, and the changes in the terrestrial ecosystem, like vegetation structure and composition, which affect these pools.

Several DVMs have been developed for use in climate models, such as TRIFFID (Cox, 2001), which is used in the Hadley Center GCM and the Lund-Potsdam-Jena Dynamic Global Vegetation Model (LPJ-DGVM; Sitch *et al.*, 2003), which has been recently coupled to the Rossby Centre Regional Climate Model. The available DVMs all differ

in characteristics and parameterisation. Sitch *et al.* (2008) compared five DVMs and showed that, despite the differences in parameterization, they all represent well the observed global land carbon budgets for the late 20th century. However, though the models simulate a net carbon uptake by the end of the 21st century, the magnitude of the land uptake vary significantly amongst the DVMs, thus indicating large uncertainties in the terrestrial biosphere response to changing climatic conditions (Sitch *et al.*, 2008). They conclude that though all models agree on the increased productivity of plants with increased atmospheric CO_2 concentrations, the carbon uptake simulated by a DVM is very dependent on the climate characteristics simulated by the climate model.

Jiang *et al.* (2012) analysed the uncertainties of vegetation distribution in the northern high-latitudes using an ensemble of LPJ-DGVM simulations under different SRES (Special Report on Emission Scenarios) scenarios. They found that the relative importance of different vegetation-related parameters, such as parameters that control plant carbon uptake and light-use efficiency, depend on the region and time of the year, and is greatly influenced by climate. The authors suggest that the uncertainties in vegetation distribution induced by vegetation-related parameters contribute significantly to the total uncertainty, though climate-induced and emission-induced uncertainties are larger. The above studies, focusing on the uncertainties coming from DVMs, lead to the conclusion that more work is necessary in the simulation of the biosphere as part of the climate system.

The dynamic vegetation model CTEM (Canadian Terrestrial Ecosystem Model) was developed at the Canadian Centre for Climate modelling and analysis (CCCma) (Arora, 2003; Arora and Boer, 2003, 2005, 2006; Li and Arora, 2011), to serve as the carbon cycle component in the CCCma atmosphere-ocean GCM. CTEM is a process-based ecosystem model, and it is able to grow vegetation from bare ground and simulates several time-varying vegetation structural attributes including leaf area index, vegetation height, root distribution and canopy mass. It includes processes of photosynthesis, autotrophic and heterotrophic respiration, phenology, turnover, allocation, fire and land-use change. CTEM simulates two dead carbon pools, litter and soil organic carbon, and three live

vegetation pools (stems, leaves and roots), and as such CTEM is able to provide net fluxes of CO_2 between the land and the atmosphere. Terrestrial ecosystem processes in CTEM are modeled for nine different plant functional types (PFTs); evergreen and deciduous needleleaf trees, broadleaf evergreen and cold and drought deciduous trees, and C_3 and C_4 crops and grasses.

CTEM was designed to be coupled to the Canadian Land Surface Scheme (CLASS; Verseghy, 1991, 2011; Verseghy *et al.*, 1993), and for this research, the coupled CLASS/CTEM was implemented in the fifth generation Canadian Regional Climate Model (CRCM5; Martynov *et al.*, 2013; Separovic *et al.*, 2013). This enables the study of biosphere-atmosphere interactions and their impact on the simulated climate at a higher resolution (0.5°) than would be possible using a CGCM. Such high-resolution studies of biosphere-atmosphere interactions are especially lacking over North America, and hence the importance of the research presented in this thesis.

It is worth noting that observation-based studies of biosphere-atmosphere interactions are also on the rise, with biosphere related observations starting to become increasingly available, and this is well reflected in the published literature. For instance, Notaro *et al.* (2006) and Wang *et al.* (2014) used observations, i.e. satellite-based fraction of photosynthetically active radiation (FPAR) and monthly climate data, to show that vegetation can substantially impact the atmosphere over North America. These studies indicate that vegetation could alter the amplitude of climate change locally and regionally through various feedbacks, and hence the need for a better understanding of biosphere-atmosphere interactions and their impact on climate.

Scientific objectives and approach

The main objective of this research is to study biosphere-climate interactions over North America in current and future climates. The main tool used in this study is CRCM5 with the Canadian Terrestrial Ecosystem Model (CTEM). Observations are used whenever possible to support model results. The systematic approach adopted to achieve the

objectives and related results are presented in Chapters I to III of this thesis.

Chapter I, entitled 'The effect of driving climate data on the simulated terrestrial carbon pools and fluxes over North America', represents a paper published in the peer-reviewed International Journal of Climatology. The focus of this chapter is on the validation of the dynamic vegetation model CTEM coupled to the Canadian Land Surface Scheme (CLASS) through offline simulations over North America. Offline CTEM/CLASS simulations driven by two different reanalysis products over North America are performed. Simulated terrestrial carbon pools and fluxes over North America are then compared with observation-based estimates. Chapter II, entitled 'Impact of dynamic vegetation on the Canadian RCM simulated climate over North America' and submitted to Climate Dynamics, assesses the impact of dynamic vegetation, i.e. CTEM, on the CRCM5 simulated climate over North America for the 1971–2010 period. This is achieved by comparing two CRCM5 simulations, with and without CTEM, paying special attention to biosphere-atmosphere interactions and its spatio-temporal variability. In the third and final chapter, entitled 'Biosphere-climate interactions in a changing climate over North America', projected changes in climate and biosphere are evaluated, and the resulting contributions of vegetation dynamics to climate change and to future climate variability are explored. Transient climate change experiments, spanning the 1971–2100 period, driven by the Canadian Earth System Model (CanEMS2) at the lateral boundaries, corresponding to two future emission scenarios - RCP4.5 and RCP8.5, with and without CTEM, are employed.

CHAPTER I

THE EFFECT OF DRIVING CLIMATE DATA ON THE SIMULATED TERRESTRIAL CARBON POOLS AND FLUXES OVER NORTH AMERICA

This chapter is presented in the format of a scientific article that has been published in the peer-reviewed journal *International Journal of Climatology*. The design of the research and its performance together with the analysis of data and the redaction of this article are entirely based on my work, with the co-authors involved in the supervision of all these tasks. The detailed reference is :

Garnaud, C., Sushama, L. and Arora, V. K. (2014). "The effect of driving climate data on the simulated terrestrial carbon pools and fluxes over North America". International Journal of Climatology, 34 : 1098-1110. DOI : 10.1002/joc.3748

Abstract

Dynamic vegetation models provide the ability to simulate terrestrial carbon pools and fluxes and a useful tool to study how these are affected by climate variability and climate change. At the continental scale, the spatial distribution of climate, in particular temperature and precipitation, strongly determines surface vegetation characteristics. Model validation exercises typically consist of driving a model with observation-based climate data and then comparing simulated quantities with their observation-based counterparts. However, observation-based datasets themselves may not necessarily be consistent with each other. Here, we compare simulated terrestrial carbon pools and fluxes over North America with observation-based estimates. Simulations are performed using the dynamic vegetation model CTEM (Canadian Terrestrial Ecosystem Model) coupled to the Canadian Land Surface Scheme (CLASS) when driven with two reanalysis-based climate datasets. The driving ECMWF reanalysis data (ERA40) and NCEP/NCAR reanalysis I data (NCEP) show differences when compared to each other, as well as

when compared to the observation-based Climate Research Unit (CRU) data. Most simulated carbon pools and fluxes show important differences, particularly over eastern North America, primarily due to differences in precipitation and temperature in the two reanalysis. However, despite very different gross fluxes, the model yields fairly similar estimates of the net atmosphere-land CO_2 flux when driven with the two forcing datasets. The ERA40 driven simulation produces terrestrial pools and fluxes that compare better with observation-based estimates. These simulations do not take into account land use change or nitrogen deposition, both of which have been shown to enhance the land carbon sink over North America. The simulated sink of 0.5 Pg C/yr during the 1980s and 1990s is therefore lower than inversion-based estimates. The analysis of spatial distribution of trends in simulated carbon pools and fluxes shows that the simulated carbon sink is driven primarily by NPP enhancements over eastern United States.

1.1 Introduction

The spatial distribution of vegetation, and terrestrial carbon pools and fluxes, at the continental to global scales is governed primarily by climate in particular temperature and precipitation (Walter and Box, 1976; Woodward, 1987; Stephenson, 1990; Prentice *et al.*, 1992). Terrestrial carbon fluxes are also sensitive to decadal and inter-annual variability in climate. Nemani *et al.* (2003) showed that a decreased cloud cover, and the resulting increase in solar radiation, led to an increase in net primary production in Amazon rain forests during the 1982–1999 period. Gobron *et al.* (2005) studied the impact of the 2003 drought on plant productivity in Europe using remote-sensing data. They found that the drought affected the growth of vegetation but that the effects of the drought were temporally limited. Zhao *et al.* (2011) studied the effect of changing climate on vegetation in the arid region of north-western China during 1982–2003 and noted an increase in productivity which was well correlated to precipitation increase during the growing season and the preceding winter.

The development of Dynamic Vegetation Models (DVMs) (e.g. Peng, 2000; Cramer *et al.*, 2001; Cox, 2001; Quillet *et al.*, 2010; den Hoof *et al.*, 2011) has allowed to model changes in vegetation structure in response to climate variability and climate change in Earth System Models. As the climate changes, a DVM can simulate the changes in structural vegetation attributes and its spatial distribution. Consequently, vegetation

becomes a dynamic component of the earth system that interacts with and provides feedback to other Earth system components. The changes in vegetation structure affect the biophysical processes at the land surface and changes in terrestrial carbon pools and fluxes affect the biogeochemical processes through carbon cycle feedbacks (Cox *et al.*, 2000; Myneni *et al.*, 2001; Foley *et al.*, 2003). DVMs represent vegetation in terms of plant functional types (PFTs). This approach broadly classifies vegetation according to its form and function into functionally similar types (Box, 1996) such as broadleaf and needleleaf trees and their deciduous and evergreen types ; crops and grasses are separated into C_3 and C_4 types according to their photosynthetic pathways. This classification does not take into account species level differences that become important at local scales but is expected to capture continental scale variability in terrestrial carbon pools and fluxes.

DVMs are typically validated against observation-based estimates of terrestrial carbon pools and fluxes when driven with observation-based climate data. However, observation-based climate datasets themselves may not necessarily be consistent with each other with consequences for model validation. The objective of this paper is to study the effect of driving climate data on the simulated terrestrial carbon pools and fluxes over North America, a region that covers several climatic zones and consequently biomes, using the Canadian Terrestrial Ecosystem Model (CTEM) (Arora, 2003; Arora and Boer, 2003, 2005) coupled to the Canadian Land Surface Scheme (CLASS) (Verseghy, 1991, 2011; Verseghy *et al.*, 1993). Coupled CLASS/CTEM are driven offline at 0.5° (~45km) resolution over North America using the European Centre for Medium range Weather Forecast's (ECMWF) ERA40 reanalysis (Uppala et al., 2005) and the National Centers for Environmental Prediction's NCEP/NCAR reanalysis I data (Kalnay *et al.*, 1996) from 1958 to 2001. Both simulations, one driven by ERA40 data and the other driven by NCEP data, are then evaluated by comparing CLASS/CTEM simulated terrestrial carbon pools and fluxes to observation-based estimates.

CTEM has been validated at selected sites and different PFTs in earlier studies (Arora and Boer, 2005; Li and Arora, 2011) and also at the global scale when implemented in an earth system model (Arora *et al.*, 2009) but coupled to earlier versions of CLASS.

The CLASS version 3.5. used here better simulates the hydraulic and thermal regimes by incorporating an improved treatment of soil evaporation, a new canopy conductance formulation, and an enhanced snow density and snow interception.

This paper is organised as follows. Section 1.2 of the paper gives a brief overview of the coupled land-surface and terrestrial ecosystem models, CLASS and CTEM, along with the description of the experimental set-up and the methodology. In section 1.3, the effect of different driving data sets on vegetation growth and productivity is analysed by comparing them with observed and modelled data. Section 1.3 also assesses the spatial and temporal evolution of the simulated biosphere in the recent past. A brief summary of the results and conclusions are given in section 1.4.

1.2 Models, Experimental Set-up and Data Sets

1.2.1 Coupled land surface and terrestrial ecosystem models

The configuration used here is comprised of the Canadian Terrestrial Ecosystem Model (CTEM) (Arora and Boer, 2005) coupled to the Canadian Land Surface Scheme (CLASS) (version 3.5) (Verseghy, 2011). In its standard formulation, CLASS uses three soil layers, 0.1 m, 0.25 m and 3.75 m thick, corresponding approximately to the depth influenced by the diurnal cycle, the rooting zone and the annual variations of temperature, respectively (Poitras *et al.*, 2011). CLASS includes prognostic equations for energy and water conservation for the three soil layers and a thermally and hydrologically distinct snowpack where applicable (treated as a fourth variable-depth layer). The energy balance and temperature calculations are performed over the three soil layers, but the hydrological balance calculations are performed only for layers above the bedrock. In an attempt to crudely mimic subgrid-scale variability, CLASS adopts a "pseudo-mosaic" approach and divides each grid cell into a maximum of four sub-areas : bare soil, vegetation, snow over bare soil and snow with vegetation. The energy and water balance calculations are first performed for each sub-area separately, and then averaged over the grid cell, using averaged structural attributes and physiological properties of the four

PFTs in CLASS : needleleaf trees, broadleaf trees, crops and grasses. These structural attributes include leaf area index (LAI), roughness length, canopy mass and rooting depth, which have to be specified if they are present in a grid cell. When coupled to CTEM, these structural vegetation attributes are dynamically simulated by CTEM as a function of environmental conditions.

CTEM is a process-based ecosystem model (Arora, 2003; Arora and Boer, 2003, 2005, 2006; Li and Arora, 2011) designed to simulate terrestrial ecosystem processes. It is able to grow vegetation from bare ground and simulates several vegetation structural attributes including leaf area index, vegetation height, root distribution and canopy mass. It includes processes of photosynthesis, autotrophic and heterotrophic respiration, phenology, turnover, allocation, fire and land-use change. The photosynthesis submodule uses the biogeochemical approach as described by Farquhar *et al.* (1980) and Collatz *et al.* (1991, 1992). CTEM simulates two dead carbon pools (litter and soil organic carbon) and three live vegetation pools (stems, leaves and roots). The structure of CTEM is shown in Figure 1.1 along with the prognostic equations for carbon in the five model pools. Terrestrial ecosystem processes in CTEM are modelled for nine different plant functional types (PFTs); evergreen and deciduous needleleaf trees, broadleaf evergreen and cold and drought deciduous trees, and C_3 and C_4 crops and grasses. The vegetation structural attributes of CTEM's nine PFTs are averaged for four PFTs (needleleaf trees, broadleaf trees, crops and grasses) when they are passed to CLASS. Figure 1.2 shows the manner in which CLASS and CTEM are coupled to each other. CLASS and CTEM's photosynthesis sub-module, simulating the fast biophysical processes, such as photosynthesis, canopy conductance and leaf respiration, operate at a 30-minute timestep while other biogeochemical processes are modelled at a daily timestep. Once coupled, CLASS and CTEM simulate energy, water and CO_2 fluxes across the land–atmosphere boundary. However, CTEM does not include the coupling of carbon with nitrogen and phosphorus cycles and so, nutrient limitation of photosynthesis is not explicitly modelled. Nevertheless, CTEM implicitly models nutrient limitation by "downregulating" photosynthesis as CO_2 increases using an empirical formulation that is calibrated on the

basis of plants grown in elevated and ambient CO_2 environments (Arora *et al.*, 2009).

1.2.2 Experimental set-up

The coupled CLASS and CTEM models are run offline over the North American domain shown in Figure 1.3, at a horizontal resolution of 0.5 degrees and a timestep of 30 minutes. The input data required to run the model include the incident solar and longwave radiation, 2-m air temperature, relative humidity, 10-m wind velocity, surface pressure and total precipitation. The soil texture information, i.e. percentage of sand and clay, for the three layers (see Section 1.2.1) is specified from Webb *et al.* (1991). Finally, the fractional coverage of CTEM's nine PFTs (Fig. 1.3) for the 0.5° grid cells are specified from Arora and Boer (2010) who use the HYDE 2 crop area data set (Wang *et al.*, 2006) to reconstruct historical land cover. The land cover is specified at its 1960 values, so land use change is not taken into account. It should be noted that, even though the geographical distribution of PFTs is fixed, the vegetation attributes (LAI, land-atmopshere CO_2 fluxes and carbon pools) are simulated as dynamic functions of driving climate.

Two simulations are performed with CLASS/CTEM models using different driving climate data. The first uses ERA40 reanalysis data (Uppala *et al.*, 2005), and the second uses NCEP reanalysis (Kalnay *et al.*, 1996). ERA40 data is available for the 1957–2002 period at 2.5° (~250 km) resolution, while NCEP data is available for the 1948–present period at 200 km resolution. These two simulations driven by ERA40 and NCEP for the common 1958-2001 period are referred to as RP_ERA and RP_NCEP, respectively.

Initial conditions for prognostic variables in CLASS and CTEM (including structural vegetation attributes) for the RP_ERA and RP_NCEP simulations are obtained by spinning the model from zero vegetation for 400 years, driven by repeated 1958–1977 ERA40 and NCEP climate data, respectively. Similarly to the CMIP5 modelling protocol (Taylor *et al.*, 2009, 2012), a constant CO_2 concentration value corresponding to the year 1765 is used for the first 207 simulation years for the spin up, followed by transient CO_2

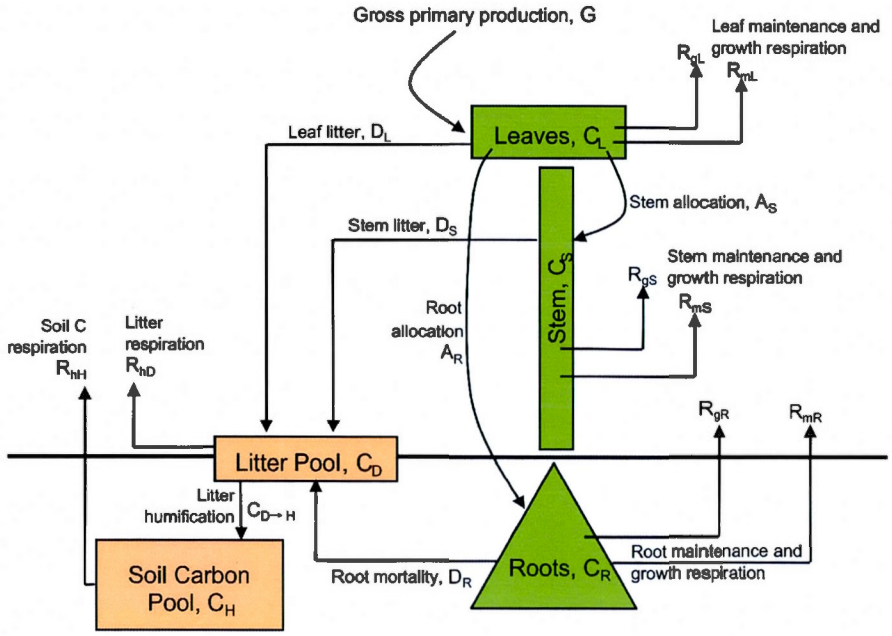

G = photosynthesis, GPP
A_S = carbon allocated to stem from leaves
A_R = carbon allocated to roots from leaves
R_{gL}= Growth respiration for leaves, and similarly for stem (S) and roots (R).
R_{mL} = Maintenance respiration for leaves and similarly for stem (S) and roots (R)
D_L = leaf litter and similarly for stem (S) and roots (R)
R_{hD} = Heterotrophic respiration from the litter or debris pool
R_{hH} = Heterotrophic respiration from the soil carbon (humus) pool
$C_{D\to H}$ = carbon transferred from the litter to the soil carbon pool

$$\frac{dC_L}{dt} = G - A_R - A_S - R_{gL} - R_{mL} - D_L$$

$$\frac{dC_S}{dt} = A_S - R_{gS} - R_{mS} - D_S$$

$$\frac{dC_R}{dt} = A_R - R_{gR} - R_{mR} - D_R$$

$$\frac{dC_D}{dt} = D_L + D_S + D_R - R_{hD} - C_{D\to H}$$

$$\frac{dC_H}{dt} = C_{D\to H} - R_{hH}$$

Figure 1.1 The structure of the terrestrial ecosystem model and the prognostic equations for carbon in five model pools "C" (Kg C/m^2) : leaves (L), stem (S), root (R), litter or debris (D), and soil organic matter or humus (H).

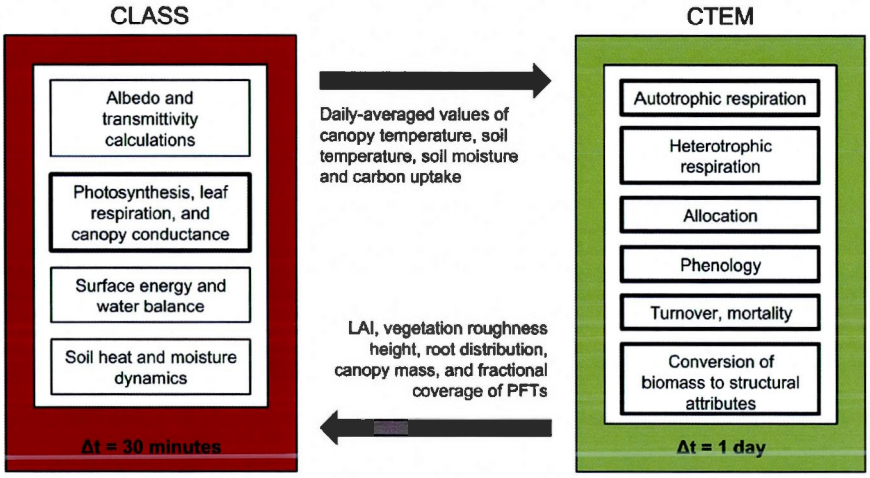

Figure 1.2 The manner in which the land surface scheme CLASS and the terrestrial ecosystem module CTEM are coupled to each other. CTEM sub-modules are shown with a thick dark outline.

concentrations corresponding to the years 1765 to 1957 for the remaining 193 years. The transient 1958–2001 simulations RP_ERA and RP_NCEP are forced with evolving CO_2 concentrations from the Mauna Loa Observatory (Keeling *et al.*, 1976; Thoning *et al.*, 1989). Because the soil carbon is much slower to reach equilibrium than any other carbon pool (Fig. 1.1), an accelerator is used to allow the soil carbon pool to reach equilibrium at a similar rate as the vegetation and the litter, so that all carbon pools have stabilised within the first part of the spinup (constant CO_2).

1.2.3 Data sets and methods

While the reanalysis data provide the sub-daily resolution of meteorological data needed for driving the CLASS and CTEM models they are not "observation-based" in a strict sense. Thus, prior to studying the impact of the climate data on vegetation, the ERA40 and NCEP seasonal mean temperature and precipitation used to drive CLASS/CTEM are compared to the gridded observational-based data from the Climate Research Unit (CRU) (Mitchell and Jones, 2005). The CRU TS 2.1 data set covers the period 1901–

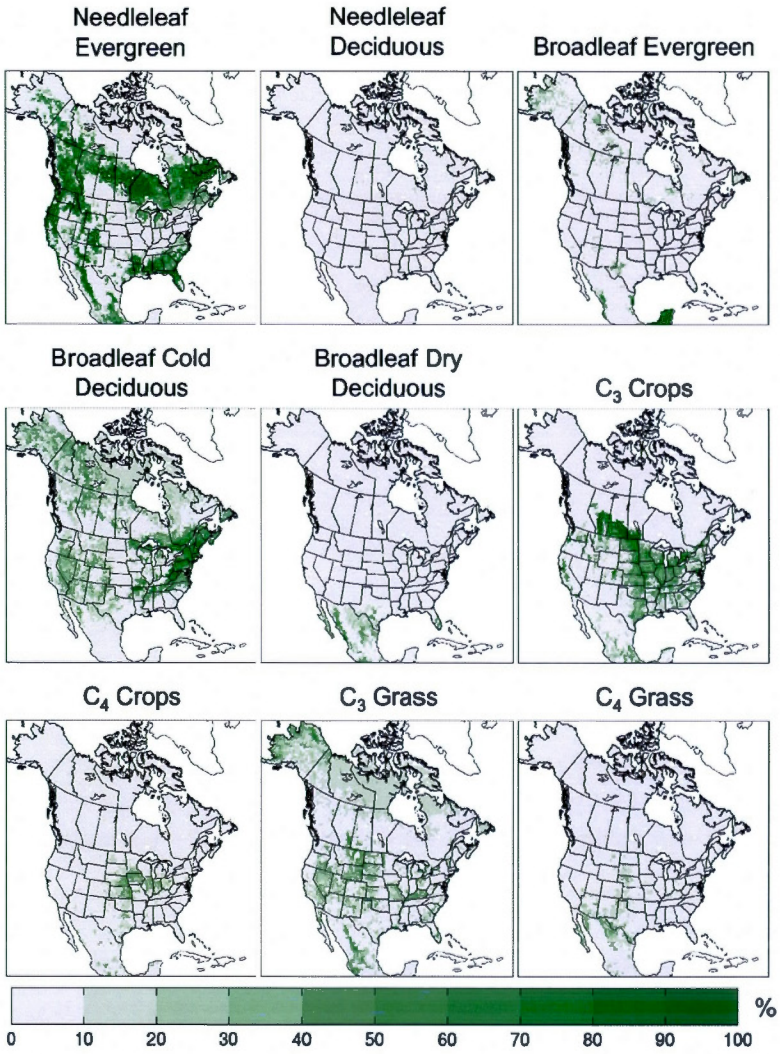

Figure 1.3 Fractional coverage (%) of the nine Plant Functional Types (PFT) modelled by CTEM for the North American domain.

2002 and has a resolution of 0.5°. This comparison helps identify biases in the two reanalysis datasets.

The simulated terrestrial pools and fluxes are analysed by comparing green leaf area index (LAI), net primary productivity (NPP), gross primary productivity (GPP) and woody biomass with observation-based estimates and multi-model results from other studies. The observation-based green leaf area index were obtained from the International Land Surface Climatology Project Initiative (ISLSCP II) FASIR-adjusted NDVI Biophysical Parameter Fields measured by the satellite mounted AVHRR sensor (Los *et al.*, 2000; Hall *et al.*, 2006; Sietse, 2010). These monthly global data are available for the 1982–1998 period at 1°x1° resolution. The net primary production (NPP) data are from the MODIS NPP/GPP project (MOD17) (Zhao *et al.*, 2005), a part of the NASA/EOS project. It is a continuous satellite-driven dataset available from 2000 to 2006 at 1-km resolution. The algorithm used in MOD17 is based on the original logic of Monteith, suggesting that NPP under non-stressed conditions is linearly related to the amount of absorbed Photosynthetically Active Radiation (PAR) during the growing season. The MOD17 product also combines the complex effects of temperature, water and radiation on the productivity and corrects the data contaminated by cloudiness or severe aerosol. The gross primary production (GPP) data were obtained from observation-based estimations of global GPP for the 1998-2005 period using eddy covariance flux data and various diagnostic models from the Beer *et al.* (2010) study. Finally, the woody biomass data are from an AVHRR GIMMS NDVI data set with an 8-km resolution and forest inventory data for stem wood volume (Dong *et al.*, 2003). An equation that relates the forest inventory data with the satellite NDVI data as a function of latitude, was developed and tested by Dong *et al.* (2003) in order to estimate the woody biomass with a high resolution across the northern hemisphere in the early 1980s and the late 1990s. The observation-based and multi-model mean data used for validation come from different sources and need not necessarily be consistent with each other.

Both RP_ERA and RP_NCEP simulations are also investigated for spatial and temporal

variability of primary carbon fluxes and trends in the carbon pools in North America. To limit the effect of initial conditions, this analysis is restricted to the last 32 years (1970–2001) of the simulation. Trends are calculated using Sen's slope method (Sen, 1968) and the statistical significance of these trends is estimated using the Mann-Kendall test (Kendall, 1975; Khaliq *et al.*, 2009) at 5% significance level.

1.3 Results and Discussion

1.3.1 Driving data validation

The seasonal mean temperature and precipitation differences between the two reanalysis and the CRU dataset for the period 1958–2001 are shown in Figure 1.4. For the winter precipitation, both NCEP and ERA40 reanalysis show similar differences compared to the CRU. There are two main regions of underestimation : up to 5 mm/day on the West Coast and in the Canadian Rocky Mountains and up to 2 mm/day in southeast USA. The NCEP and ERA40 summer precipitation compare differently to the CRU data. NCEP tends to overestimate precipitation by up to 5 mm/day in southeast USA and Mexico and by 4 mm/day in Alaska. It underestimates summer precipitation in some parts of northeast Canada and northwest Mexico by up to 4 mm/day. ERA40 tends to generally underestimate summer precipitation, particularly over the USA, by 1 or 2 mm/day, but as high as up to 4 mm/day in southeast USA and up to 5 mm/day in Mexico (Fig. 1.4a). Overall, ERA40 precipitation appears to compare better with the CRU data set, especially during summer when most of the vegetation growth occurs.

In Figure 1.4b, ERA40 generally overestimates the seasonal mean winter temperature by 1 to 2°C in the southern half of North America, and by up to 10°C in the high-latitude regions of northwest Canada and Alaska. NCEP generally tends to underestimate the winter temperatures, especially in the highlands of western USA (up to 6°C). For seasonal mean summer temperature, ERA40 shows a constant overestimation of between 2 and 6°C that is enhanced over the high elevations in western US (up to 10°C). Similar to ERA40, NCEP tends to overestimate the temperatures in summer except along the

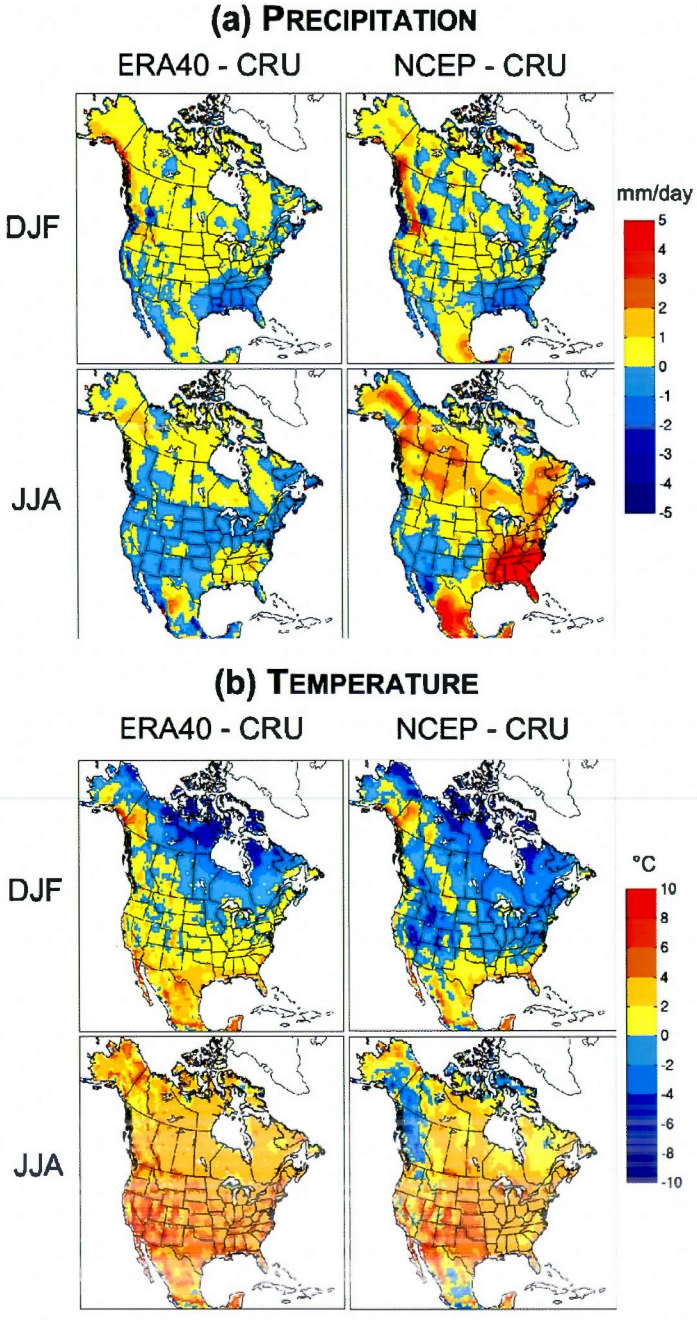

Figure 1.4 Difference between the 1958–2001 NCEP and ERA40 (a) precipitation (mm/day) and (b) mean air temperature (°C) and that of CRU for the winter (DJF) and summer (JJA) periods.

Canadian West Coast where it underestimates the temperature by up to 10°C.

In their comparison of ERA40 and NCEP reanalyses to CRU over the 1958–2001 period, Simmons *et al.* (2004) have shown that there is a warm bias in the surface temperature in the middle and high latitudes, especially prior to the 1970s due to the lack of satellite observations. Their study also showed that when comparing ERA40 to the NCEP reanalysis, ERA40 is closest to the CRU analysis for all but the earliest years (prior to 1967).

1.3.2 CLASS/CTEM evaluation and analysis

The simulated terrestrial carbon pools and fluxes from the offline CLASS and CTEM simulations (RP_ERA and RP_NCEP) for the 1958–2001 period are compared with observations where possible and also analysed to investigate the trends for the 1970–2001 period.

1.3.2.1 Evaluation of the mean state

Simulated NPP, GPP, woody biomass and green LAI, are compared with observation-based where available or with multi-model mean data as described in section 1.2.3. In Figure 1.5a, RP_ERA GPP compares reasonably well with the observation-based estimate from Beer *et al.* (2010). The model captures the spatial distribution of GPP relatively well, with high values located mostly in southeast US and along the coasts of Mexico. The model also somewhat captures the high GPP values along the West Coast. The simulated higher GPP for the RP_NCEP case over southeast US is the result of higher summer precipitation in the NCEP reanalysis (Figure 1.4a). While simulated GPP compares well with its observation-based estimate, simulated NPP for the RP_ERA case (Figure 1.5b) is higher over the eastern US and generally low elsewhere when compared to the satellite-based NPP from MODIS (Zhao *et al.*, 2005). Similar to GPP, NPP for the RP_NCEP case is too high compared to the estimate from Zhao *et al.* (2005), especially over eastern US, again due to higher than observed summer precipitation.

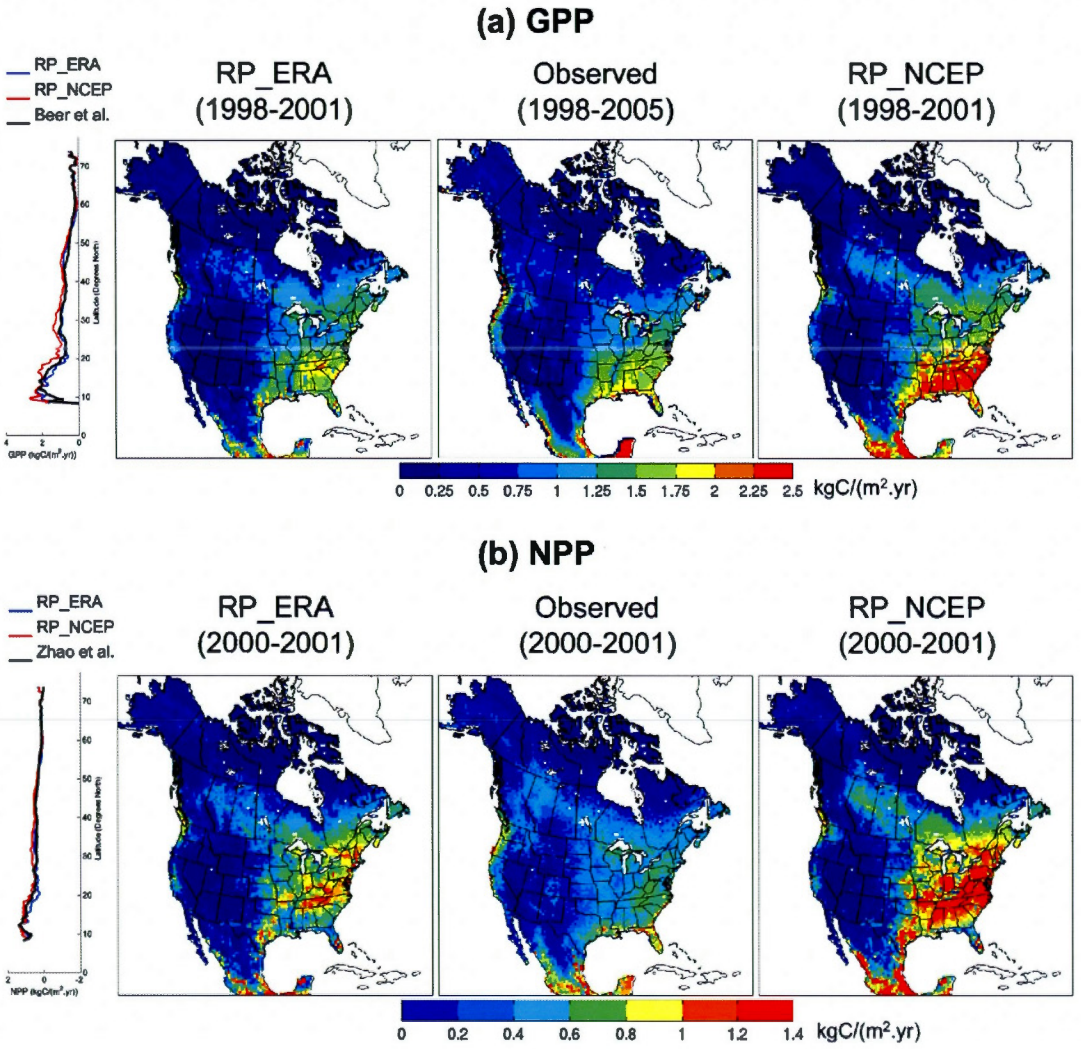

Figure 1.5 The spatial plots correspond to the mean annual (a) GPP ($kgC.m^{-2}.yr^{-1}$) (1998–2001 or 1998–2005) and (b) NPP ($kgC.m^{-2}.yr^{-1}$) (2000-2001) for RP_ERA (2^{nd} column), RP_NCEP (4^{th} column) and their respective validation data (3^{rd} column) from Beer *et al.* (2010) and Zhao *et al.* (2005). Zonal distributions along the northern latitudes of the studied variable are shown in the 1^{st} column.

	NPP		GPP	
	R^2	RMSE	R^2	RMSE
RP_NCEP	0.5307	0.2338	0.6483	0.3546
RP_ERA	0.5630	0.2924	0.6716	0.4392

Table 1.1 Coefficient of determination (R^2) and root mean square error (RMSE) values from the NPP and GPP values against the respective evaluation data for both RP_ERA and RP_NCEP simulations.

CTEM uses a single-leaf photosynthesis approach and the coupling between photosynthesis and canopy conductance is based on vapour pressure deficit (Leuning, 1995). The effect of water stress on maximum potential temperature-based photosynthetic rate is taken into account by reducing the potential photosynthetic rate via a non-linear soil moisture function, which takes into account the degree of soil saturation, the wilting point and the field capacity soil moisture contents and the fraction of roots in the three soil layers (Arora, 2003). The coefficient of determination (R^2) and root mean square error (RMSE) of both NPP and GPP values against their respective evaluation data are shown in Table 1.1. For both net and gross primary productivities, the RMSE values confirm that RP_NCEP has the larger errors. Interestingly, the R^2 values show that the spatial patterns are better captured by RP_NCEP. In Figure 1.6a, simulated woody biomass for the RP_ERA case is generally higher than its observation-based estimate except in the Pacific northwest region of the United States and interior British Columbia. This is possibly related to only one PFT dedicated to needleleaf evergreens. Validation of CTEM over British Columbia in another project at a 40 km resolution shows that an additional needleleaf evergreen PFT, with higher leaf life span as well as higher drought and cold resistance, is needed for interior British Columbia to simulate realistic spatial distribution of LAI (Dr. Yiran Peng, CCCma, personal communication). Finally, the use of the NCEP reanalysis leads to even higher simulated woody biomass.

Even though the simulated GPP (Fig. 1.5a) compares reasonably well with its observation-based estimate, the simulated NPP (Fig. 1.5b) is overestimated compared to the

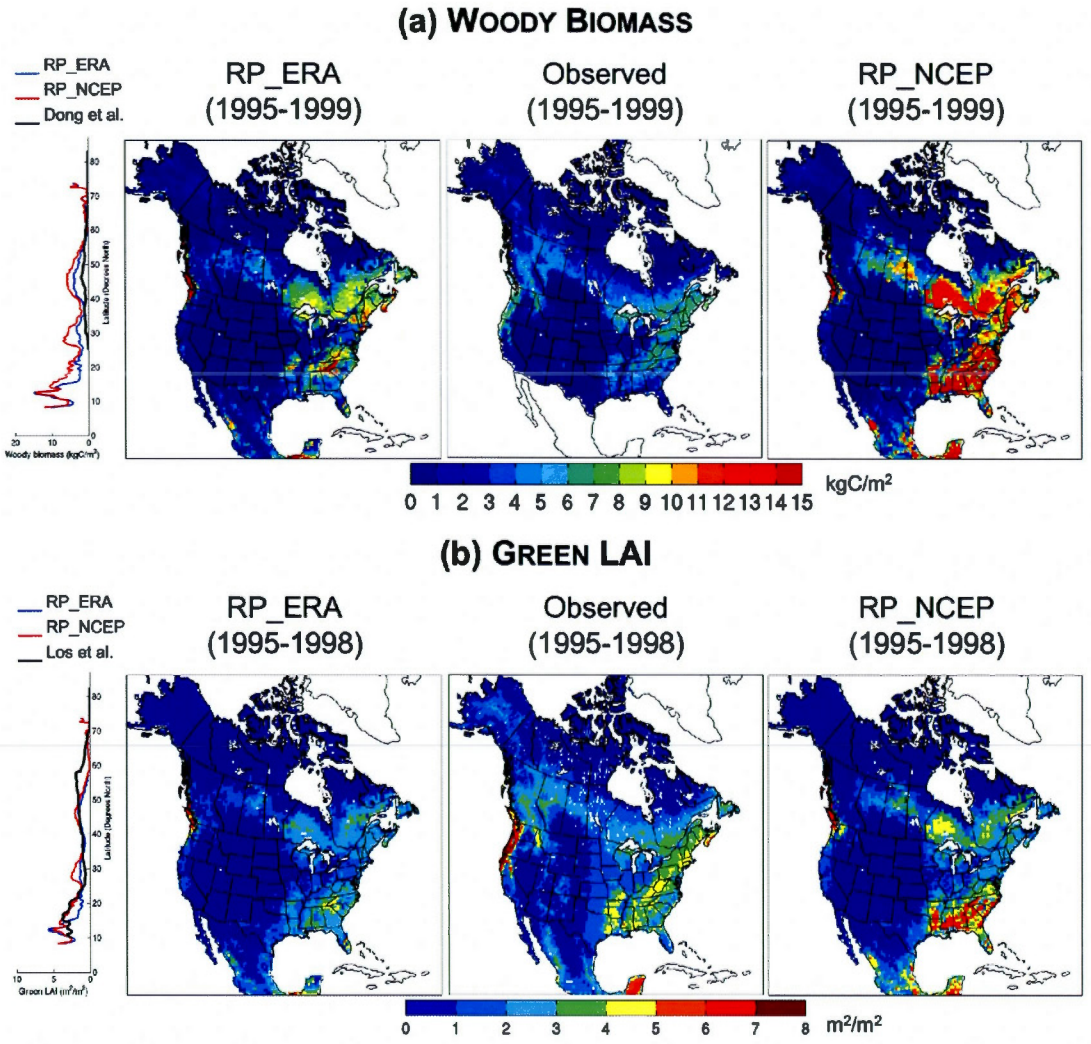

Figure 1.6 The spatial plots correspond to the mean annual (a) woody biomass (kgC/m^2) (1995–1999) and (b) green LAI (m^2/m^2) (1995–1998) for RP_ERA (2^{nd} column), RP_NCEP (4^{th} column) and their respective validation data (3^{rd} column) from Dong *et al.* (2003) and from ISLSCP II (Los *et al.*, 2000; Hall *et al.*, 2006; Sietse, 2010). Zonal distributions along the northern latitudes of the studied variable are shown in the 1^{st} column.

MODIS estimates from Zhao et al. (2005) and woody biomass (Fig. 1.6a) is overestimated compared to observation-based estimates from Dong *et al.* (2003). These inconsistencies are most likely the result of different sources of the validation data.

With its higher temperatures and greater precipitation in summer, compared to the CRU data set, the NCEP reanalysis yield values of GPP and NPP (Figures 1.5 a-b) that are much too high in southeast USA. This overestimation is, indeed, well correlated with the higher summer precipitation shown in Figure 1.4a. The woody biomass (Figure 1.6a) is, as a result, also overestimated when compared to observations. These patterns are also seen in the zonal distribution of GPP, NPP and woody biomass in Figures 1.5a, 1.5b and 1.6a, respectively. The zonal distribution of both GPP and NPP, for the RP_ERA case, compares well the observation-based estimates from Beer *et al.* (2010) and satellite-driven data from Zhao *et al.* (2005), respectively, while for the RP_NCEP case both quantities are overestimated in the tropics and mid-latitudes regions. In regards to the woody biomass, both simulations yield values that are higher than the observation-based estimates although the RP_ERA case is closer to the observations.

In Figure 1.6b, CTEM tends to underestimate the green LAI when driven by the ERA40 reanalysis. The underestimation, when compared to the observation-based data, is greatest in areas covered mostly by forests such as the boreal forest in central and western Canada and the temperate forests covering most of eastern US. This is most likely a model limitation, although satellite-based LAI products also have their limitations. Many different approaches are used to calculate the normalized difference vegetation index (NDVI), used to derive LAI, and this leads to different results, as shown by Alcaraz-Segura *et al.* (2010). Furthermore, Garrigues *et al.* (2008) have shown that LAI datasets derived from remote sensing data all have their weaknesses. Most datasets agree over croplands and grasslands, but large differences appear over forests "where differences in vegetation structure representation between algorithms and surface reflectance uncertainties lead to substantial discrepancies between products" (Garrigues *et al.*, 2008). The RP_NCEP case shows similar spatial pattern to that for RP_ERA, but it tends to overestimate the LAI especially in southeast US. The zonal distribution of the LAI

shows that both simulations tend to overestimate LAI between 25 and 35°N but tend to underestimate LAI north of 50°N, similarly to what found Gibelin *et al.* (2006) when comparing their LAI, simulated by ISBA terrestrial ecosystem model, with the ISLSCP data (their Figure 2). In addition, Gibelin *et al.* (2006) show that ISLSCP values of LAI are generally rather high compared to MODIS and ECOCLIMAP (Champeaux *et al.*, 2005) data.

The different sources of observation-based data and inconsistencies between them make it difficult to draw firm conclusions about model behavior. For example, the simulated GPP in the RP_ERA case over the southeastern USA (Figure 1.5a) compares well with its observation-based estimate but simulated woody biomass is higher compared to observation-based estimates and simulated LAI is lower. Nevertheless, despite the differences in the absolute magnitude of simulated GPP, NPP, woody biomass and LAI, the spatial patterns of these quantities and their zonal distributions compare reasonably well to those from the observation-based analysis. However, the productivity and the LAI in the Yucatan peninsula are underestimated by both simulations (RP_ERA and RP_NCEP). This could be due to a combination of the low resolution of both climate dataset, and its impact on the quality of the datasets, and of problems with model performance in tropical regions.

Simulated results may also be assessed on the basis of vegetation carbon use efficiency (CUE), the ratio of net to gross primary productivity, which describes the ability of plants to transfer carbon from the atmosphere to terrestrial biomass (DeLucia *et al.*, 2007). CUE may also be used to assess the consistency between the NPP and GPP data used for validating simulated results. DeLucia *et al.* (2007) show that the CUE of forests can vary from 0.23 to 0.83, with an average value of 0.53, depending on the tree type, their stand age and leaf mass to total mass ratio. Figure 1.7 shows the simulated mean CUE for the 1990–1999 period obtained from both RP_ERA and RP_NCEP simulations, together with two observation-based CUE calculated using NPP estimates from Zhao *et al.* (2005) and GPP estimates from Beer *et al.* (2010) and Zhao *et al.* (2005). The comparison between the two observation-based CUE demonstrates

the lack of consistency that can occur between "observational" datasets. The CUE calculated using Beer *et al.* (2010) GPP generally has much higher values than those suggested by DeLucia *et al.* (2007) and obtained with Zhao *et al.* (2005). Simulated CUE values vary between 0.15 and 0.80, with an average of 0.573 over North America for the RP_ERA case and 0.585 for the RP_NCEP case. Terrestrial ecosystem models that do not model autotrophic respiration explicitly usually assume a constant value of 0.5 for the CUE for all types of plants (DeLucia *et al.*, 2007). The values of CUE obtained from our recent past experiments (RP_ERA and RP_NCEP) are generally similar to that suggested by DeLucia *et al.* (2007), though the RP_NCEP case gives somewhat higher values than RP_ERA. In addition, simulated values of CUE are greatest for temperate deciduous forests and lowest for boreal forests, similar to DeLucia *et al.* (2007). The areas covered mostly by crops show higher values of CUE, consistent with the observations made by Frantz and Bugbee (2005) and Choudhury (2000), the latter stating that in general the CUE values for forests are about 30% lower than those for crops and grasses.

1.3.2.2 Trends in biospheric fluxes and pools

Both RP_ERA and RP_NCEP simulations are further analysed to investigate trends in terrestrial carbon pools and fluxes. To limit the effect of initial conditions, results from the last 32 years (1970–2001) of the simulations are used.

Figure 1.8 shows the trends in the driving data (CO_2, precipitation and temperature), in simulated fluxes (net atmosphere-land CO_2 flux, GPP, NPP, autotrophic and heterotrophic respiration) and in carbon pools (LAI and woody biomass). The temperature and precipitation data, and the GPP, NPP, both respiration fluxes and LAI are domain averaged. The net atmosphere-land CO_2 flux and woody biomass are summed over the domain.

The rising atmospheric CO_2 (Fig. 1.8a) and temperatures (Figure 1.8c) over the domain for the 1970–2001 period, along with nearly constant precipitation in both reanalysis

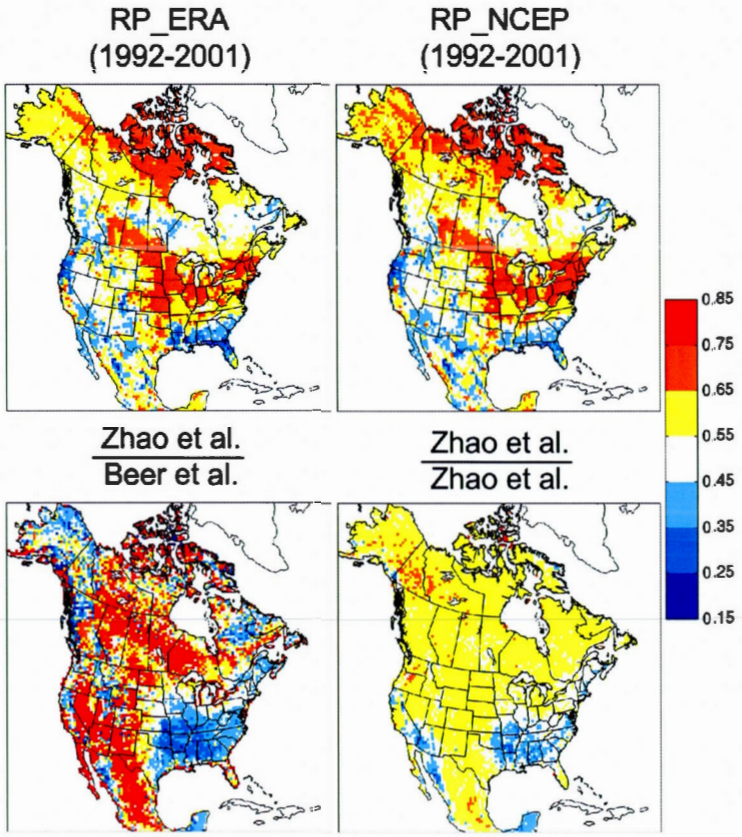

Figure 1.7 Mean annual Carbon Use Efficiency (NPP/GPP) during the 1990–1999 period for RP_ERA (top left; spatial mean = 0.573), RP_NCEP (top right; spatial mean = 0.585) and the CUE calculated using NPP estimates from Zhao *et al.* (2005) and GPP estimates from Beer *et al.* (2010) (bottom left), and using both NPP and GPP estimates from Zhao *et al.* (2005) (bottom right).

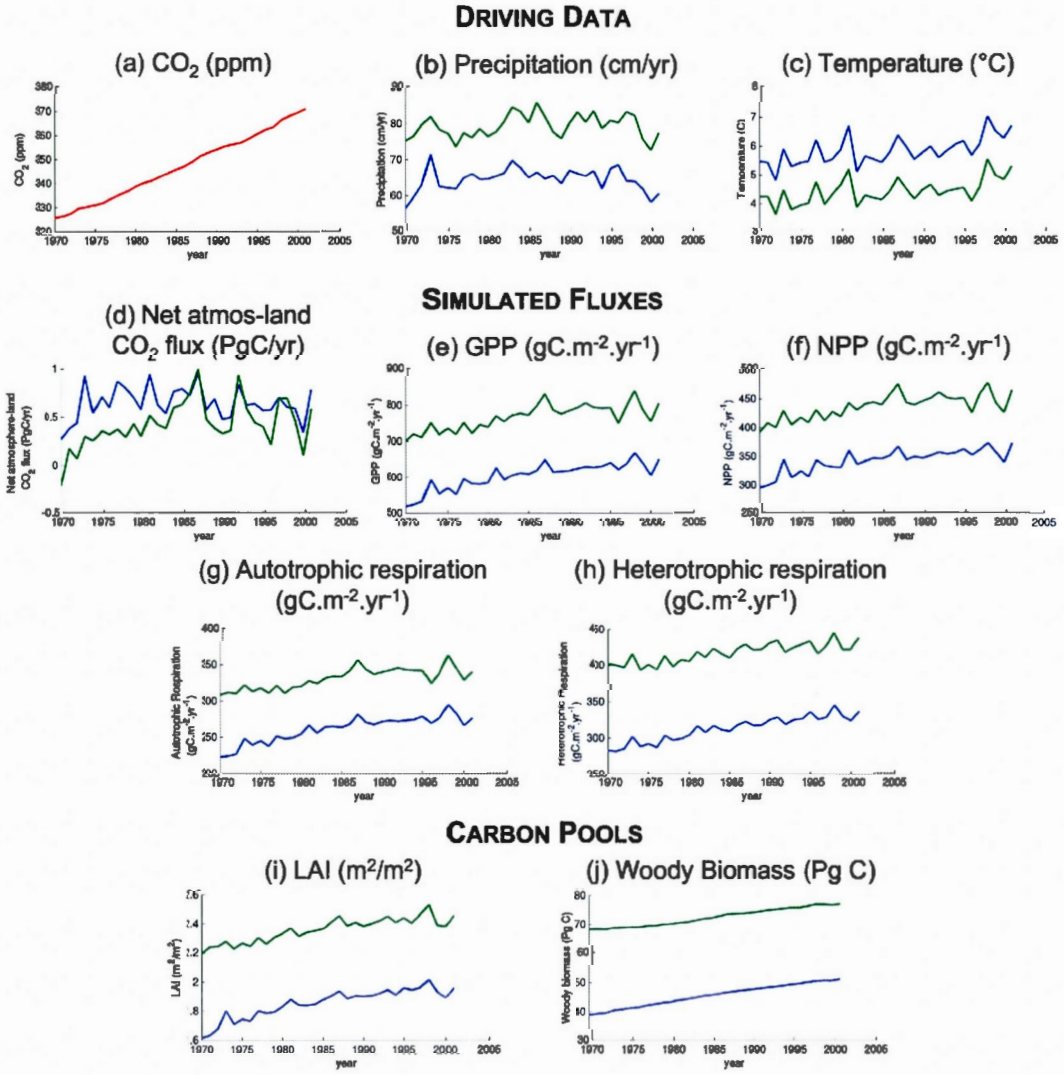

Figure 1.8 Trends in the driving data (CO_2 (in red), precipitation and temperature), in simulated fluxes (net atmosphere-land CO_2 flux, GPP and NPP) and in carbon pools (LAI, woody biomass and soil carbon mass) over the study domain from 1970 to 2001 for the RP_ERA simulation (in blue) and the RP_NCEP (in green) simulations.

(Fig. 1.8b), yield a simulated carbon sink of around 0.5 Pg C/yr for both RP_ERA and RP_NCEP simulations during 1980s and 1990s (Fig. 1.8d), despite very different gross production fluxes. This is in part explained by the fact that both autotrophic and heterotrophic respirations (Fig. 1.8g and 1.8h, respectively) are much greater in RP_NCEP than RP_ERA, effectively counteracting the greater primary production in RP_NCEP. These simulations do not include the effect of land use change, which is expected to yield an additional carbon sink in the eastern United States due to abandonment of croplands (Arora and Boer, 2010), nor do they include the effect of nitrogen deposition that is also expected to increase the sink strength (Holland *et al.*, 1997). As expected then, our simulated sink of 0.5 Pg C/yr, which includes only the effects of increasing CO_2 and warming temperatures, is consistently lower than other estimates. Pacala *et al.* (2001) provide a model-based estimate of a sink of 0.37 to 0.71 Pg C/yr for 1980s for North America. Inversion-based estimates from five studies range from 0.81 ± 0.72 to 1.26 ± 0.23 during 1990s as reported in Crevoisier *et al.* (2010) (their Table 1). The simulated sink is primarily associated with an increase in woody biomass (Fig. 1.8j). There is also a marginal contribution from the soil carbon (figure not shown). However, CTEM only includes a single soil carbon pool and studies show that multi-pool models are able to capture the response to soil warming experiments more realistically (Knorr *et al.*, 2005). The simulated LAI also increases over the 1970–2001 period (Fig. 1.8i). The increase in LAI and woody biomass, which yields the simulated sink, is associated with an increase of about 22% in GPP and NPP over the 1970–2001 period (Figs. 1.8 e-f).

Figures 1.9 and 1.10 show the spatial distribution of trends associated with the live (stem and roots) and dead (litter and soil) carbon pools for the 1970–2001 period for RP_ERA and RP_NCEP simulations, respectively, computed using Sen's slope method. Trends are also shown for total carbon in the system that includes these four pools in panel (a) of both figures. For both simulations, most of North America shows an increasing trend, except for parts of the central United States, the high latitudes of Canada and segments along the southern West Coast, mostly due to the decreasing

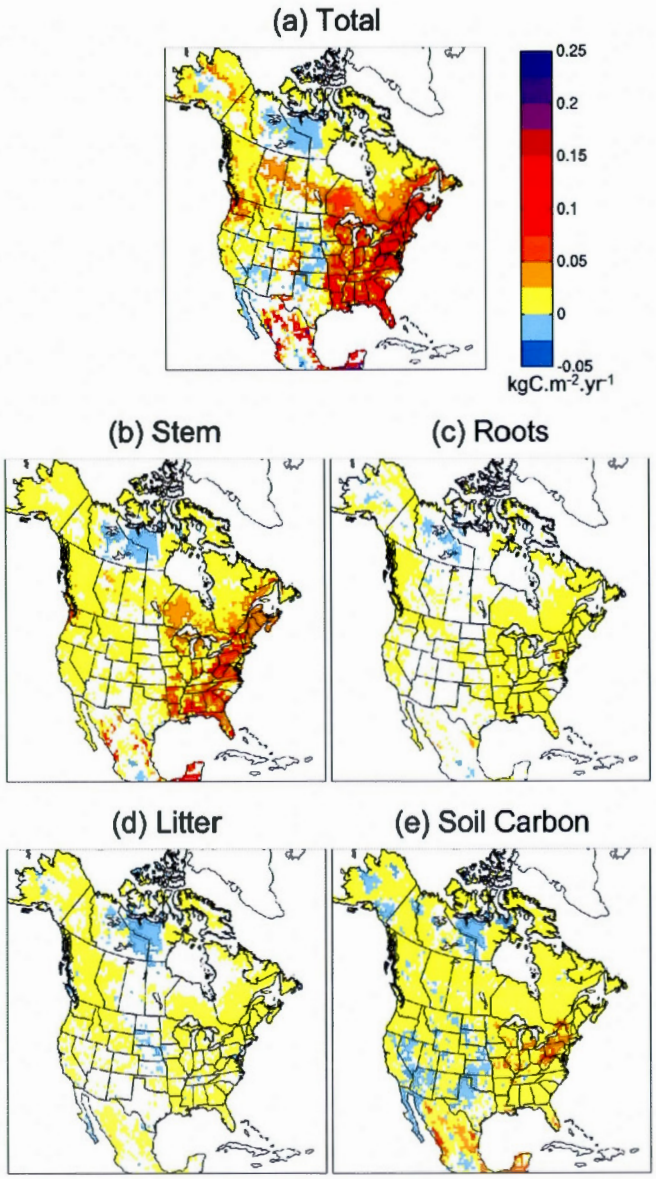

Figure 1.9 Trends in the RP_ERA simulated carbon uptake ($kgC.m^{-2}.yr^{-1}$) for the 1970 to 2001 period, for (a) the biosphere as a whole and by its different components : (b) stem, (c) roots, (d) litter and (e) soil carbon. Regions where trends are not significant are shown in white.

trend in the soil carbon pool in these regions, especially for the RP_NCEP case. The marginal decrease in soil carbon is explained by the positive trend in temperature that results in greater heterotrophic respiration rates that overwhelms the increase in NPP, causing a net loss of soil carbon. The simulated general positive trend of carbon uptake averaged over the 1970–2001 period is strongest in eastern United States, where NPP and GPP are generally the highest (Figure 1.5). The simulated trends are highest for the stem component, followed by soil carbon, roots and the litter components.

Figure 1.11 shows the simulated trends in NPP (in $gC/m^2.yr^2$) for the 1970–2001 for the RP_ERA and RP_NCEP simulations. The trend in NPP is either not significant or positive over the North American domain. Most regions that show increase in NPP are similar to those found in the observation-based study from Hicke *et al.* (2002), except the area east of the Great Lakes. Hicke *et al.* (2002) found that northeast North America shows an increasing trend in NPP from 1982 to 1998 and this is likely related to higher spring temperatures.

1.4 Summary and Conclusions

The effect of driving climate data on the simulated terrestrial carbon pools and fluxes over North America is assessed using the Canadian Terrestrial Ecosystem Model (CTEM) coupled to the Canadian Land Surface Scheme (CLASS). The offline simulations are driven with NCEP and ERA40 reanalysis data from 1958 to 2001 over North America and simulated quantities are compared with observation- and model-based estimates.

Both the NCEP and ERA40 reanalysis data differ from each other, especially in terms of summer precipitation, as well as with the observation-based CRU climate data and both reanalysis data show generally warmer temperatures also during summer. Overall, the ERA40 reanalysis data compares better with the observation-based CRU climate data than the NCEP. The observation-based GPP, LAI and woody biomass data and the model-based NPP data, that are used to validate simulated quantities, are not derived from the same source so are expected to be inconsistent with each other. The

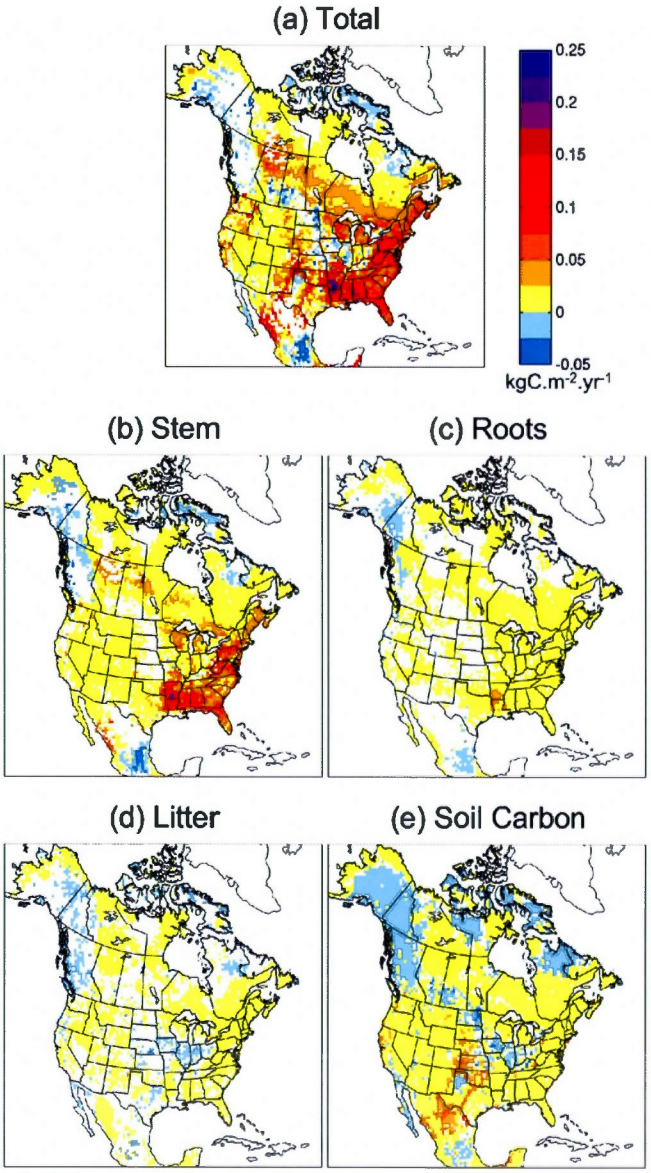

Figure 1.10 Trends in the RP_NCEP simulated carbon uptake ($kgC.m^{-2}.yr^{-1}$) for the 1970 to 2001 period, for (a) the biosphere as a whole and by its different components : (b) stem, (c) roots, (d) litter and (e) soil carbon. Regions where trends are not significant are shown in white.

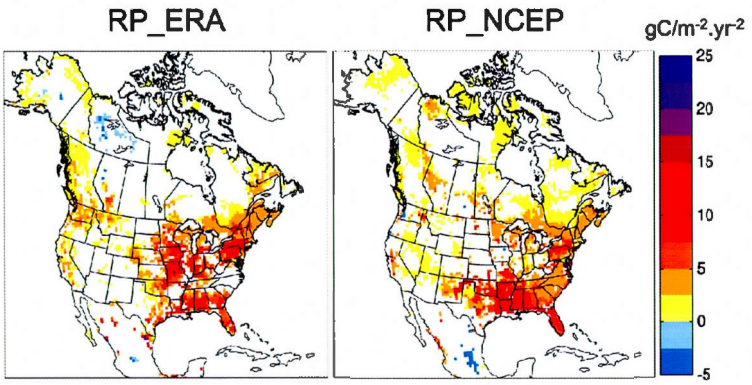

Figure 1.11 Trends in the net primary productivity (NPP, in $gC.m^{-2}.yr^{-2}$) for the 1970—2001 period for grid-cells where trends are significant at α =5% significance level for the RP_ERA (left) and RP_NCEP (right) simulations.

inconsistency between Zhao *et al.* (2005) NPP estimates and Beer *et al.* (2010) GPP estimates is reflected in large CUE values that generally do not compare well with the observation-based estimates from DeLucia *et al.* (2007).

Both the limitations in the driving climate data as well as the inconsistencies in the data used for model validation make the task of model assessment somewhat difficult. However, the simulations are able to provide broad insight into the behaviour of the CTEM model. The model is able to reproduce the broad spatial patterns of LAI, woody biomass, NPP and GPP as well their zonal distributions. The range in the simulated values of carbon use efficiency and its average value also compare reasonably well with observation-based estimates of DeLucia *et al.* (2007). Limitations, however, remain in simulated quantities. In particular, the simulated LAI is low compared to the ISLSCP satellite based estimates, although Gibelin *et al.* (2006) show that the LAI estimates in this product are higher than other satellite based estimates, especially in the boreal forest, and the model does not capture the GPP of the productive needleleaf evergreen forests along the interior of west coast of the United States. This model limitation is also obvious in the comparisons of simulated woody biomass with their observation-

based estimates. Despite its generally higher than observed woody biomass, the model is not able to simulate enough woody biomass along the United States west coast as well as in the interior British Columbia (BC). Both the interior BC and the interior west coast of the United States are characterized by drier summers and colder winters than at the coast. Results from another study under progress (Dr. Yiran Peng, CCCma, personal communication) show that, while the only needleleaf evergreen PFT of the model performs well at the coast of British Columbia, it yields lower than observed GPP in the interior of the province. These results indicate that while the broad classification of PFTs in CTEM is sufficient to capture terrestrial ecosystem process at the global scale, it is insufficient for representing continental scale processes and another needleleaf evergreen PFT is required.

The simulations are also used to assess the land carbon sink over the North American domain. Despite very different gross fluxes, the model yields fairly similar estimates of the net atmosphere-land CO_2 flux with the two forcing datasets. The simulated sink of 0.5 Pg C/yr during the 1980s and 1990s compares well with another model-based estimates during the 1980s (Pacala *et al.*, 2001) but is lower than the inversion-based estimates which vary from 0.81 to 1.26 Pg C/yr during the 1990s. This is expected since our simulations do not include land use change and the effect of nitrogen deposition. The analysis of spatial distribution of trends in simulated carbon pools and fluxes shows that the simulated carbon sink is driven primarily by NPP enhancements over eastern United States and the resulting carbon sequestration in the woody biomass. Future efforts will attempt to include land use change, which will help to quantify the contribution of cropland abandonment in eastern United States on the simulated sink.

The choice of ECMWF's ERA40 and ERA-Interim as the driving data in this study was based on how far back in time each of them went. Ideally, the spinup simulation should be performed with climate that shows minimal warming trends. Although the ERA-Interim reanalysis are available at a higher resolution, we chose ERA40 given its availability since 1958 allowing us to perform our spinup simulation with repeated 1958–1977 climate followed by the recent past simulation from 1958 to 2001. Preliminary

analysis of a simulation using ERA40 for the 1958–1978 period, followed by ERA-Interim during the 1979–2001 period, suggests similar spatial patterns (figures not shown) as in the case RP_ERA. However, the use of ERA-Interim data tends to overestimate the productivity and the biomass in areas that were already overestimated (mainly south-eastern US) in RP_ERA when compared to observations.

Our simulations do not take into account competition between PFTs and as a result the fractional coverage of PFT does not change in time. As shown by Smith *et al.* (2011), competition is important to model vegetation shifts and changing tree line which can have non-negligible effects on temperature and precipitation through biophysical feedbacks, particularly in the context of a changing climate. Work is in progress to implement competition in CTEM based on competition parameterisation of Arora and Boer (2006), and we expect to be able to use it in future simulations.

CHAPTER II

IMPACT OF DYNAMIC VEGETATION ON THE CANADIAN RCM SIMULATED CLIMATE OVER NORTH AMERICA

This chapter is presented in the format of a scientific article that has been submitted to the peer-reviewed journal *Climate Dynamics*. The design of the research and its performance together with the analysis of data and the redaction of this article are entirely based on my work, with Dr. Sushama involved in the supervision of all these tasks and Dr. Diana Verseghy giving constructive comments on the content of the manuscript. The detailed reference is :

Garnaud, C., Sushama, L, and Verseghy, D."Impact of dynamic vegetation on the Canadian RCM simulated climate over North America". Submitted to Climate Dynamics.

Abstract

Biosphere-atmosphere interactions play a very important role in modulating regional climate. To capture these bi-directional interactions, a dynamic vegetation model, the Canadian Terrestrial Ecosystem Model (CTEM), has been implemented in the fifth generation of the Canadian Regional Climate Model (CRCM5). CTEM can grow vegetation from bare ground and includes processes of photosynthesis, autotrophic and heterotrophic respiration, phenology, turnover, mortality and allocation. This study focuses on assessing the impact of dynamic vegetation, i.e. CTEM, on the CRCM5 simulated climate over North America. This is achieved by comparing two CRCM5 simulations – one with dynamic vegetation and the other with static vegetation, driven by ECMWF reanalysis data (ERA40 and ERA-Interim) at the lateral boundaries, for the 1971–2010 period. Comparison of simulated vegetation attributes, temperature and precipitation in both simulations to those observed indicates that introduction of dynamic vegetation improves the performance of CRCM5 in some regions, although it introduces new biases

in other regions, which are related to the underestimation of leaf area index (LAI). Dynamic vegetation enhances biosphere-atmosphere interactions, which are reflected in the higher values of correlation between atmosphere and biosphere variables. Dynamic vegetation also introduces long-term memory in CRCM5, estimated via lagged correlations between precipitation/temperature and LAI. Improved biosphere-atmosphere interactions and long-term memory in the CRCM5 simulation with dynamic vegetation leads to better interannual variability, particularly noticeable in the biosphere and atmosphere states during anomalously wet and dry years. This study thus provides useful insights related to the added value of dynamic vegetation in CRCM5 as well as the nature and variability of biosphere-atmosphere interactions over North America.

2.1 Introduction

It is well recognized that climate has a strong influence on the distribution and characteristics of terrestrial ecosystems (Woodward, 1987; Stephenson, 1990; Prentice *et al.*, 1992; Zhao *et al.*, 2011). In turn, vegetation forcings on climate, through surface characteristics such as albedo and roughness length, have been proven to be important by previous studies based on observations (Liu *et al.*, 2006; Notaro *et al.*, 2006; Wang *et al.*, 2014) and by climate model simulations using static vegetation, i.e. vegetation with prescribed characteristics (Snyder *et al.*, 2004; Dubreuil *et al.*, 2012). However, the study of vegetation impacts on climate using climate models with static vegetation is limited by the fact that these models cannot be expected to adequately capture long-term evolution of vegetation attributes and variability, particularly in the context of changing climate. Pielke *et al.* (1998) suggest that terrestrial ecosystems could significantly influence atmospheric processes on short-term (biophysical pathway) as well as on long-term (biogeochemical and biogeographical pathways) timescales, confirming the important role of the biosphere in climate simulations.

Dynamic vegetation models (DVMs) are increasingly being used for applications in climate models to improve the representation of biosphere-atmosphere interactions (Peng, 2000; Cox, 2001; Quillet *et al.*, 2010; den Hoof *et al.*, 2011). A DVM takes into account different terrestrial carbon pools (stems, roots, leaves) and the changes in the terrestrial ecosystem, like vegetation structure and composition, which affect these pools. In these models, vegetation is represented as patches of plant functional types (PFTs) such as

crops, grass, deciduous trees, and evergreen trees, with prognostic properties : leaf area index, stem area index, vegetation height, rooting depth, etc. The vegetation attributes change in response to changes in climate in a DVM. These changes include those affecting the biogeochemical, biogeophysical and hydrological cycles, and more specifically alterations in the biomass, productivity and energy fluxes. Consequently, climate models with DVMs are able to simulate vegetation-atmosphere interactions more realistically, particularly in the long term.

Wramneby *et al.* (2010) studied vegetation-climate feedbacks over Europe under future greenhouse warming using the Rossby Centre's Regional Climate Model (RCM) RCA-GUESS, which includes the dynamic vegetation model LPJ-GUESS (Smith *et al.*, 2001), based on two simulations with and without feedbacks of vegetation dynamics. They found that vegetation feedbacks on the climate are small compared to the radiative forcing of increased global CO_2 concentrations, but may alter warming projections locally, regionally and seasonally compared to the simulation lacking a dynamic vegetation module. Similarly, using the University of Wisconsin's fully coupled global atmosphere–ocean–land Fast Ocean Atmosphere Model (FOAM) with dynamic vegetation model LPJ, Notaro *et al.* (2007) showed that, although the majority of the projected future warming is associated with the radiative forcing of rising CO_2, the vegetation physiological forcing augments the warming by weakening the hydrological cycle due to reduced evapotranspiration, particularly for tropical forests. Using the Hadley Centre's HadCM3LC with the DVM TRIFFID, Pinto *et al.* (2009) demonstrated that the lifting condensation level over the Amazon in future conditions could be 1000m higher compared to current climate due to reduced vegetation cover, and therefore decreased evapotranspiration, leading to low atmospheric humidity resulting in increased sensible heat flux (SHF) and therefore warmer temperatures.

Several other studies have looked at the effect of vegetation dynamics on the climate variability. Hughes *et al.* (2006), using the Hadley Centre GCM including TRIFFID, found that the variability of the vegetation structure, which is determined by environmental conditions through photosynthesis, and feedbacks can dampen or amplify

atmospheric variability through a shift in the response timescale. Delire *et al.* (2011) using two coupled atmosphere-vegetation models, CCM3-IBIS from the National Center for Atmospheric Research (NCAR) and LMDz-ORCHIDEE from the Institut Pierre Simon Laplace (IPSL), demonstrated that vegetation dynamics introduces a long-term memory into the climate system by slowly modifying the physical characteristics of the vegetated surface. Furthermore, they found that phenology alone could enhance the variability of the climate system.

Similarly to most of the existing state-of-the-art climate models, both GCMs and RCMs, the fifth generation of the Canadian RCM (CRCM5) (Martynov *et al.*, 2013; Separovic *et al.*, 2013) is evolving to include a dynamic vegetation module. The land surface scheme used in CRCM5 is the latest version of the Canadian LAnd Surface Scheme (CLASS, version 3.5) (Verseghy, 1991, 2011; Verseghy *et al.*, 1993). CLASS recognizes four vegetation types : broadleaf, needleleaf, crops and grass. Vegetation is assumed static in CLASS. The dynamic vegetation model CTEM (Canadian Terrestrial Ecosystem Model : Arora, 2003; Arora and Boer, 2003, 2005), developed at the Canadian Centre for Climate Modelling and Analysis (CCCma), has been implemented in CRCM5. In this framework, CTEM simulates the vegetation biomass as a function of climate, which is used by CLASS to compute water and energy fluxes at the land-atmosphere interface, allowing a two-way interaction between vegetation and regional climate. The CLASS/CTEM framework has been used in offline simulations and validated against site-specific biophysical and biogeochemical measurements from flux towers (Li and Arora, 2011), as well as over all of North America, as detailed in Garnaud *et al.* (2014a). The latter compared two simulations driven by different reanalysis products over North America. They found that the simulated biosphere is relatively sensitive to the driving data, as most simulated carbon pools and fluxes showed important differences, particularly over eastern North America, primarily due to the differences in precipitation and temperature in the driving reanalysis products. Nonetheless, Garnaud *et al.* (2014a) concluded that the simulated biosphere in offline CLASS/CTEM simulations responds adequately to climate change, such as rising CO_2 and temperatures.

The main objective of this study is to assess the impact of dynamic vegetation on the CRCM5-simulated climate over North America, particularly the role played by biosphere-atmosphere interactions in modulating the interannual the climate variability. This is achieved by comparing two experiments with CRCM5 – one with static vegetation (i.e. CLASS only) and the other with dynamic vegetation (i.e. CLASS/CTEM), for the 1971–2010 period. The paper is organized as follows. Section 2.2 gives a brief overview of the model along with a description of the experimental set-up and methods used. Section 2.3 presents analysis of the RCM simulations, with and without dynamic vegetation, focusing on the mean state of the simulated climate, biosphere-atmosphere interactions quantified using correlations, long-term memory of the atmosphere and biosphere through lagged correlations, and interannual variability including the state of the biosphere and atmosphere during anomalously dry and wet years. A brief summary and conclusions are given in section 2.4.

2.2 Model, Experiments and Methods

2.2.1 The Canadian Regional Climate Model

The regional climate model used in this study, CRCM5, is based on a limited-area version of the Global Environment Multiscale (GEM) model used for numerical weather prediction at Environment Canada (Côté *et al.*, 1998). GEM employs semi-Lagrangian transport and a (quasi) fully implicit marching scheme. In its fully elastic nonhydrostatic formulation (Yeh *et al.*, 2002), GEM uses a vertical coordinate based on hydrostatic pressure (Laprise, 1992). The following GEM parameterisations are used in CRCM5 : deep convection following Kain and Fritsch (1990), shallow convection based on a transient version of the Kuo (1965) scheme (Belair *et al.*, 2005), large-scale condensation (Sundqvist *et al.*, 1989), correlated-K solar and terrestrial radiation (Li and Barker, 2005), subgrid-scale orographic gravity-wave drag (McFarlane, 1987), low-level orographic blocking (Zadra *et al.*, 2003), and turbulent kinetic energy closure in the planetary boundary layer and vertical diffusion (Benoit *et al.*, 1989; Delage and Girard, 1992;

Delage, 1997).

The land surface scheme CLASS in CRCM5 models three soil layers, 0.1 m, 0.25 m and 3.75 m thick in its standard formulation, corresponding approximately to the depth influenced by the diurnal cycle, the rooting zone and the annual variations of temperature, respectively. CLASS includes prognostic equations for energy and water conservation for the three soil layers and a thermally and hydrologically distinct snowpack where applicable (treated as a fourth variable-depth layer). The thermal budget is performed over the three soil layers, but the hydrological budget is done only for layers above the bedrock. In order to simply mimic subgrid-scale variability, CLASS adopts a "pseudo-mosaic" approach and divides the land fraction of each grid cell into a maximum of four sub-areas : bare soil, vegetation, snow over bare soil and snow with vegetation. The energy and water budget equations are first solved for each sub-area separately and then averaged over the grid cell, using spatially varying structural attributes and physiological properties of the four CLASS PFTs (needleleaf trees, broadleaf trees, crops and grass) derived from high-resolution land cover datasets. These structural attributes include albedo, leaf area index (LAI), roughness length, canopy mass and rooting depth.

The dynamic vegetation model CTEM that has recently been implemented in CRCM5 is a process-based ecosystem model (Arora, 2003; Arora and Boer, 2003, 2005, 2006; Li and Arora, 2011) designed to simulate the terrestrial carbon cycle. It is able to grow vegetation from bare ground and to simulate several vegetation structural attributes such as leaf area index, vegetation height, root distribution and canopy mass. It includes processes such as photosynthesis, autotrophic respiration, heterotrophic respiration, phenology, turnover, allocation, fire and land-use change. CTEM simulates two dead carbon pools – litter and soil organic carbon – and three live vegetation pools – stems, leaves and roots. Terrestrial ecosystem processes in CTEM are modeled for nine different plant functional types (PFTs) : evergreen and deciduous needleleaf trees, broadleaf evergreen and cold and drought deciduous trees, and C_3 and C_4 crops and grasses. The manner in which CLASS and CTEM interact is explained in the following section.

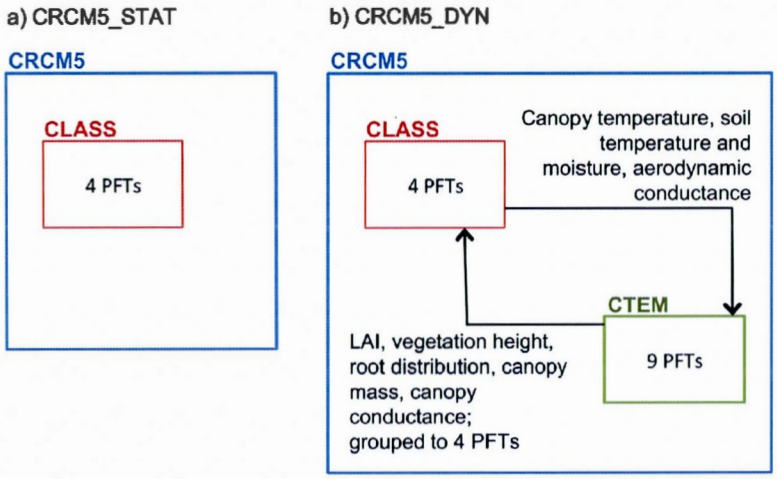

Figure 2.1 Schematic diagram demonstrating the representation of vegetation PFTs in (a) CRCM5_STAT and (b) CRCM5_DYN simulations. The interactions between CTEM and CLASS are also shown in CRCM5_DYN. PFT stands for Plant Functional Type, and LAI for Leaf Area Index

2.2.2 Experiments

As discussed earlier, this study investigates the effects of vegetation dynamics on the regional climate and its variability over North America. Two simulations are performed for the 1958–2010 period at 0.5° resolution; these simulations are forced by the European Centre for Medium range Weather Forecast's (ECMWF) ERA40 reanalysis data (Uppala *et al.*, 2005) for the 1958–1978 period and by ERA-Interim reanalysis data (Dee *et al.*, 2001) for the 1979–2010 period at the lateral boundaries. The ERA40 reanalysis is available for the period 1957–2001 at 2.5° (~250 km) resolution. The ERA-Interim reanalysis is available from 1979 to the present day at a resolution of 1.5°.

The first simulation uses static vegetation and the second uses dynamic vegetation (i.e. CTEM; Fig. 2.1). These two simulations will be referred to hereafter as CRCM5_STAT and CRCM5_DYN, respectively. The two simulations are run at a 20-minute time step and are forced with observed CO_2 concentrations from the NASA Earth Sciences Divi-

sion (Hansen and Sato, 2001, 2004). Thus, the carbon cycle feedbacks are not included. The soil type, i.e. percentage of sand and clay, for the 3 layers modeled in CLASS is taken from (Webb *et al.*, 1991). The grid cell fractional coverage of nine PFTs, shown in Fig. 2.2, is obtained from the HYDE 2 database (Arora and Boer, 2010) for crops and from (Wang *et al.*, 2006) for other PFTs. The land fractional cover is specified at its 1960 values. It should be noted that in CRCM5_DYN, even though the geographical distribution of PFTs is fixed, the vegetation attributes (LAI and carbon pools) are simulated as dynamic functions of driving climate. The sea surface temperatures (SST) and sea ice concentrations (SIC) in the CRCM5 simulations are prescribed from AMIP2 (Atmospheric Model Intercomparison Project; Taylor *et al.*, 2000) for the 1958–1978 period and from ERA-Interim (Dee *et al.*, 2001) for the 1979–2010 period. Consequently, the differences in simulated climate between CRCM5_STAT and CRCM5_DYN are due only to the differences in interactions between the vegetation and the atmosphere. Initial conditions of soil and vegetation state were obtained by running CLASS/CTEM offline for 300 years driven by repeated temperature, humidity and wind variables from a 20-year CRCM5 simulation (with CTEM, and initialized using data from Garnaud *et al.* (2014a)), until equilibrium conditions were obtained, using a fixed 1765 CO_2 concentration during the first 107 years and a transient 1765-1957 CO_2 concentration for the following 193 years. The vegetation parameters prescribed in CRCM5_STAT (albedo, max and min LAI, rooting depth, etc.) are derived from the biosphere state during the last 50 years of the above-mentioned 300-year offline simulation.

CRCM5_STAT vs. CRCM5_DYN

The most important differences between CRCM5_STAT and CRCM5_DYN, i.e. simulations with static and dynamic vegetation respectively, relate to the canopy resistance and photosynthesis, phenology, root distribution, canopy mass and vegetation height.

Photosynthesis and canopy conductance are of crucial importance in vegetation modelling. In CRCM5_STAT, the canopy conductance ($g_c = 1/r_c$) formulation handled in CLASS is similar to that of Schulze *et al.* (1995), where the canopy resistance (r_c) is

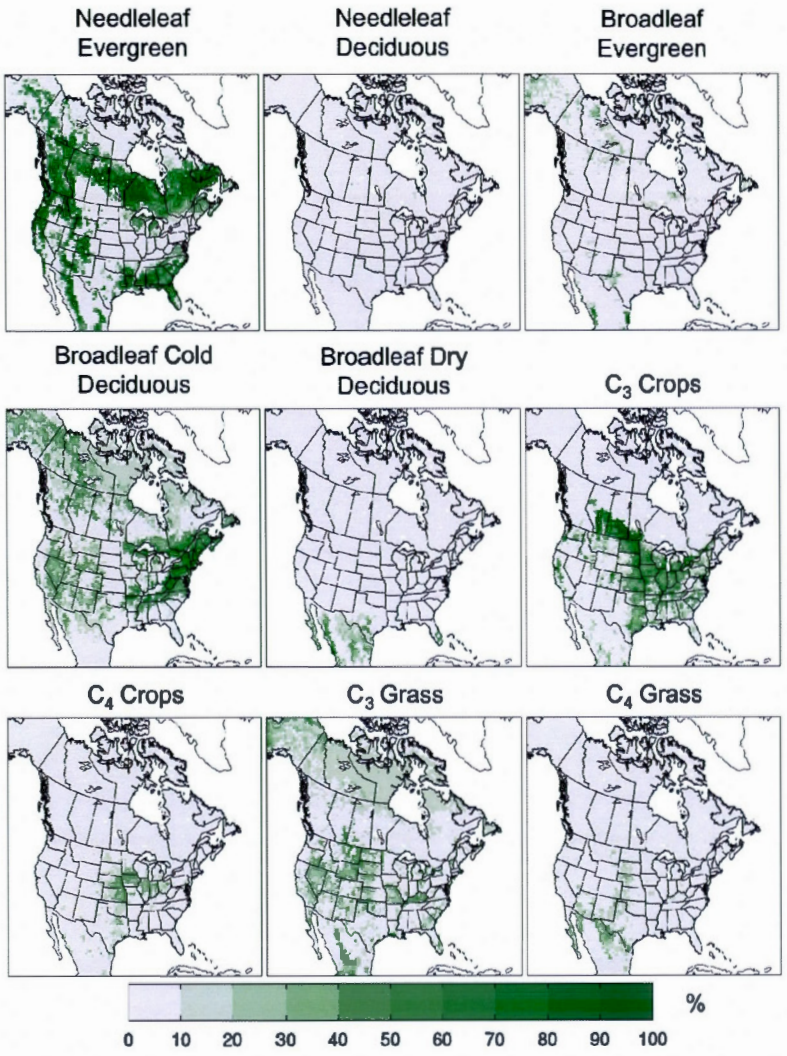

Figure 2.2 Fractional coverage (%) of the nine Plant Functional Types (PFT) considered in CTEM for the North American study domain

expressed as a function of minimum stomatal resistance (r_{min}) and a series of environmental dependences, such as incoming solar radiation, air temperature, vapour pressure deficit, and soil moisture suction. Thus, the effect of atmospheric CO_2 concentration on canopy resistance is not explicitly modeled in this formulation.

In CRCM5_DYN, CTEM models photosynthesis, as described in details in Arora (2003). In addition to the environmental variables cited above, the CTEM formualtion includes the effect of atmospheric CO_2 concentration on stomatal conductance. This is essential to simulate the physiological effects of increasing CO_2 amounts on stomatal conductance, and thus canopy resistance, in climate simulations. The photosynthesis sub-module used in CTEM is based on the biochemical approach (Farquhar *et al.*, 1980; Collatz *et al.*, 1991, 1992) with some minor differences. The photosynthesis rate, A, is co-limited by assimilation rates based on the photosynthetic enzyme Rubisco, the amount of available light, and the photosynthetic product transport capacity. CTEM can also simulate the effect of soil moisture stress on photosynthesis in order to account for soil moisture stress via stomatal closure. Net canopy photosynthesis rate, A_n, is then used to estimate canopy conductance. A_n is obtained by subtracting canopy leaf maintenance respiration from the canopy photosynthesis rate (Arora, 2003).

With respect to phenology, in CRCM5_STAT, CLASS adopts an approach where the air temperature and the temperature of the top soil layer determine leaf onset and offset, as described in Verseghy (2011). A threshold temperature of 2°C is used and when this threshold is exceeded the LAI increases linearly from a specified minimum to specified maximum value in certain number of days : two months for needleleaf trees and one month for broadleaf trees. With respect to crops, the Earth is divided into 10° latitude bands, and as specified in Verseghy (2011), the beginning of crop growth and the end of harvest are specified for each band as occurring on certain days of the year. It is assumed that crops take two months to reach maturity, and that one month elapses between the time that senescence begins and the time that harvest is over. Since the annual variations in height and leaf area index of grass can be considered as negligible, its height and LAI are assigned to a maximum value throughout the year. Thus, seasonality is modeled but

not long-term variations in canopy cover or vegetation structure.

In CRCM5_DYN, CTEM simulates the leaf onset through a carbon benefit approach, and the leaf offset is initiated by unfavorable environmental conditions that stress the plant and imply carbon loss. These unfavorable conditions include shorter day length, cooler temperatures, and drier soil moisture conditions. These processes are fully described in Arora and Boer (2005). In CTEM, four plant growth states determine the plant behavior and allocation patterns, as summarized in Table 2 of Arora and Boer (2005). These are maximum growth, normal growth, leaf-fall/crop-harvest and dormancy/no-leaves. During maximum growth, for trees and crops, all net primary productivity is allocated to leaves. For grass, the allocation is to leaves and roots for structural stability reasons. During normal growth, the allocation is shared between leaves, stem (if applicable) and roots. During leaf fall and crop harvest, the allocation to leaves ceases but continues for stem and roots. During dormancy/no-leaf state, no allocation occurs in the absence of CO_2 uptake. The set of conditions used to trigger transition from one plant state to another for each PFT in CTEM are described in Arora and Boer (2005).

In CRCM5_STAT, CLASS calculates the vegetation height and the canopy mass as a function of a PFT-dependent roughness length for momentum at vegetation maturity and maximum value of canopy mass, respectively. For trees, these values are invariant; for crops and grass, the vegetation effective height and the canopy mass vary annually with snow depth and growth stage. The rooting depth remains at its PFT-dependent maximum value for trees and grass; for crops, it is further corrected for growth stage.

In CRCM5_DYN, CTEM allocates positive net primary production (NPP) between leaf, stem, and root components, which increases their biomass, while negative NPP results in the decrease of component biomass because of respiration. As a result of these allocation processes, the vegetation biomass may vary diurnally. CTEM then uses the simulated leaf biomass to calculate the LAI, which is passed on to CLASS and used in energy and water balance calculations over the vegetated fraction of the grid cell. The root biomass is converted to a rooting depth and root distribution profile that are then used

to estimate the fraction of roots in each soil layer required for calculating transpiration in CLASS. The aboveground canopy mass from CTEM is used to estimate the canopy heat capacity.

In CRCM5_DYN, the vegetation structural attributes of CTEM's nine PFTs are clustered to four PFTs (needleleaf trees, broadleaf trees, crops and grass) when they are passed on to CLASS. CLASS and CTEM's photosynthesis sub-module that simulates the fast biophysical processes, such as photosynthesis, canopy conductance and leaf respiration, operates at a 30 minutes timestep while the rest of CTEM runs at a daily timestep.

2.2.3 Methods of model output evaluation and analysis

Prior to studying the impact of dynamic vegetation on the simulated climate over North America, the climate and biosphere simulated by CRCM5_STAT are compared to observations in order to assess the model performance and to help identify biases. CRCM5_STAT simulated temperature and precipitation are compared to gridded observational datasets available from the Climate Research Unit (CRU) (Mitchell and Jones, 2005) and from the University of Delaware (UDEL) (Willmott and Matsuura, 1995). The CRU TS 2.1 dataset covers the period 1901–2002 at a monthly temporal resolution and has a spatial resolution of 0.5°. The UDEL V3.01 dataset is composed of monthly values from 1901 to 2010 with a 0.5° global coverage. The simulated biosphere is evaluated against the observation-based green leaf area index product from the International Land Surface Climatology Project Initiative (ISLSCP II) FASIR-adjusted NDVI Biophysical Parameter Fields measured by the satellite mounted AVHRR sensor (Los *et al.*, 2000; Hall *et al.*, 2006; Sietse, 2010). This monthly global dataset is available for the 1982–1998 period at 1°x1° resolution. To limit the impact of initial conditions on results, the analysis presented in this study focuses on the 1971–2010 period. The impact of dynamic vegetation on the simulated climate over North America is then investigated by comparing CRCM5_DYN and CRCM5_STAT, particularly with respect to biosphere-atmosphere interactions.

To assess the strength of the simulated biosphere-atmosphere interactions, statistical analyses are performed. First Pearson correlation coefficients are computed to determine the strength of the linear relationships between maximum leaf area index, precipitation, temperature, and sensible and latent heat fluxes (SHF and LHF) during spring and summer seasons. Where required, this is followed by a path analysis (Pinto *et al.*, 2009) to decompose the Pearson correlations into direct (β_i) and indirect (β_j) effects of two independent variables (x_i and x_j) on a dependent variable (y), using the relation :

$$r_i = \beta_i + \beta_j c(x_i, x_j), \tag{2.1}$$

for $i = 1, 2$ and $i \neq j$, where r_i is the Pearson correlation coefficient between x_i and y, β_i is the standardized coefficient of x_i estimated from multiple linear regression and $c(x_i, x_j)$ is the correlation coefficient between x_i and x_j. The indirect effect can be seen as the effect of x_j on y resulting from interaction with x_i.

Any long-term memory introduced by vegetation dynamics is studied through lag correlations. Also, the interannual variability of selected biosphere and climate characteristics in both simulations is investigated using the coefficient of variation (i.e. the ratio of the standard deviation to mean). In connection with the interannual variability, modeled atmosphere and biosphere states for observed anomalously dry/hot and wet years are also studied. To this end, the year 1988, which was a very dry and warm year over large regions of the United States, covering the central and eastern parts, is selected. The year 1993, which was an anomalously wet year over approximately the same region, is also considered. For the dry and warm year of 1988, the simulated number of hot days (NHD) is compared to that observed. Using a similar approach to Fischer *et al.* (2007), NHD is defined as the number of days with maximum temperature exceeding the long term (1981–2010) 90th percentile daily maximum temperatures, calculated for each month of the summer (JJA) season. Since no single high-resolution dataset of daily temperature is available over the study domain, two observation datasets, covering Canada and the USA, were used. The gridded observational dataset over Canada

(Hopkinson *et al.*, 2011) is generated from daily observations at Environment Canada climate stations using a thin plate smoothing spline surface fitting method. The gridded meteorological data from the University of Washington (UW; Maurer *et al.*, 2002) is used over the USA. The response of the biosphere in CRCM5_STAT and CRCM5_DYN to the anomalous amounts of precipitation and temperatures for the studied dry and wet years is also explored in detail.

2.3 Results and Discussion

2.3.1 CRCM5_STAT evaluation

The mean seasonal temperature and precipitation modeled by CRCM5_STAT for the 1971–2010 period are compared with those from the CRU and UDEL datasets in Fig. 2.3. It should be noted that there are large differences between CRU and UDEL datasets, especially in the northern high latitudes where observations are scarce. In winter (DJF) and spring (MAM), CRCM5_STAT exhibits a warm bias over Canada, which is more pronounced when compared to the CRU data. From Mexico to western US, a cold bias persists most of the year. The comparison with the UDEL dataset also shows a cold bias along the east coast of the US that is more widespread during summer (JJA) and autumn (SON). CRCM5_STAT generally overestimates precipitation. There is a wet bias over the Canadian West Coast that is strongest in winter and autumn, and weakest in summer. A wet bias is also noticeable over large parts of central and eastern US in winter, and it extends over Canada in spring. Since CRCM5_STAT is driven by ERA-40/ERA-Interim, the so-called perfect boundary conditions, these biases, generally referred to as performance errors, are related to the internal dynamics and physics of the model.

The mean annual and summer values of LAI from CRCM5_STAT are compared to the ISLSCP II data for the 1982–1998 period in Fig. 2.4. With respect to the annual mean LAI, though the general spatial pattern is reasonably well captured, CRCM5_STAT tends to overestimate the LAI over central and western US, and over north-eastern

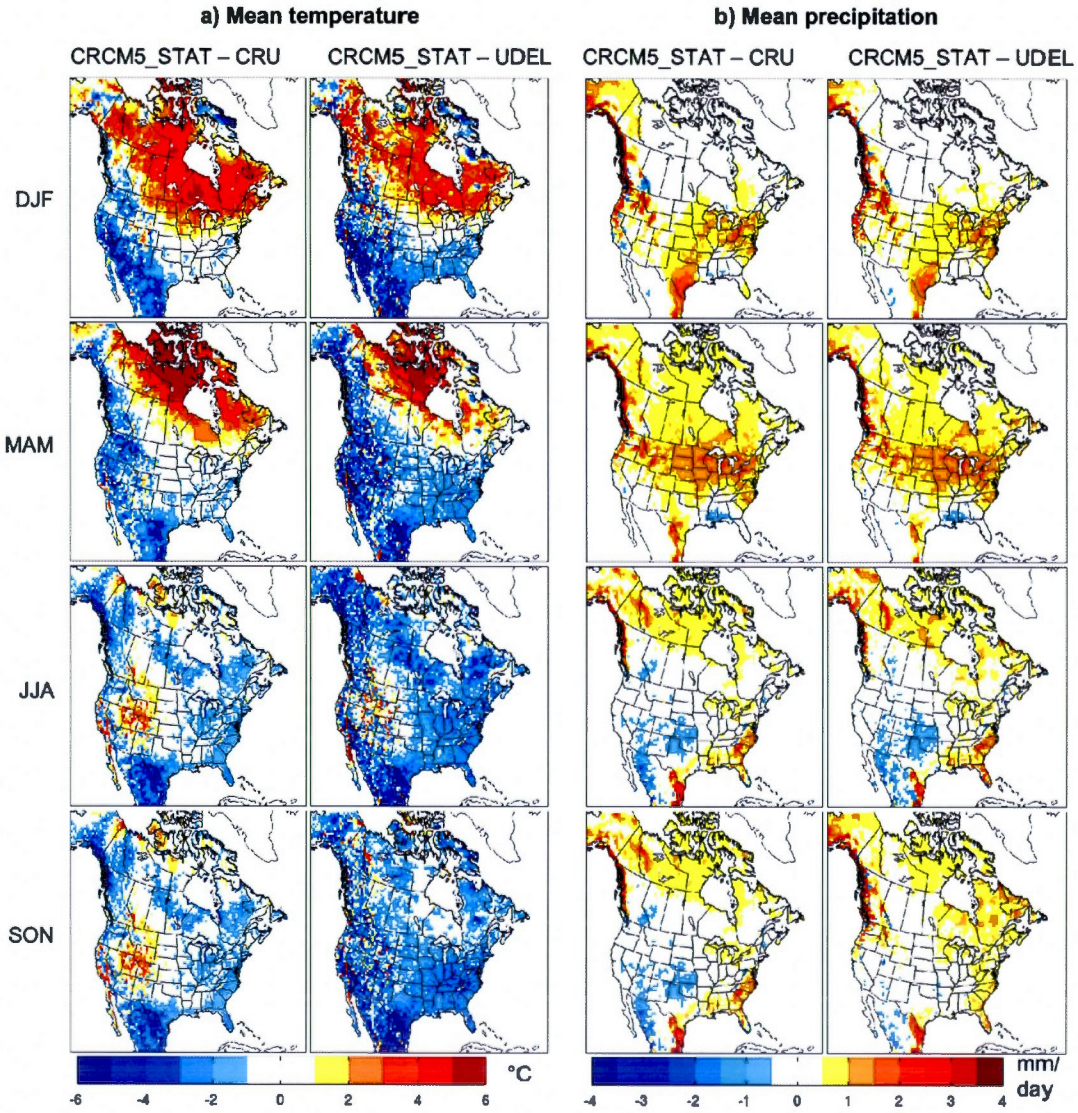

Figure 2.3 Differences in mean seasonal (a) temperature (°C) and (b) precipitation (mm/day) between CRCM5_STAT and CRU (columns 1 and 3) and between CRCM5_STAT and UDEL (columns 2 and 4) for the 1971–2010 period

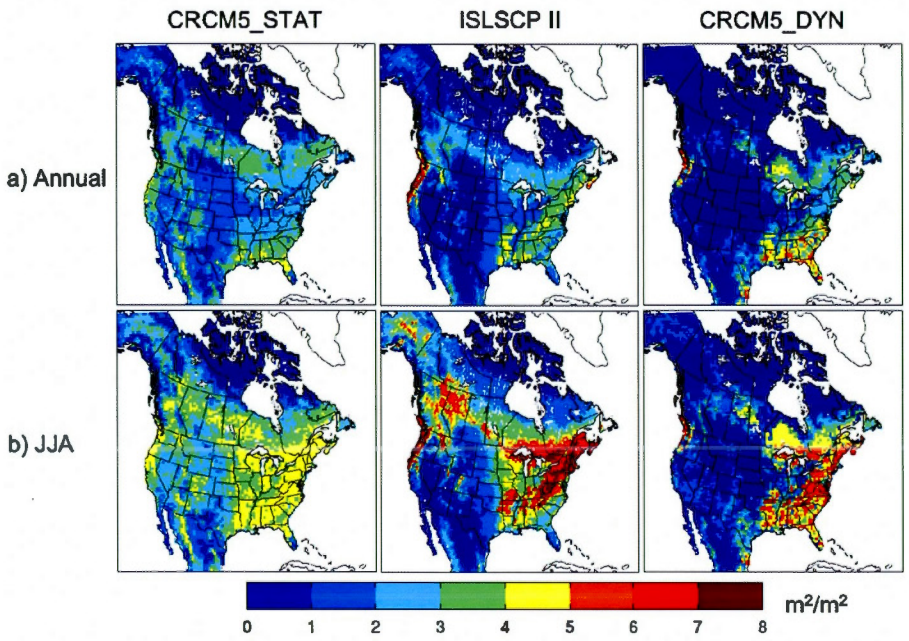

Figure 2.4 Spatial plots of the mean (a) annual and (b) summer LAI (m^2/m^2) (1982–1998) for CRCM5_STAT (1^{st} column), CRCM5_DYN (3^{rd} column) and the ISLSCPII data (2^{nd} column)

Canada, where most of the vegetation consists of crops and/or grass in the model. LAI is underestimated along the central West Coast. Since the annual LAI is an average of all seasons, Fig. 2.4b focuses more specifically on the summer season, where the overestimation over central and western US is more pronounced. There is also a strong underestimation of LAI over eastern US and southeastern Canada, which are mainly covered by broadleaf trees. Underestimation of LAI along the central West Coast is still present. These PFT-specific biases are probably due to the formulation of the vegetation attributes in CLASS, particularly the LAI. Furthermore, it is not possible to make direct linkages with precipitation and temperature, as interannual variations in climate do not affect the prescribed vegetation attributes in CRCM5_STAT.

2.3.2 Mean climate : CRCM5_STAT vs. CRCM5_DYN

Both CRCM5_STAT and CRCM5_DYN simulations have the same grid cell fractional vegetation coverage (Fig. 2.2). However, the vegetation state and its evolution are different in the two simulations, as discussed in section 2.2.2. This results in dissimilarities in the simulated LAI. When looking at the annual mean LAI simulated by CRCM5_DYN (Fig. 2.4), there is an overall improvement over eastern North America compared to CRCM5_STAT, but not over western Canada, where the boreal forest is underestimated by CRCM5_DYN. However, the LAI along the central West Coast is much improved, which could come from an LAI-precipitation positive feedback since CRCM5_DYN has more precipitation than CRCM5_STAT in this area, as seen in Fig. 2.5a. There is a slight overestimation of LAI over southeast US in CRCM5_DYN. More specifically, during summer, CRCM5_DYN does a better job compared to CRCM5_STAT at portraying the LAI over eastern North America, although it is still underestimated.

The underestimation of LAI in CRCM5_DYN over the western boreal forest is clearly visible for summer. This could be due to a negative LAI-temperature feedback in spring. Comparison of CRCM5_DYN and CRCM5_STAT in Fig. 2.5b shows that CRCM5_DYN simulates much cooler temperatures in spring over the boreal region, which may lead to a lower annual and summer LAI by delaying the annual increase in LAI of evergreen needleleaf trees. It is worth noting that, in Garnaud *et al.* (2014a), ERA40- and NCEP-driven CLASS/CTEM offline simulations showed a similar underestimation of LAI in the western boreal forest. Also, results from Peng *et al.* (2014) show that, while the needleleaf evergreen PFT of the model performs well for the coast of British Columbia, it yields lower than observed GPP in the interior of the province. This is due to the colder and drier climate in the interior of British Columbia, to which CTEM's needleleaf evergreen trees are not adapted. These results indicate that while the broad classification of PFTs in CTEM is sufficient to capture terrestrial ecosystem process at the global scale, it is inadequate for representing regional scale processes and another needleleaf evergreen PFT is probably required, as suggested by Peng *et al.* (2014). However, it must

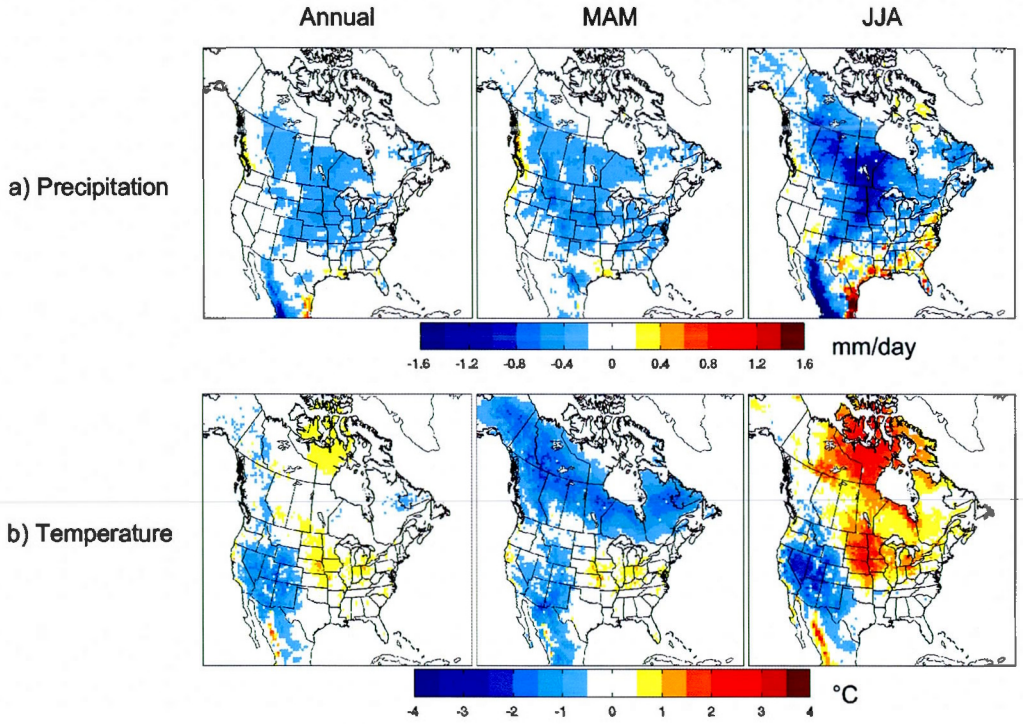

Figure 2.5 Differences in the annual (1^{st} column), spring (MAM; 2^{nd} column) and summer (JJA; 3^{rd} column) mean (a) precipitation (mm/day) and (b) temperatures (°C) between CRCM5_DYN and CRCM5_STAT for the 1971–2010 period

be noted that there are large uncertainties in the observation datasets. For example, Gibelin *et al.* (2006) showed that the ISLSCP II LAI is higher than other satellite-based estimates, especially for the boreal forest. Garrigues *et al.* (2008) also showed that LAI datasets derived from remote sensing data all have their weaknesses, especially over forests. The underestimation of LAI over central and eastern North America is mainly due to the weak representation of C_3 crops in CTEM, and this bias was also reported in Garnaud *et al.* (2014a), but it is probably amplified by the lower precipitation in CRCM5_DYN over central North America (Fig. 2.5a). On the contrary, the LAI of crops is overestimated in CRCM5_STAT compared to observations, thus creating large differences between the two simulations.

The LAI is the vegetation characteristic that has the largest impact on the biosphere-atmosphere interactions, and is thus the best characteristic to describe the state of the biosphere with respect to surface energy and water fluxes (Delire *et al.*, 2004). Therefore, one could assume that the large differences in the LAI between CRCM5_STAT and CRCM5_DYN would lead to differences in climate, especially during the growing season. Figure 2.6 shows the differences in the mean temperature and precipitation (columns a and b, respectively) between CRCM5_DYN and the CRU and UDEL datasets during the 1971–2010 period. As shown in Fig. 2.5b, the largest differences between CRCM5_DYN and CRCM5_STAT in temperature occur in spring and summer. A comparison of Fig. 2.3a with Fig. 2.6a shows that CRCM5_DYN tends to decrease the overestimation of the temperature over Canada in CRCM5_STAT in the high latitudes in spring, but increases the cold bias over Mexico and southwest US.

Figure 2.7 shows the seasonal differences in LAI, albedo, SHF and LHF between the two simulations CRCM5_DYN and CRCM5_STAT for the 1971–2010 period; values are shown only for grid cells where the differences are statistically significant at 5% significance level, estimated using Student's t-test. During spring season in CRCM5_DYN, for the mid- to high-latitudes, cooler temperatures lead to greater snow depth (figure not shown), partially masking the vegetation (particularly grass) and thus reducing the exposed LAI compared to CRCM5_STAT (Fig. 2.7a), resulting in higher albedo, as shown

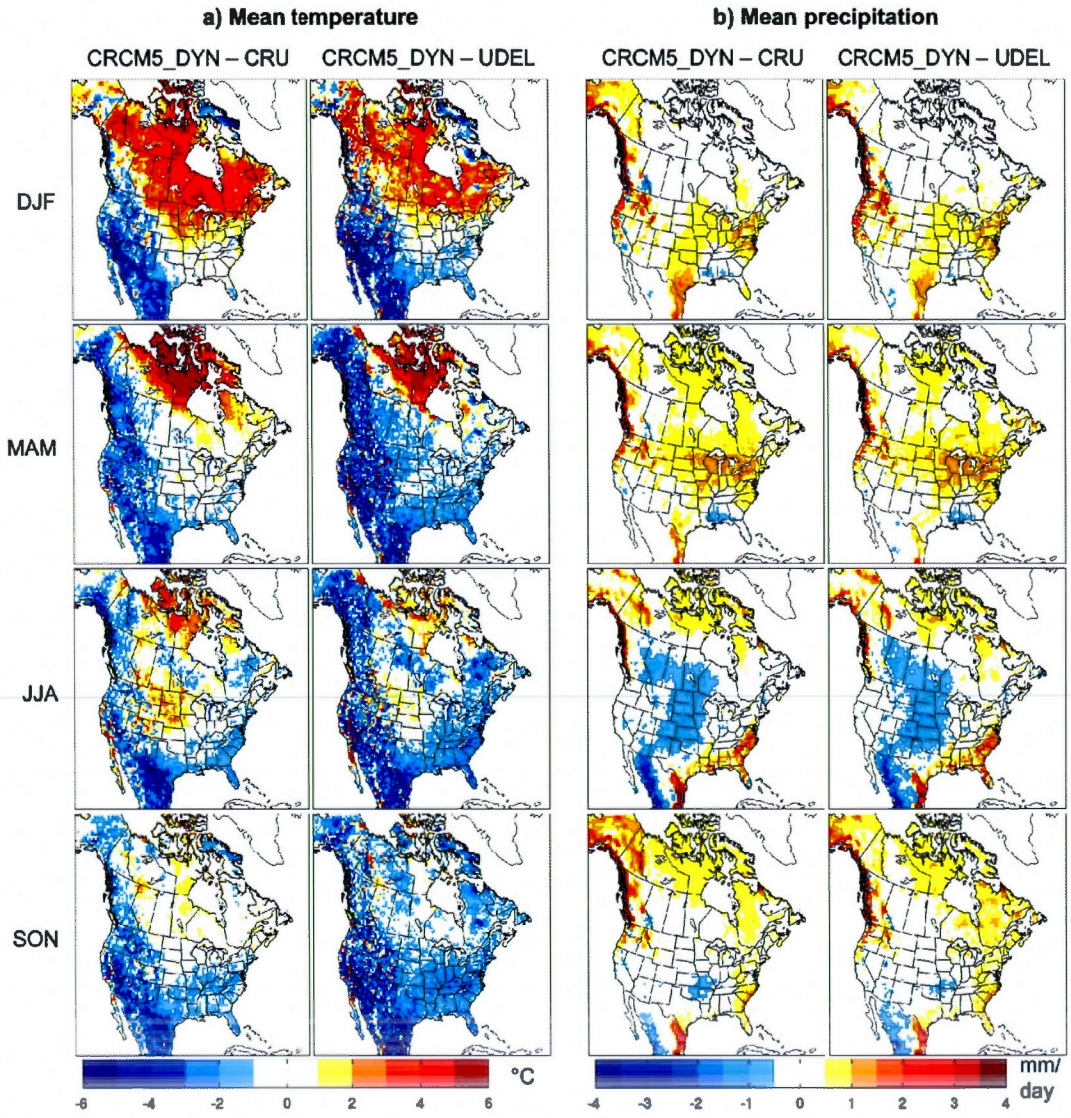

Figure 2.6 Differences in mean seasonal (a) temperature (°C) and (b) precipitation (mm/day) between CRCM5_DYN and CRU (columns 1 and 3) and between CRCM5_STAT and UDEL (columns 2 and 4) for the 1971–2010 period

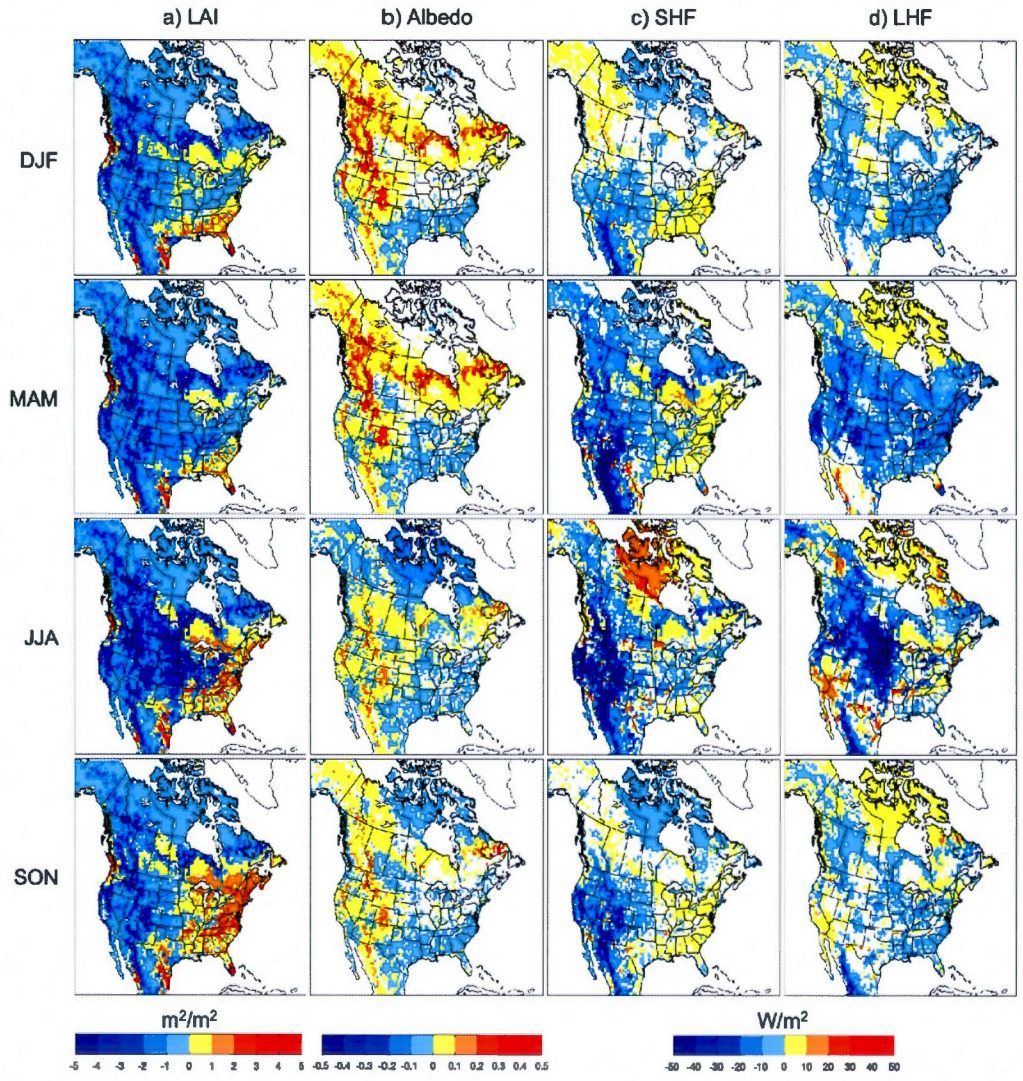

Figure 2.7 Seasonal differences in (a) LAI (m^2/m^2), (b) albedo, and (c) sensible and (d) latent heat fluxes (W/m^2) between CRCM5_DYN and CRCM5_STAT for the 1971–2010 period. Regions where differences are not statistically significant are shown in white; significance is calculated using the Student's t-test at 5% significance level

in Fig. 2.7b. This leads to further reduction of the temperatures in CRCM5_DYN compared to CRCM5_STAT (Fig. 2.5b) through decreased SHF (Fig. 2.7c). The dynamic vegetation module also reduces the cold bias over Canada in summer in CRCM5_STAT (Fig. 2.3a) due to the lower albedo (Fig. 2.7b), but in some areas warm biases are introduced in CRCM5_DYN (Fig. 2.6a). The albedo effect in the boreal regions is strong and leads to an increased SHF (Fig. 2.7c) in CRCM5_DYN, resulting in warmer temperatures in summer (Fig. 2.3b) compared to CRCM5_STAT. Furthermore, CRCM5_DYN mostly reduces the warm bias over the Rockies in western US in summer (Fig. 2.6a) compared to CRCM5_STAT because of a significant decrease in SHF (Fig. 2.7c) due to a decrease in LAI (Fig. 2.7a) and an increase in albedo (Fig. 2.7b), which once again leads to cold biases in some areas in CRCM5_DYN. These arid regions with large fractional areas of bare ground have higher albedo values. Moreover, CRCM5_STAT shows a cold bias over Mexico and western US (Fig. 2.3a) all year long, thus the significantly lower LAI in CRCM5_DYN (Fig. 2.7a) in these regions generally increases the temperature bias (Fig. 2.6a), although CRCM5_DYN's LAI is closer to the observations (Fig. 2.4). In this area, a decrease in LAI leads to an increase in albedo and to a cooling of the 2-m temperature.

The effect of the biosphere on precipitation is more complex as the precipitation source could be local recycling or convergence of moisture advected into the region. As shown in Figs. 2.5a and 2.6b, similar to the temperatures, the largest differences between the two simulations occur in spring and summer, when the biosphere-atmosphere interactions are strong. CRCM5_DYN only slightly improves the dry bias along the West Coast compared to CRCM5_STAT, despite the difference in LAI (Fig. 2.7a), as the main source of precipitation in this region is the moisture advected into the region. In spring, the lower LAI in CRCM5_DYN (Fig. 2.7a) across western and central US implies reduced LHF (Fig. 2.7d), which could lead to reduced contribution of local moisture to the total atmospheric westerly transport of transpired water. In summer, the differences in LAI are strongest between the two simulations (Fig. 2.7a). This is the season with maximum convective activity and therefore the biosphere has a more direct effect on the local

precipitation. The model is able to reproduce these biosphere-atmosphere interactions : in summer, the spatial patterns of the difference in LHF (Fig. 2.7d), which is greatly affected by LAI, and precipitation (Fig. 2.5a) are very similar.

Thus, although the impact of dynamic vegetation on the 1971–2010 mean climate can be significant depending on the region and the season, it does not always improve the model simulation when compared to observations. However, the possible improvement from the dynamic vegetation module is limited by its own internal biases, along with the biases from the simulated climate, greatly influencing the simulated vegetation. Indeed, Garnaud *et al.* (2014a) have shown that the vegetation simulated by CLASS/CTEM is sensitive to the driving climate. Despite these limitations, the implementation of CTEM in CRCM5 enables better representation of certain aspects of biosphere-atmosphere interactions, as discussed in the following section.

2.3.3 Biosphere-atmosphere interactions : CRCM5_STAT vs. CRCM5_DYN

Figure 2.8 shows spatial plots of the correlations between the annual maximum LAI and the mean spring–summer (MAMJJA) precipitation, LHF, temperature and SHF. In CRCM5_STAT, the correlations between maximum LAI and precipitation, LHF and SHF (Figs. 2.8a, 2.8b and 2.8d, respectively) are mostly non-significant, which is expected since the links between these variables in the model are weak. However, positive correlations are seen between the LAI and the temperature (Fig. 2.8c) in the high-latitudes in CRCM5_STAT. This is because temperature is the main determining factor of leaf phenology in this simulation. Once the conditions with respect to 2-m air temperatures are favorable (i.e. above 2°C), LAI increases from a minimum value to a maximum value (both prescribed) in a predefined amount of time. Thus, if the temperatures are too low in a given year, the plants will not have time to reach their maximum LAI, and hence the positive correlations in the high latitudes.

In CRCM5_DYN, the correlations between the LAI and precipitation are very strong with mainly positive values (Fig. 2.8a). Over southern North America for example, where

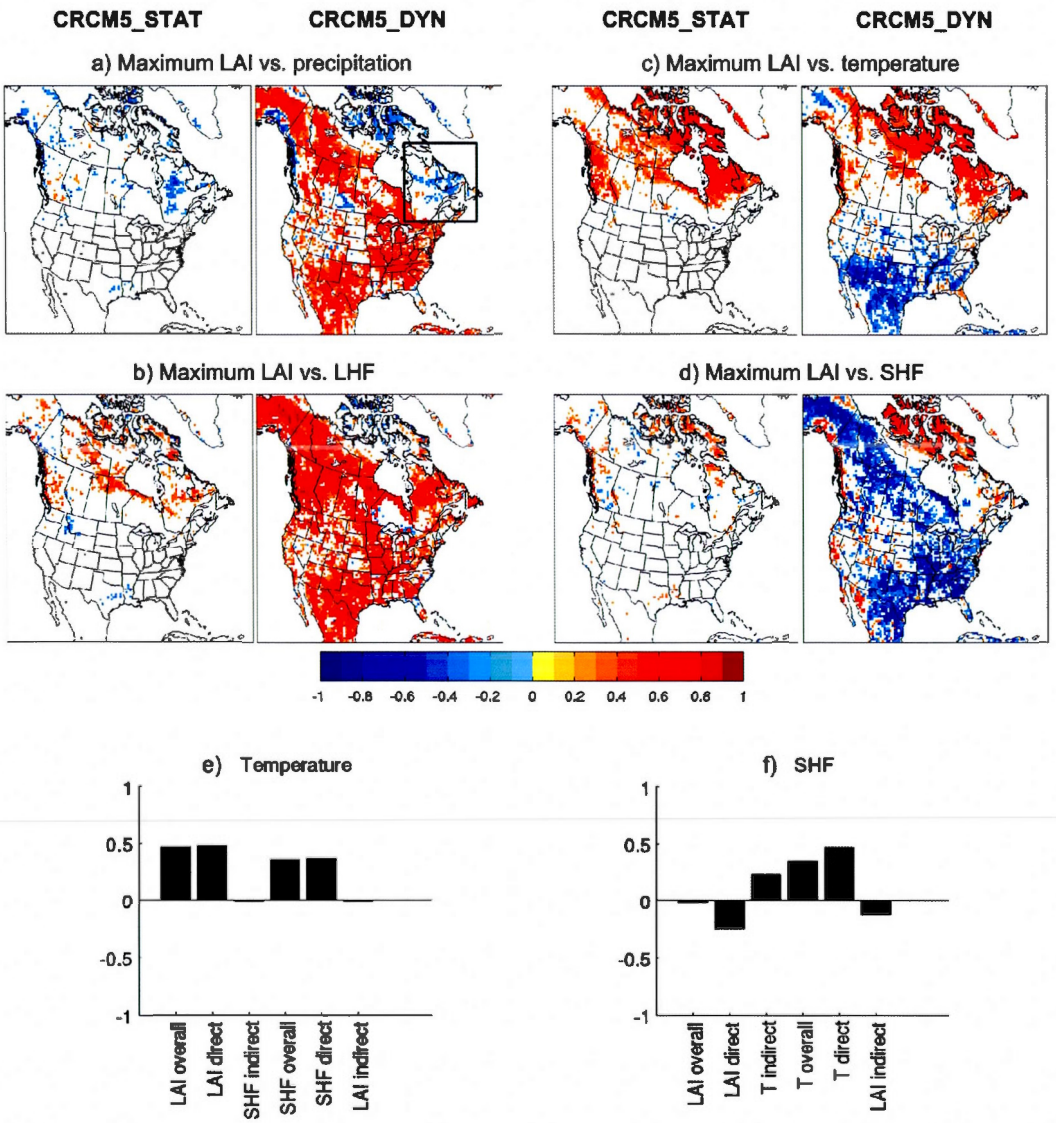

Figure 2.8 Spatial plots of the correlations between the maximum LAI and mean spring/summer (a) precipitation, (b) LHF, (c) temperature, and (d) SHF for the 1971–2010 period. Regions where correlations are not significant are shown in white; significance is calculated using the Student's t-test at 10% significance level. Path analysis illustrating the direct, indirect and overall effects of (e) maximum LAI and SHF on temperature, and (f) maximum LAI and temperature (T) on SHF, in CRCM5_DYN in the region defined by the black box in (a)

water is a growth-limiting factor, vegetation is largely dependent on precipitation. This leads to a positive LAI-precipitation feedback loop, with a positive precipitation anomaly boosting plant productivity and LAI, which leads to increased evapotranspiration, as shown in Fig. 2.8b, and possibly the amount of local rainfall. The correlations between the LAI and temperature (Fig. 2.8c) are negative over southern North America, since plants suffer from heat stress at higher temperatures in these regions, consequently decreasing the vegetation productivity. The correlations are positive in the higher latitudes, where vegetation will benefit from warmer temperatures due to the lengthening of the growing season. Over most regions, where correlations between LAI and SHF are negative, correlations between LAI and LHF are positive. However, in CRCM5_DYN, the region of eastern Canada, shown in Fig. 2.8a, stands out. Indeed, in this region, though the LAI-LHF correlations are positive, the LAI-precipitation correlations are mostly non-significant. This leads to the conclusion that vegetation does not suffer from moisture limitation in this region.

For the same region, the correlations between LAI and temperature are positive, though the correlations between LAI and SHF are mostly non-significant. To better understand the interactions, a path analysis is performed to decompose the effect of (1) LAI and SHF on temperature, and (2) LAI and temperature on SHF, as explained in section 2.2.3 and shown in Fig. 2.8 e-f. The magnitudes of the direct effect of SHF and the indirect effect of LAI (through SHF) on temperature-SHF correlations (Fig. 2.8e) confirm that an increase in SHF leads to an increase in temperature. This suggests that the missing link in the LAI-SHF-temperature-LAI interactive loop resides in the correlation between LAI and SHF. Figure 2.8f shows that the LAI-SHF correlation is non-significant due to the counteracting direct effect of LAI on SHF (-0.25) and indirect effect of temperature on SHF through its effect on LAI (0.22).

Long-term memory

Delire *et al.* (2011) suggested that the implementation of a dynamic vegetation module in a climate model introduces long-term memory in the system. Indeed, the biosphere is

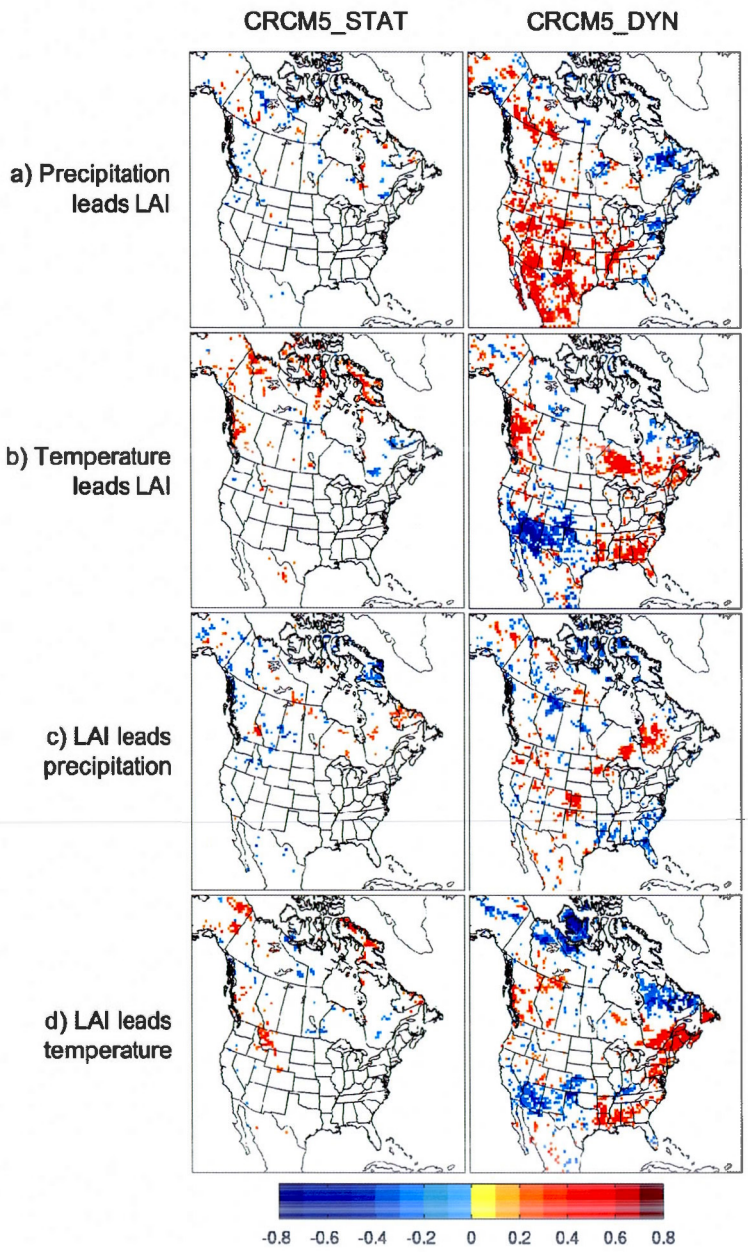

Figure 2.9 Spatial plots of 1-year lagged-correlations between (a) precipitation and peak LAI, (b) temperature and peak LAI, (c) peak LAI and precipitation, and (d) peak LAI and temperature, with the first variable leading the second by one year in all cases, for CRCM5_STAT (column 1) and CRCM5_DYN (column 2) for the 1971–2010 period. Regions where correlations are not significant are shown in white; significance is calculated using the Student's t-test at 10% significance level

a slow integrator of short-term climate changes, thus influencing the climate in the long-term. To assess the impact of the vegetation memory on the CRCM5 climate, 1-yr lagged correlations between the peak LAI and the annual mean precipitation and temperature were calculated, as shown in Fig. 2.9. For instance, Fig. 2.9a shows the correlation of precipitation with the LAI when the precipitation leads the LAI by one year. Whether looking at the biosphere (LAI) leading the climate or vice-versa, CRCM5_DYN shows significant correlations over many regions compared to CRCM5_STAT. The correlations with the precipitation leading the LAI are mostly positive in CRCM5_DYN over the south-western parts of North America, since an increase in precipitation benefits vegetation in these regions where water is somewhat a limiting factor to vegetation growth. If the NPP increases during the year with increased precipitation, the LAI will most likely be greater the following year. As can be seen from Fig. 2.9b, an increase in temperature has a different effect on the vegetation depending on location. Over southwest North America where the climate is hot and dry, an increase in temperature leads to heat stress, resulting in a decrease in vegetation live carbon pools and thus in the LAI the following year. In other regions, vegetation benefits from higher temperature since it may lengthen the growing season, thus increasing the vegetation carbon uptake and the LAI the following year. The atmosphere memory relative to the biosphere (Figs. 2.9c and 2.9d) is weaker than the biosphere memory (Figs. 2.9a and 2.9b), which concurs with the observed results from Notaro *et al.* (2006). However, CRCM5_DYN indicates that changes in biosphere could lead to significant alterations in the climate in the long-term in sensitive regions, especially since it is the temperature that seems most affected by changes in vegetation coverage, similarly to the findings of Liu *et al.* (2006).

The results presented above for instantaneous correlations and lead-lag correlations show great resemblance in patterns to those of Notaro *et al.* (2006) who used observed data in order to study the vegetation-atmosphere feedbacks across the United States. Thus, the model simulation CRCM5_DYN is consistent with observations and other studies. It was discussed in section 2.3.2 that CRCM5_DYN does not clearly improve the model with respect to the mean climate. However, since it introduces biosphere-

atmosphere feedbacks and long-term memory in the model, it could be hypothesized that CRCM5_DYN captures better the variability of biosphere and climate.

2.3.4 Interannual variability and extremes

Several studies have shown that vegetation can dampen or amplify climate variability through changes in vegetation structure and feedbacks (Hughes *et al.*, 2006; Delire *et al.*, 2004, 2011). Thus, in order to study the impact of dynamic vegetation on the interannual variability of the simulated climate, the coefficient of variation (CV) – defined as the ratio of the standard deviation to mean value – of the seasonal maximum LAI and the seasonal means of LHF, SHF, precipitation, temperature and diurnal temperature range are computed for spring (MAM ; Fig. 2.10) and summer (JJA ; Fig. 2.11), for the 1971–2010 period, for CRCM5_DYN and CRCM5_STAT. CV is used as a measure of variability as it facilitates comparison across variables and seasons.

The interannual variability, quantified in terms of CV, of maximum LAI is clearly higher for CRCM5_DYN, compared to CRCM5_STAT (Figs. 2.10a, 2.11a) for both seasons, and is closer to that observed (figure not shown). In spring, the interannual variability of the maximum LAI in CRCM5_STAT (Fig. 2.10a) can be high as it depends on the date of budburst. In summer however (Fig. 2.11a), most of the vegetation has reached its prescribed maximum LAI, except in the high latitudes, where the length of the growing season has a great impact on the maximum LAI. In these high latitude regions, a link can be made with Fig. 2.8c where the spatial pattern of the correlation between the maximum LAI and mean spring/summer temperature is very similar to the interannual variability of the maximum LAI in summer. As explained previously, this is due to the fact that in CRCM5_STAT the phenology of the plants is driven by the 2-m air and the soil temperatures. However, the interannual variability of LAI does not seem to be linked to the interannual variability of the energy fluxes and the climate in CRCM5_STAT, which is expected since the maximum LAI is prescribed in CRCM5_STAT.

In CRCM5_DYN, the region of maximum LAI variability shifts from the high-latitude

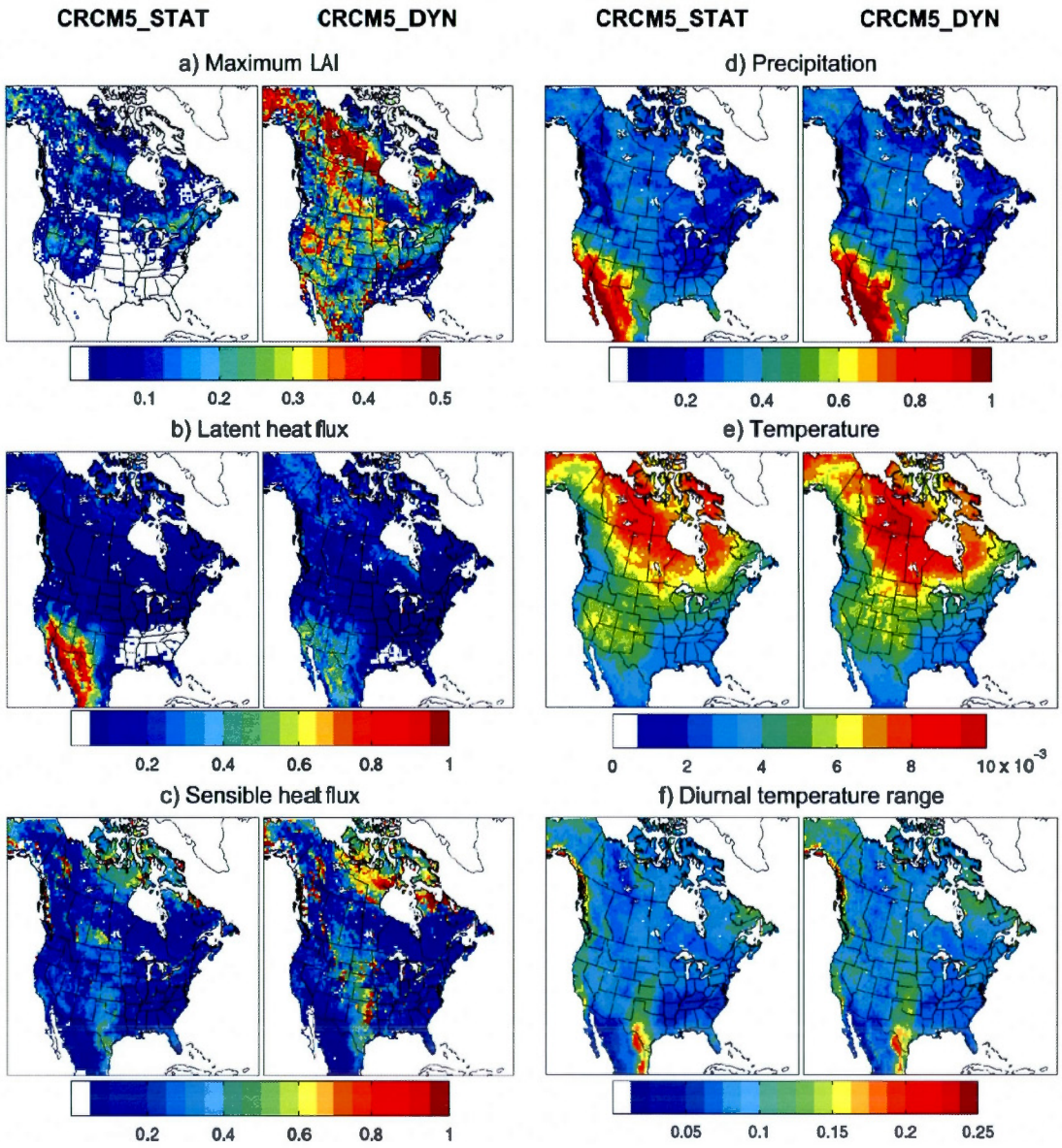

Figure 2.10 Spatial plots of the coefficient of variation of the (a) maximum LAI and mean (b) latent heat flux, (c) sensible heat flux, (d) precipitation, (e) temperature, and (f) diurnal temperature range for the CRCM5_STAT and CRCM5_DYN simulations, for the 1971–2010 period, for spring (MAM) season

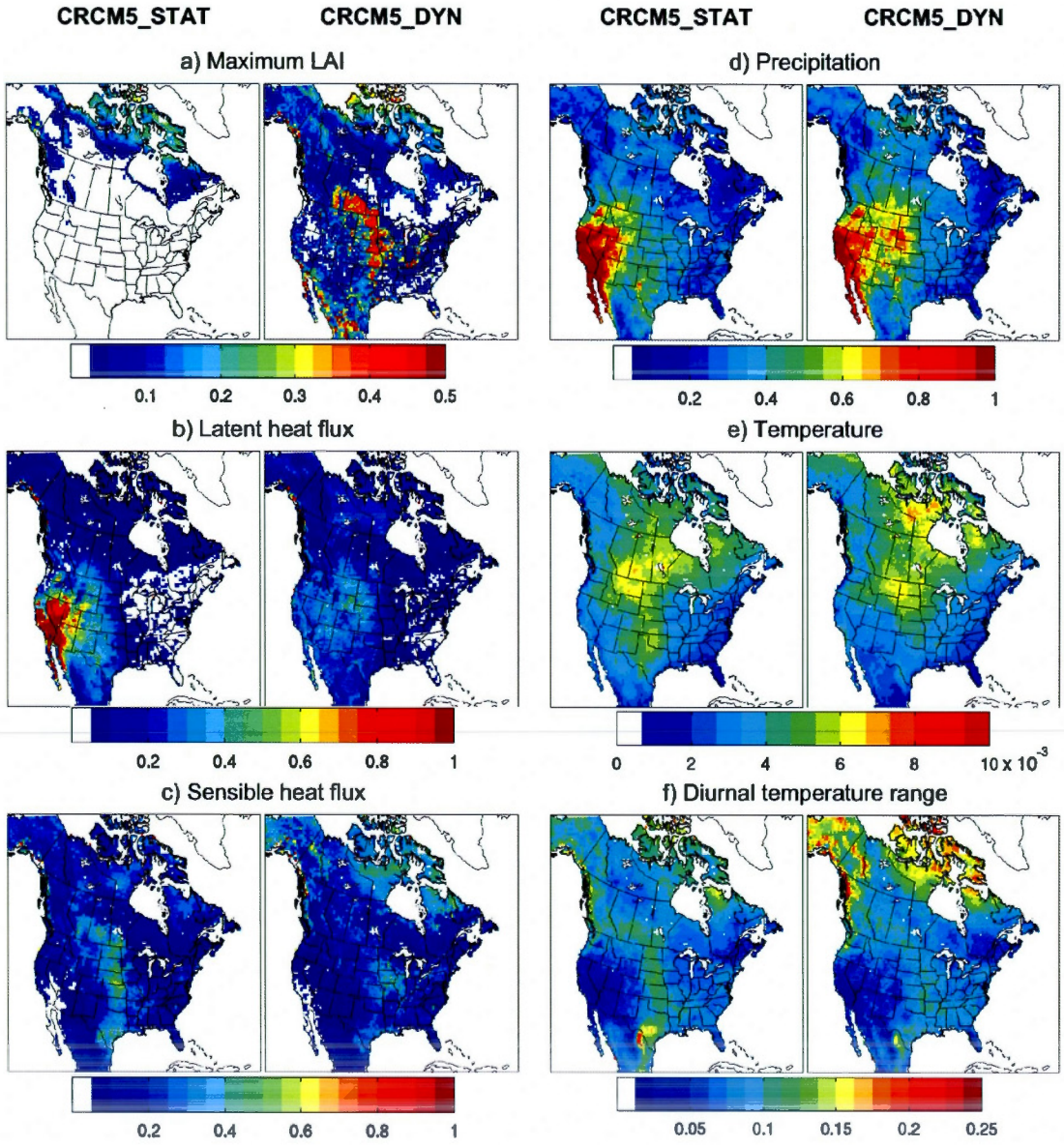

Figure 2.11 Spatial plots of the coefficient of variation of the (a) maximum LAI and mean (b) latent heat flux, (c) sensible heat flux, (d) precipitation, (e) temperature, and (f) diurnal temperature range for the CRCM5_STAT and CRCM5_DYN simulations, for the 1971–2010 period, for summer (JJA) season

regions in spring to a southerly location, dominated by crops, in summer. For spring, amplification of interannual variability can be noticed for SHF in CRCM5_DYN, for the same high-latitude regions where higher interannual variability in maximum LAI is noted, which is also reflected in the interannual variability of mean spring temperature (Fig. 2.10e). The amplification in LHF variability for the same region is much smaller compared to SHF and is expected since the impact of LAI on albedo and therefore on SHF is dominant compared to LHF in these regions.

In spring, despite the higher interannual variability in the southern parts of the domain for maximum LAI in CRCM5_DYN, a dampening of LHF variability is noted for the south-western regions of the North American landmass (Fig. 2.10b) and some amplification in SHF over the central Great Plains (Fig. 2.10c). The dampened interannual variability in LHF over central North America is not reflected in precipitation, as the source of precipitation for these regions is not only related to local recycling of moisture, but also to moist air advected into the region by winds from the adjoining oceans (Pacific and Gulf of Mexico). The impact of the increased interannual variability in SHF for the central Great Plains on the mean temperature is less evident. As for summer, similar to spring, dampening of LHF variability can be noted in CRCM5_DYN. Though variability in SHF is higher in high-latitude regions in CRCM5_DYN in summer compared to CRCM5_STAT, no important changes are noticed for other regions.

To investigate further the impact of higher and improved interannual variability of maximum LAI in CRCM5_DYN on climate, we turn our attention to anomalous dry and wet years. In particular, anomalous dry/wet years over the region with high interannual variability in LAI in summer are selected. For a drought year, we focus on year 1988 when droughts affected central parts of North America, and for an anomalous wet year, we look at year 1993, which affected approximately the same region as the drought of 1988. Figure 2.12 shows observed (based on Hopkinson *et al.* (2011) and Maurer *et al.* (2002) datasets) and CRCM5_DYN and CRCM5_STAT simulated NHD for the summer of 1988. Although the spatial pattern of the NHD in CRCM5_DYN is slightly shifted to the north, the improvement in the simulation of the NHD, compared to CRCM5_STAT,

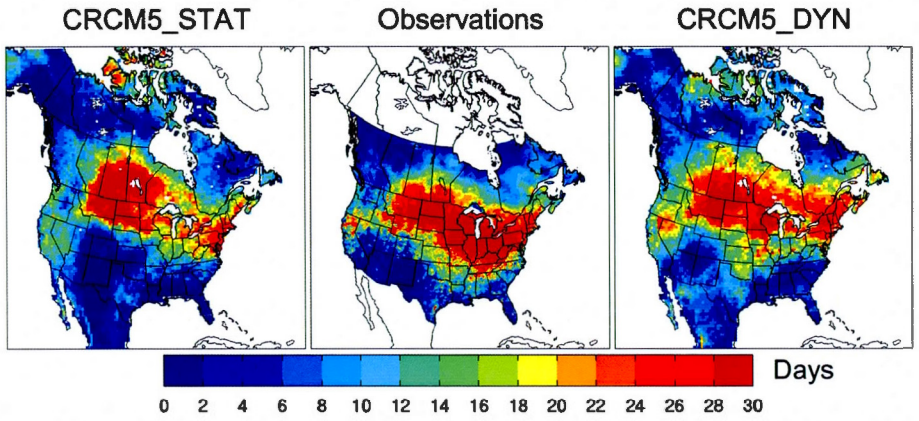

Figure 2.12 Number of hot days derived from (centre) observed data (Canada : Hopkinson *et al.*, 2011 and USA : Maurer *et al.*, 2002) daily maximum temperature series, and the (left) CRCM5_STAT and (right) CRCM5_DYN simulations during the summer (JJA) of 1988

is notable. In CRCM5_STAT, the NHD is substantially reduced over eastern North America, where the differences in summer LAI (see Fig. 2.4b) between CRCM5_DYN and CRCM5_STAT are more pronounced, which suggests that a better representation of vegetation cover and the interactions at the land-atmosphere interface leads to better simulation of the NHD.

The impact of the very dry and warm conditions, during the summer of 1988, on the simulated biosphere in CRCM5_DYN and CRCM_STAT can be assessed from Fig. 2.13, which shows time series of summer mean values of precipitation, temperature and LAI for the 1971–2010 period, for the drought affected region (between 41°N and 50°N, and 116°W and 88°W). Both simulations capture the 1988 drought, reflected in the below normal precipitation values and the related above normal positive temperatures. The impact of these anomalies on the biosphere is different in CRCM5_STAT and CRCM5_DYN. Indeed, in CRCM5_STAT, since precipitation has no direct effect on the LAI, the below normal precipitation apparently has no influence on LAI. On the contrary, the above normal warmer temperature increases the length of the growing

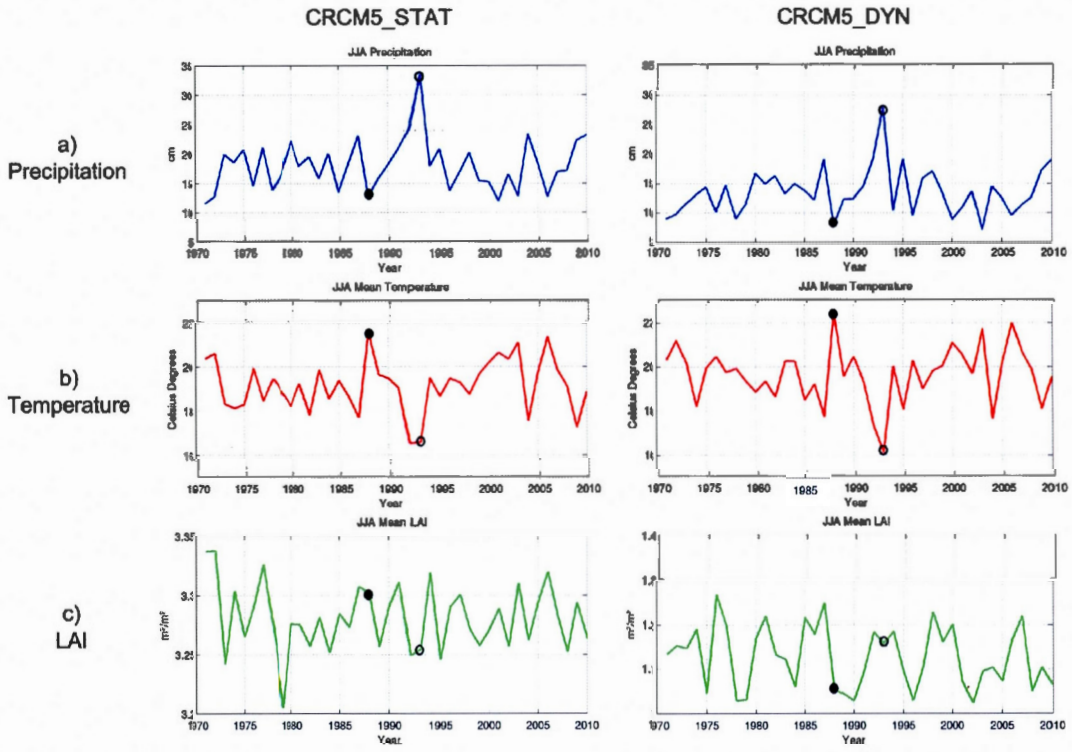

Figure 2.13 Evolution of CRCM5_STAT (left column) and CRCM5_DYN (right column) simulated mean summer (a) precipitation (cm), (b) temperature (°C) and (c) LAI (m^2/m^2) for the 1988 drought affected region (between 41°N and 50°N, and 116°W and 88°W) shown in Fig. 2.12, for the 1971–2010 period. The filled (empty) circles correspond to year 1988 (1993)

season and thus the mean LAI. However, CRCM5_DYN captures the drought-stress effect on the vegetation. The below normal precipitation leads to water stress, to which the vegetation responds through increased stomatal resistance, thereby reducing the productivity and therefore LAI. Though precipitation picks up and temperature cools in the subsequent years, the LAI continues to drop till 1990 in CRCM5_DYN, possibly due to the long-term memory of the biosphere and its impact on the atmosphere.

As for the wet summer of 1993, both simulations capture the positive precipitation anomaly, accompanied by anomalously cooler temperatures. Once again, these two climate factors have different effects on the biosphere in the two simulations. In CRCM5_STAT, the lower temperatures in 1993 and 1994 cause the mean LAI to drop, with precipitation having no direct effect on the biosphere. In CRCM5_DYN however, vegetation benefits from the increased precipitation although this effect is dampened by the cooler temperatures. It should be noted that overly large precipitation, resulting in flooding, could lead to unfavorable conditions for the biosphere, but this is not currently represented in CTEM.

2.4 Summary and Conclusions

The impact of dynamic vegetation on CRCM5 simulated climate over North America for the 1971–2010 period is studied by comparing two simulations – CRCM5_STAT with static vegetation represented by the land surface scheme CLASS and CRCM5_DYN which models vegetation as a dynamic component through CTEM coupled with CLASS. Both simulations are driven by ERA-40/ERA-Interim reanalyses at the lateral boundaries.

Comparison of simulated and observed spatial distribution of the biospheric state variable, i.e. LAI, suggests that CRCM5_DYN, particularly in summer, captures better the distribution, except over western Canada where it underestimates the LAI. This bias in the simulated biosphere over western Canada in CRCM5_DYN could lead to underestimation of biosphere-atmosphere feedbacks, particularly due to the strength of the albedo effect in this region (Loranty *et al.*, 2014), and it could possibly be rectified

by creating a 10th PFT adapted to this region, as suggested by Peng *et al.* (2014). It must however be noted that there are large uncertainties in the LAI observation datasets. For example, Gibelin *et al.* (2006) have shown that the ISLSCP II LAI is higher than other satellite based estimates, especially in the boreal forest.

The differences in LAI, the vegetation characteristic that has the greatest impact on the atmosphere-biosphere interactions, between CRCM5_DYN and CRCM5_STAT lead to differences in surface albedo, SHF and LHF between the two simulations over various regions, which are reflected in the simulated temperature and precipitation fields. In fact, CTEM improves the model (CRCM5) in some regions, although it introduces new biases in other regions such as western USA. Thus the impact of dynamic vegetation on the 1971–2010 mean climate can be significant depending on the region and the season. It should be noted that biases in the simulated climate stemming from other sources could influence the simulated vegetation. Garnaud *et al.* (2014a) have shown that the vegetation simulated by CLASS/CTEM is sensitive to the driving climate.

Despite these limitations, the implementation of CTEM in CRCM5 introduces feedbacks between the biosphere and the atmosphere. In fact, the correlations between biospheric and atmospheric variables are significantly stronger in CRCM5_DYN, particularly with respect to precipitation and surface fluxes. Furthermore, since the biosphere is a slow integrator of short-term climate changes, the implementation of a dynamic vegetation module in a climate model introduces long-term memory in the climate system, thus influencing the climate in the long term, as suggested by Delire *et al.* (2011) and noted in CRCM5_DYN. The strongest lagged correlations are between the LAI and temperature, with the average temperature of a given year having a significant impact on the LAI of the following year. Although not as pronounced, the impact of LAI on temperature the following year shows a similar behavior. Once again, this is an indication that CRCM5_DYN is able to simulate feedback between the biosphere and the climate that could lead to significant alterations in the climate in sensitive regions in the long term. These findings are similar to those obtained by Liu *et al.* (2006) and Wang *et al.* (2014) using observations. CRCM5_DYN simulates better the interannual variability in LAI,

which is also reflected in the ability of the model to simulate more realistically the state of the atmosphere and biosphere during anomalously wet and dry years.

This study thus provides important insights on the impact of dynamic vegetation on the regional climate of North America, particularly related to the variability, both in space and time, in biosphere-atmosphere interactions over the region. As mentioned earlier, this study does not take into account competition between plant functional types. As shown by Smith *et al.* (2011), competition is important to model vegetation shifts and changing tree line, due to non-negligible effects that this can have on temperature and precipitation feedbacks, particularly in the context of a changing climate. Work is in progress to implement competition in CTEM, and thus future work will focus on the impact of competition on regional climate.

CHAPTER III

BIOSPHERE-CLIMATE INTERACTIONS IN A CHANGING CLIMATE OVER NORTH AMERICA

This chapter is presented in the format of a scientific article that will soon be submitted to a peer-reviewed journal. The design of experiments and methods, as well as the analysis of data and preparation of the article were entirely carried out by myself, with Dr. Sushama involved in the supervision of all these tasks.

Abstract

This study focuses on projected changes to vegetation characteristics and their interactions with the atmosphere in future climate over North America, using four transient climate change simulations of the Canadian Regional Climate Model (CRCM5). Here, CRCM5 performs dynamical downscaling of CanESM2 simulated data, for RCP4.5 and RCP8.5 radiation forcing scenarios. For each scenario, two CRCM5 simulations are performed - one with static vegetation and the other with dynamic vegetation - for the 1950–2100 period over North America. The dynamic vegetation model used in this study is the Canadian Terrestrial Ecosystem Model (CTEM). Results show that the extension of the growing season in future climate in the dynamic vegetation simulations leads to higher annual vegetation productivity and biomass. In comparison with projected changes based on CRCM5 with static vegetation, CRCM5 with vegetation dynamics leads to an albedo-mediated warming enhancement in the northern latitudes, while an attenuation of warming due to hydrological feedbacks is suggested for more southern regions. Most of North America shows an increase in leaf area index (LAI) in future climate, although precipitation decreases over time during summer season, particularly for southern regions. This suggests that vegetation enhances its water use efficiency with rising atmospheric CO_2 concentrations in future climate. Over southeastern US, in the dynamic vegetation simulation corresponding to the RCP8.5 scenario, the adverse effects of the projected increase in temperatures and decrease in precipitation on vegetation dominate the CO_2 fertilization effect, leading to decreasing trends in net

productivity during the 2071–2100 period. Thus, this study demonstrates that vegetation dynamics modulates greenhouse gas-mediated warming through various feedbacks, which vary from region to region.

3.1 Introduction

Biosphere-atmosphere interactions and feedbacks constitute an important part of the climate system and can modulate climate, particularly in the context of a changing climate (Pielke *et al.*, 1998; Bonan, 2008; Brovkin, 2002; Notaro *et al.*, 2006). Dynamic Vegetation Models (DVMs) have therefore been developed (e.g., Foley *et al.*, 1996; Bonan *et al.*, 2003; Hughes *et al.*, 2006) for use in climate models to enable the simulation of large-scale structural vegetation changes in response to variations in atmospheric CO_2 concentrations and the climate, and to incorporate the relevant biosphere-atmosphere feedback mechanisms (Denman *et al.*, 2007).

Several studies have been performed to assess the impact of vegetation dynamics on future climate using global climate models (GCMs) (e.g., Thompson *et al.*, 2004; Port *et al.*, 2012). Based on their study on the influence of dynamic vegetation on climate change arising from doubled/quadrupled CO_2, O'ishi and Abe-Ouchi (2009) suggest an enhancement of warming by 10-30% globally and an amplification of climate sensitivity by 10%, mainly due to albedo changes associated with vegetation changes. By separating the effects of rising CO_2 and temperatures on vegetation, they found that warmer temperatures alter the vegetation mostly in northern latitudes, while CO_2 fertilization effects - the biochemical stimulation of photosynthesis at higher CO_2 concentration (Hickler *et al.*, 2008) - mostly contribute to greening in arid/semi-arid regions. Similarly, using the fully coupled global atmosphere–ocean–land Fast Ocean Atmosphere Model (FOAM) with dynamic vegetation model LPJ, Notaro *et al.* (2007) showed that, although the majority of the projected future warming is associated with the radiative forcing of rising CO_2, the vegetation physiological forcing augments the warming by weakening the hydrological cycle due to reduced evapotranspiration, particularly for tropical forests.

Most of the studies focusing on biosphere-atmosphere interactions in future climate are based on coarse resolution GCMs. As pointed out by Snyder and Liess (2013), such coarse resolution simulations can overlook hot spots of biosphere-atmosphere interactions, such as alpine and coastal sites. Thus, the use of high-resolution regional climate models (RCM) is key to better understanding the biosphere-climate interactions and feedbacks.

Using the Rossby Center RCM coupled with a DVM (RCA-GUESS), Wramneby *et al.* (2010) showed that, although the biosphere forcing is modest compared to the radiative forcing of increased CO_2, the biosphere-atmosphere feedbacks may modify warming projections locally and seasonally over Europe. They were able to identify hotspots where vegetation-climate feedbacks were strongest, suggesting that the strength and nature of the biosphere-atmosphere interactions vary regionally. Despite the need for high-resolution simulations with dynamic vegetation, only very few studies are available, especially over North America.

The main objective of this study is thus to assess biosphere-climate interactions over North America in future climate. In particular, changes to vegetation in terms of phenology and productivity, and their role in modulating increasing CO_2 mediated warming, are assessed. This is achieved through four transient climate change simulations of the fifth generation Canadian Regional Climate Model (CRCM5). CRCM5 performs dynamical downscaling of the second generation Canadian Earth System Model (CanESM2) simulated data, for RCP4.5 and RCP8.5 radiation forcing scenarios. For each RCP scenario, two CRCM5 simulations are performed – one with static vegetation and the other with dynamic vegetation (i.e. CTEM) – for the 1950–2100 period at 0.5° resolution over North America. The DVM used in CRCM5 is the Canadian Terrestrial Ecosystem Model (CTEM ; Arora, 2003; Arora and Boer, 2005).

The performance of CRCM5 with CTEM has been evaluated for current climate in Garnaud *et al.* (2014b). This was achieved by comparing two CRCM5 simulations, one with dynamic vegetation and the other with static vegetation, for the 1971–2010 period, with available observations. Their results show that dynamic vegetation improves

the performance of CRCM5 in some regions through better representation of the leaf area index (LAI). It, however, introduces new biases in other regions, compared to the CRCM5 simulation with static vegetation. The authors suggest that the implementation of vegetation dynamics introduces memory and enables realistic representation of interannual variability.

This paper is organized as follows. Section 3.2 of the paper gives a brief overview of the regional climate model, CRCM5, and the coupled land-surface and terrestrial ecosystem models, the Canadian Land Surface Scheme (CLASS; Verseghy, 1991, 2011; Verseghy *et al.*, 1993) and CTEM, along with the description of the experimental set-up and the methodology. Section 3.3 evaluates the performance and boundary forcing errors, and assesses projected changes to biosphere and how it modulates future climate. A brief summary of the results and conclusions are given in section 3.4.

3.2 Models, Experiments and Methods

3.2.1 The Canadian Regional Climate Model (CRCM5)

The regional climate model used in this study, CRCM5, is based on a limited-area version of the Global Environment Multiscale (GEM) model used for numerical weather prediction at Environment Canada (Côté *et al.*, 1998). GEM employs semi-Lagrangian transport and (quasi) fully implicit marching scheme. In its fully elastic nonhydrostatic formulation (Yeh *et al.*, 2002), GEM uses a vertical coordinate based on hydrostatic pressure (Laprise, 1992). The following GEM parameterisations are used in CRCM5 : deep convection following Kain and Fritsch (1990), shallow convection based on a transient version of the Kuo (1965) scheme (Belair *et al.*, 2005), large-scale condensation (Sundqvist *et al.*, 1989), correlated-K solar and terrestrial radiations (Li and Barker, 2005), subgrid-scale orographic gravity-wave drag (McFarlane, 1987), low-level orographic blocking (Zadra *et al.*, 2003), and turbulent kinetic energy closure in the planetary boundary layer and vertical diffusion (Benoit *et al.*, 1989; Delage and Girard, 1992; Delage, 1997).

The land surface scheme CLASS (Verseghy, 1991, 2011; Verseghy *et al.*, 1993) in CRCM5 models three soil layers, 0.1m, 0.25m and 3.75m thick, in its standard formulation, corresponding approximately to the depth influenced by the diurnal cycle, the rooting zone and the annual variations of temperature, respectively. CLASS includes prognostic equations for energy and water conservation for the three soil layers and a thermally and hydrologically distinct snowpack where applicable (treated as a fourth variable-depth layer). The thermal budget is performed over the three soil layers, but the hydrological budget is done only for layers above the bedrock. In order to simply mimic subgrid-scale variability, CLASS adopts a 'pseudo-mosaic' approach and divides the land fraction of each grid cell into a maximum of four sub-areas : bare soil, vegetation, snow over bare soil and snow with vegetation. The energy and water budget equations are first solved for each sub-area separately and then averaged over the grid cell, using spatially varying structural attributes and physiological properties of the four CLASS PFTs (needleleaf trees, broadleaf trees, crops and grass) derived from high-resolution land cover datasets. These structural attributes include albedo, leaf area index (LAI), roughness length, canopy mass and rooting depth.

The dynamic vegetation model CTEM implemented in CRCM5 is a process-based ecosystem model (Arora, 2003; Arora and Boer, 2003, 2005, 2006; Li and Arora, 2011) designed to simulate the terrestrial carbon cycle. It is able to grow vegetation from bare ground and to simulate several vegetation structural attributes such as leaf area index, vegetation height, root distribution and canopy mass. It includes processes such as photosynthesis, autotrophic respiration, heterotrophic respiration, phenology, turnover, allocation, fire and land-use change. CTEM simulates two dead carbon pools, litter and soil organic carbon, and three live vegetation pools (stems, leaves and roots). Terrestrial ecosystem processes in CTEM are modeled for nine different plant functional types (PFTs) : evergreen and deciduous needleleaf trees, broadleaf evergreen and cold and drought deciduous trees, and C_3 and C_4 crops and grasses.

The vegetation structural attributes of CTEM's nine PFTs are aggregated to four PFTs (needleleaf trees, broadleaf trees, crops and grass) when they are passed on to CLASS.

CTEM computes leaf biomass and therefore LAI, which is used by CLASS to estimate surface albedo used in the energy and water balance calculations over the vegetated fraction of a grid cell. The root biomass in CTEM is converted to rooting depth and root distribution profile that is then used to estimate the fraction of roots in each soil layer required for estimating transpiration in CLASS. The aboveground canopy mass from CTEM is used in CLASS to estimate the canopy heat capacity. In turn, CTEM uses the canopy temperature, soil temperature and moisture, and aerodynamic conductance calculated in CLASS to simulate dynamic vegetation characteristics.

3.2.2 Transient climate experiments

As discussed earlier, this study investigates biosphere-climate interactions in future climate and their regional differences using four CRCM5 transient climate change simulations. CRCM5 performs dynamical downscaling of the second generation Canadian Earth System Model (CanESM2) simulated data, for RCP4.5 and RCP8.5 radiation forcing scenarios. Sea surface temperatures (SST) and sea ice concentrations (SIC) are prescribed from the driving CanESM2 simulations. For each RCP scenario, two CRCM5 simulations are performed – one with static vegetation and the other with dynamic vegetation (i.e. CTEM) – for the 1950–2100 period at 0.5° resolution over North America. These four simulations will be referred to as STAT_RCP45, STAT_RCP85, DYN_RCP45, and DYN_RCP85, as described in Table 3.1. The simulations are run at a 20-minute time step and are forced with greenhouse gas (GHG) concentrations, including CO_2, from the RCP scenarios. It should be noted that the concentrations of GHGs are the same in all four simulations from 1950 to 2005 inclusively. From 2006 to 2100, the GHG concentrations follow the respective concentration scenario (RCP), with an atmospheric CO_2 concentration of 538 ppm by 2100 in RCP4.5 and 936 ppm in RCP8.5.

The soil type, i.e. percentage of sand and clay, for the 3 layers modeled in CLASS follows Webb *et al.* (1991). The grid cell fractional coverage of the nine PFTs (Fig. 2.2, Garnaud *et al.*, 2014b) is obtained from the HYDE 2 database (Arora and Boer, 2010) for crops and from Wang *et al.* (2006) for the other PFTs. The land fractional cover is specified at

Simulation	Vegetation	Driving data
STAT_ERA	Static	ERA40/ERA-Interim
DYN_ERA	Dynamic	ERA40/ERA-Interim
STAT_RCP45	Static	CanESM2 (RCP4.5)
DYN_RCP45	Dynamic	CanESM2 (RCP4.5)
STAT_RCP85	Static	CanESM2 (RCP8.5)
DYN_RCP85	Dynamic	CanESM2 (RCP8.5)

Table 3.1 Experimental setup and names given to simulations.

its 1960 values. It should be noted that in DYN_RCP45 and DYN_RCP85, even though the geographical distribution of PFTs is fixed, the vegetation attributes (LAI and carbon pools) are simulated as dynamic functions of driving climate. Initial conditions of soil and vegetation state were obtained by running CLASS/CTEM offline for 300 years driven by repeated temperature, humidity and wind variables from a 20-year CRCM5 simulation (with CTEM, and initialized using data from Garnaud *et al.* (2014a)), until equilibrium conditions were obtained, using a fixed 1765 CO_2 concentration during the first 107 years and a transient 1765-1957 CO_2 concentration for the following 193 years. The vegetation parameters prescribed in CRCM5_STAT (albedo, max and min LAI, rooting depth, etc.) are derived from the biosphere state during the last 50 years of the above-mentioned 300-year offline simulation. Since the SST and SIC in the simulations are prescribed from the driving CanESM2 simulation, the differences in climate between the dynamic and static vegetation simulations for the same RCP scenario are due only to the differences in interactions between the vegetation and the atmosphere.

Though the transient climate change simulations span the 1950–2100 period, analysis presented in this article focuses on the 1971–2000 current and 2071–2100 future periods. It must be noted that the period 1971–2000 of simulations DYN_RCP45 and DYN_RCP85, and similarly of STAT_RCP45 and STAT_RCP85, are identical since the GHGs are the same.

The most important differences between simulations with static vegetation and dynamic

vegetation relate to the canopy resistance and photosynthesis, phenology, root distribution, canopy mass and vegetation height, as described in details in Garnaud *et al.* (2014b). In simulations using static vegetation, canopy resistance is dependent on incoming solar radiation, vapour pressure deficit, soil moisture suction, and air temperature, and does not explicitly take into account the effect of atmospheric CO_2 concentration. In addition to the environmental variables cited above, the CTEM formulation includes the effect of atmospheric CO_2 concentration on stomatal conductance. This is essential to simulate the physiological effects of increasing CO_2 amounts on stomatal canopy resistance in transient climate simulations.

With respect to phenology, in simulations using static vegetation, CLASS adopts an approach where the air temperature and the temperature of the top soil layer determine leaf onset, as described in details in Verseghy (2011). When the air and top soil temperatures exceed 2°C, the LAI increases linearly from a specified minimum to mature state with maximum LAI (prescribed) in specified number of days. The duration of the transition period from dormancy to mature state depends on the PFT. Similarly, the transition to dormancy occurs when the air temperature falls below 2°C. Therefore, seasonality is modeled but not long-term variations in canopy cover or vegetation structure. On the other hand, CTEM simulates leaf onset through a carbon benefit approach, and leaf offset is initiated by unfavorable environmental conditions that stress the plant and imply carbon loss. This allows the simulated vegetation to grow or perish in the long-term, depending on the environmental conditions such as CO_2 concentrations, temperature and soil moisture. When conditions are favorable, CTEM allocates positive net primary production (NPP) between leaf, stem, and root components, which increases their biomass, while negative NPP results in decrease of component biomass because of respiration. As a result of these allocation processes, the vegetation biomass may vary.

3.2.3 Methods of analysis

Errors in an RCM simulation driven by a GCM at its boundaries is the sum of performance and boundary forcing errors (Sushama *et al.*, 2006). Performance errors are related to model dynamics and physics, while boundary forcing errors are due to errors in the driving data. Performance errors can be assessed by comparing reanalysis-driven RCM simulations with observations, while boundary forcing errors can be assessed by comparing GCM-driven RCM simulations with reanalysis-driven RCM simulations.

In order to assess performance errors associated with CRCM5 with static and dynamic vegetation, two additional CRCM5 simulations were performed for the 1971–2000 period driven by the ECMWF reanalyses ERA40 (Uppala *et al.*, 2005) until 1978 inclusively and ERA-Interim (Dee *et al.*, 2001) from 1979 onwards, with dynamic vegetation and static vegetation. These simulations will be refered to as DYN_ERA and STAT_ERA, respectively (see Table 3.1). Selected climate variables, namely temperature and precipitation, from these two simulations are compared to gridded observational data from the Climate Research Unit (CRU) (Mitchell and Jones, 2005). The CRU TS 2.1 data set covers the period 1901–2002 and has a resolution of 0.5°. The boundary forcing errors associated with biospheric and atmospheric variablesare investigated by comparing STAT_RCP45 and DYN_RCP45 simulations with STAT_ERA and DYN_ERA, respectively, for the 1971–2000 period.

Only DYN_RCP45 and DYN_RCP85 are expected to capture changes to vegetation characteristics in the context of changing climate. Thus, the response of the biosphere to rising atmospheric CO_2 concentrations and climate change in these two simulations is assessed by studying projected changes in leaf onset, productivity and biomass by comparing mean values for the future 2071–2100 period with that for the current 1971–2000 period. Trends in the net primary productivity are also estimated using Sen's slope method (Sen, 1968) for different time slices. The statistical significance of these trends is estimated using the Mann-Kendall test (Kendall, 1975; Khaliq *et al.*, 2009) at 5% significance level.

Similar to biosphere variables, projected changes to climate variables of interest, namely mean temperature and precipitation that are important for vegetation, are assessed by comparing their mean values for the future 2071–2100 period with that for the current 1971–2000 period. Projected changes based on DYN_RCP45 and DYN_RCP85 are compared to those from STAT_RCP45 and STAT_RCP85, respectively, to identify regions where vegetation dynamics is important. To assess the strength of the simulated biosphere-atmosphere interactions, Pearson correlation coefficients are computed for the annual maximum LAI and annual mean precipitation, as well as for the annual maximum LAI and mean spring/summer temperatures, for the current 1971–2000 and future 2071–2100 periods. The statistical significance of Pearson correlation coefficients is estimated using the Student's t-test at 10% significance level.

3.3 Results and Discussion

The analysis presented here focuses on summer (JJA) season only, when biosphere-atmosphere interactions are strongest. However reference is made to other seasons where required.

3.3.1 Performance and boundary forcing errors

Figure 3.1 shows the performance errors associated with temperature and precipitation, for DYN_ERA and STAT_ERA, for summer, when compared with CRU data. When compared to the gridded observational CRU data, STAT_ERA shows cold biases over most of North America, particularly the southernmost part. Some warm biases are noted for the high latitudes and parts of western US. DYN_ERA reduces the cold bias over Canada in summer, but in some areas, warm biases are enhanced compared to STAT_ERA and extend across central North America. Garnaud *et al.* (2014b) suggest that this is due to a strong albedo effect in forested regions, which leads to an increased sensible heat flux in DYN_ERA, resulting in warmer temperatures in summer compared to STAT_ERA.

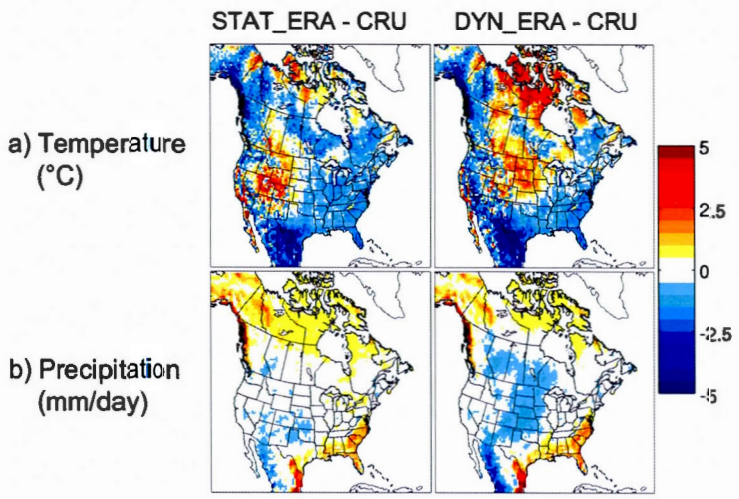

Figure 3.1 Differences between STAT_ERA and CRU (left) and DYN_ERA and CRU (right) mean summer (JJA) (a) temperature (°C) and (b) precipitation (mm/day) for the 1971–2000 period

With respect to precipitation, STAT_ERA overestimates across northern Canada and over south-eastern North America. A weak underestimation of precipitation in STAT_ERA is present over central US and southwestern coast. In DYN_ERA, the dry bias along the southwestern coast is enhanced and extends further north. This difference in performance errors in STAT_ERA and DYN_ERA is largely due to the differences in LAI in the two simulations, as suggested in Garnaud *et al.* (2014b).

The boundary forcing errors (BFE) are depicted in Fig. 3.2, which shows the differences between the DYN_RCP45 (STAT_RCP45) and DYN_ERA (STAT_ERA), for the 1971–2000 period, for mean summer temperature and precipitation. With respect to temperature, both STAT_RCP45 and DYN_RCP45 show positive BFE across most of Canada and northern US, and the error is larger in STAT_RCP45. This is consistent with the warmer temperatures in the driving CanESM2 as reported in Separovic *et al.* (2013). Weak negative BFE can be seen over Alaska and south-western USA. Regarding precipitation, the BFEs in both STAT_RCP45 and DYN_RCP45 are negative across

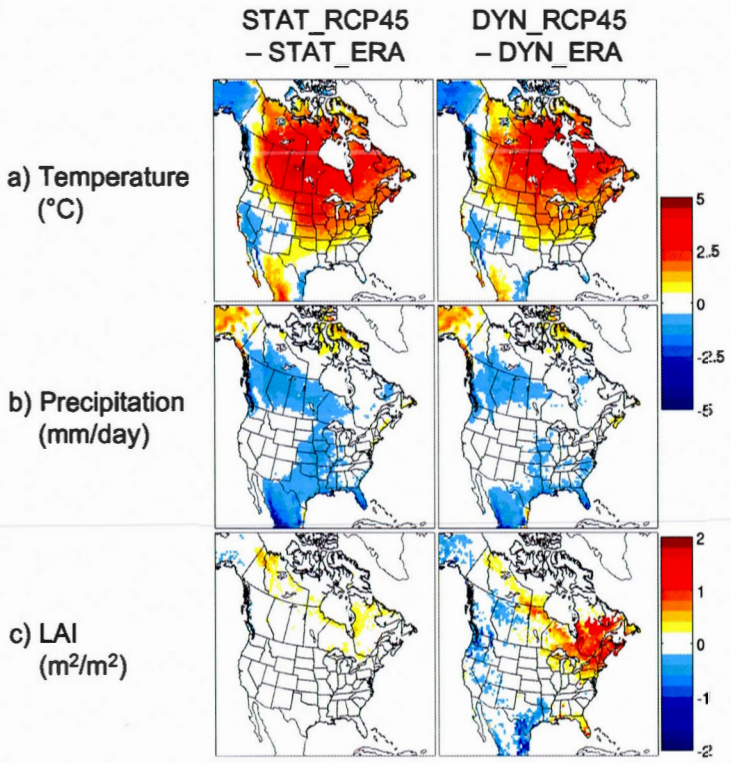

Figure 3.2 Differences between DYN_RCP45 and DYN_ERA simulated mean summer (JJA) (a) temperature (°C), (b) precipitation (mm/day), and (c) leaf area index (m^2/m^2) for the 1971–2000 period

most of North America, except over high-latitudes where positive BFE are present.

The differences in precipitation and temperature are reflected in the state of the biosphere (Fig. 3.2c), mostly in DYN_RCP45. Positive BFE in temperature for the mid- to high-latitudes lead to positive BFE in LAI, mostly over eastern Canada. Similarly, regions with negative BFE in LAI in DYN_RCP45 generally are somewhat co-located with regions of negative BFE in temperature. Furthermore, negative BFE in LAI over the southern part of the domain corresponds to the region with negative BFE in precipitation. This information is useful when interpreting confidence associated with projected changes.

3.3.2 Projected changes to biosphere characteristics

Projected changes in the biosphere productivity and biomass are presented here for DYN_RCP45 and DYN_RCP85 simulations. Note that STAT_RCP45 and STAT_RCP85 simulations have fixed values of vegetation biomass and maximum LAI, and do not model vegetation productivity. Since biosphere is the main focus of this study, projected changes in the biosphere are assessed before the impact of the biosphere on climate is analysed.

In response to rising atmospheric CO_2 concentrations and climate change, the length of the growing season increases, in line with other studies (e.g. Richardson *et al.*, 2013). Figure 3.3 represents the phenological leaf onset for broadleaf cold deciduous trees across North America in Julian days. Earlier leaf onset in future 2071–2100 period for both DYN_RCP45 and DYN_RCP85, particularly for the mid- to high-latitudes, can be noted. The mean change in leaf onset over North America in DYN_RCP45 is 21 days earlier than the historical period, while it is 27 days in DYN_RCP85. The simulated leaf onset in DYN_RCP85 can be up to 25 days earlier compared to DYN_RCP45 over south-eastern Canada, along the Canadian west coast and high altitudes. No significant changes to leaf onset dates are noticed for southerly regions, as expected, since broadleaf cold deciduous trees are mostly mostly fully-leaved throughout the year due to year-long favourable

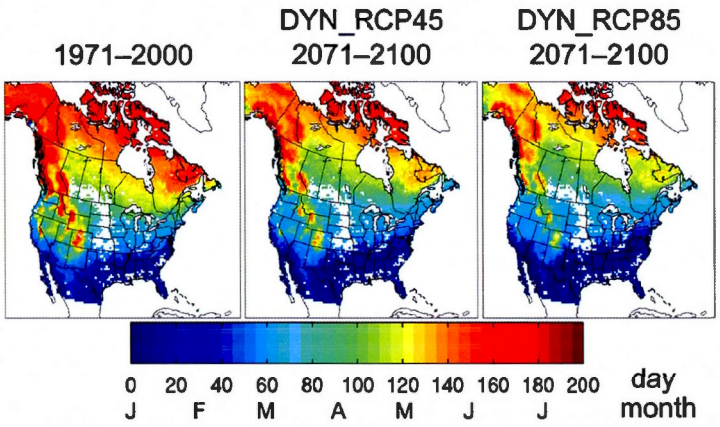

Figure 3.3 Average julian day of leaf onset for broadleaf cold deciduous trees for (a) current 1971–2000 period for DYN_RCP45, and future 2071–2100 period for (b) DYN_RCP45 and (c) DYN_RCP85 simulations.

temperature conditions, in the current 1971–2000 and future 2071–2100 periods.

The above noted extension of the growing season in future climate leads to higher annual productivity of vegetation and therefore biomass (Fig. 3.4). The largest increases are noted over the forested areas of eastern North America, particularly in DYN_RCP85. It is however interesting to note that for some parts of southeast US in DYN_RCP85, the gross primary productivity (GPP) in future (2071–2100) is lower than in DYN_RCP45, which suggests that the conditions for optimum photosynthesis are not met in this region in DYN_RCP85. This coastal region is mostly covered by evergreen needleleaf trees, and this PFT is subject to heat stress above 34°C. The heat stress threshold temperatures for broadleaves and crops are 37°C and 42°C, respectively. Thus, above 34°C needleleaf evergreen trees decrease their photosynthesis rate, and thus decrease their productivity, which is reflected in GPP, NPP, maximum LAI and biomass.

Figure 3.5a shows the trends in net primary productivity (NPP) in DYN_RCP45 and DYN_RCP85 over the 1971–2100 period. Most of the significant trends in both simulations are positive, indicating an increase in carbon uptake, particularly over eastern

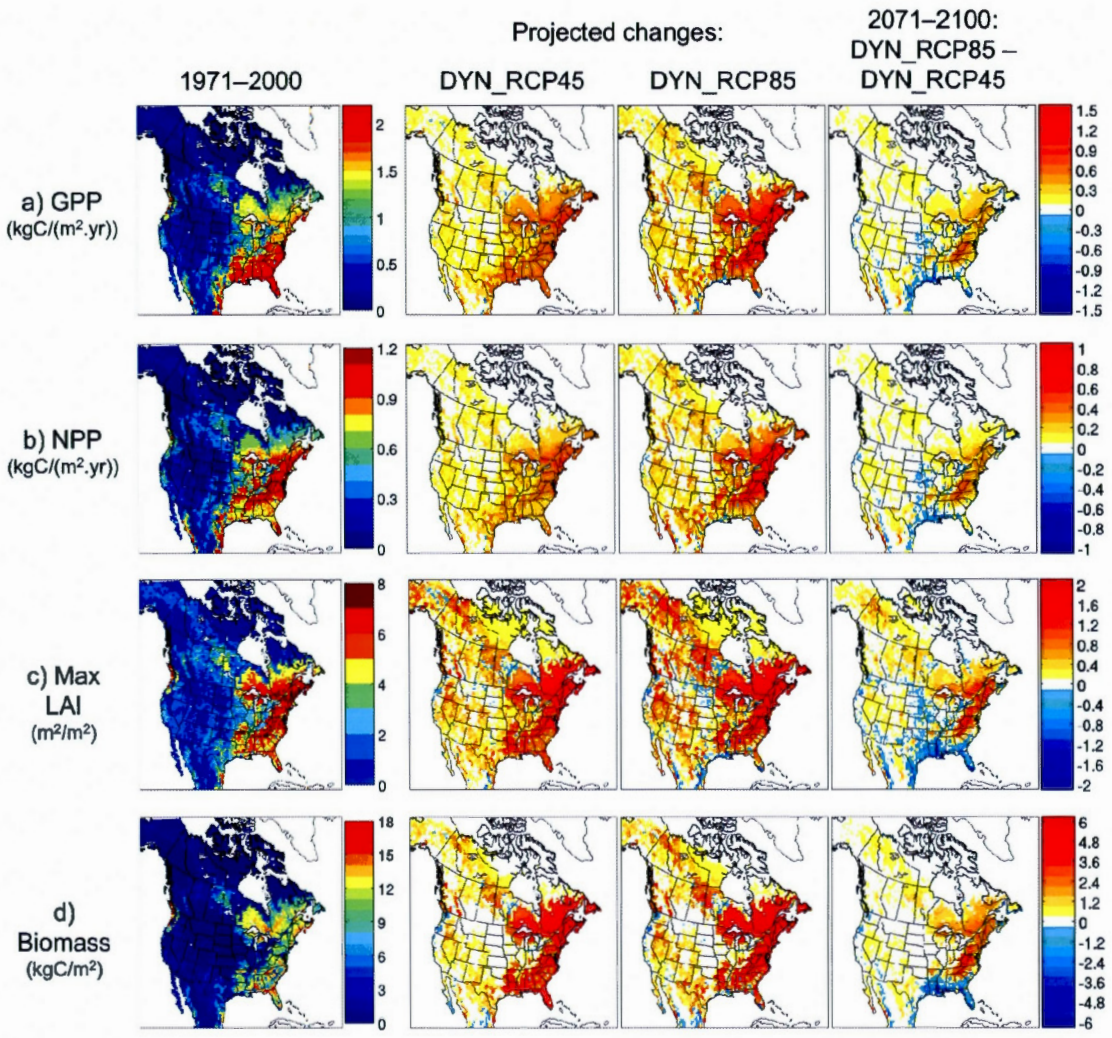

Figure 3.4 Average value in current 1971–2000 period for DYN_RCP45 (1^{st} column), projected change in DYN_RCP45 (2^{nd} column) and DYN_RCP85 (3^{rd} column), and differences between DYN_RCP85 and DYN_RCP45 (4^{th} column) in the future 2071–2100 period of the (a) gross primary productivity (GPP ; kgC.m^{-2}.yr^{-1}), (b) net primary productivity (NPP ; kgC.m^{-2}.yr^{-1}), (c) maximum LAI (m^2.m^{-2}) and (d) total vegetation biomass (kgC.m^{-2})

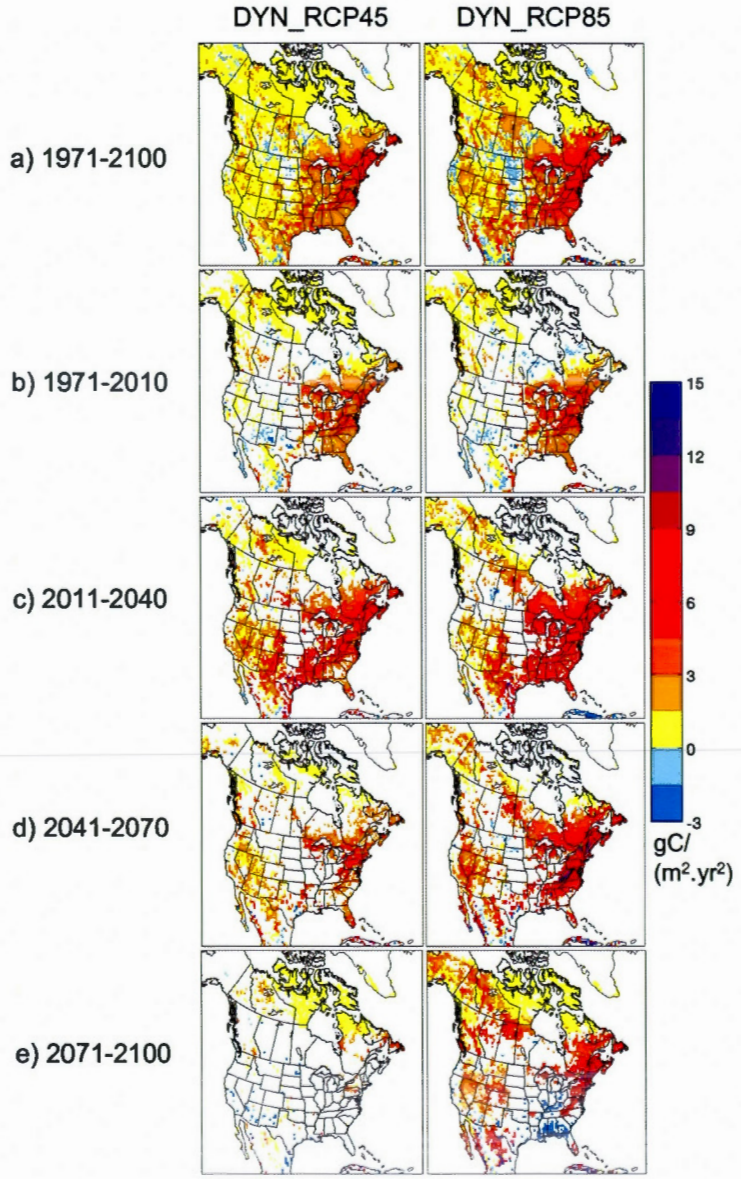

Figure 3.5 Trends in NPP (in $gC.m^{-2}.yr^{-2}$) for (a) 1971–2100, (b) 1971–2010, (c) 2011–2040, (d) 2041–2070 and (e) 2071–2100 periods for grid cells where trends are significant at α=5% significance level for the DYN_RCP45 (left) and DYN_RCP85 (right) simulations.

North America. However, studying trends over a long period is not representative of shorter periods. Thus, Figs. 3.5 b-d represent the trends in NPP for four 30- to 40-year time slices within the 1971–2100 period. The results are different from Figure 3.5a and show the evolution of NPP trends through time.

For DYN_RCP45, maximum positive trends are noted for the 2011–2040 period, following which smaller trends are noted for the 2041–2070 and 2071–2100 periods. This corresponds well with the evolution of atmospheric CO_2 concentrations, which decreases its positive trend around 2065 in RCP4.5. At this point, the beneficial effect of CO_2 fertilization is subdued by the continually rising temperatures causing heat and water stress to the biosphere. In DYN_RCP85, however, NPP trends continue to increase through to 2070, except over southern US. Although CO_2 concentrations continue to rise, in southern latitudes, vegetation is subject to heat stress, which reduces photosynthesis. Trends in NPP even turn negative over southeast USA during the 2071–2100 period, as reflected in Figs. 3.4b and 3.5e. Interestingly, trends in DYN_RCP85 simulated NPP in mid to high latitudes and over the Rocky Mountains increase significantly throughout the simulation but not in DYN_RCP45. These regions are where the largest increase in growing season length occur in DYN_RCP85, which favors vegetation.

3.3.3 Impact of the biosphere on future climate

Projected changes to mean summer temperature and precipitation for STAT_RCP45, STAT_RCP85, DYN_RCP45 and DYN_RCP85 are presented. Figure 3.6 shows that, as expected, temperatures increase throughout North America, with an average of 3.5°C in STAT_RCP45, 3.9°C in DYN_RCP45, 5.0°C in STAT_RCP85 and 5.6°C in DYN_RCP85. Differences between projected changes based on simulations with dynamic and static vegetation (i.e., Δ_{DYN} and Δ_{STAT}) show that vegetation dynamics cause an albedo-mediated warming enhancement in the northern regions (left column of Fig. 3.6), in line with other studies (Bonan *et al.*, 1992; Notaro *et al.*, 2006; Loranty *et al.*, 2014), for both RCP scenarios. In these regions, an increase in maximum LAI in future climate, as seen in Fig. 3.4, leads to reduced land-surface albedo, and the-

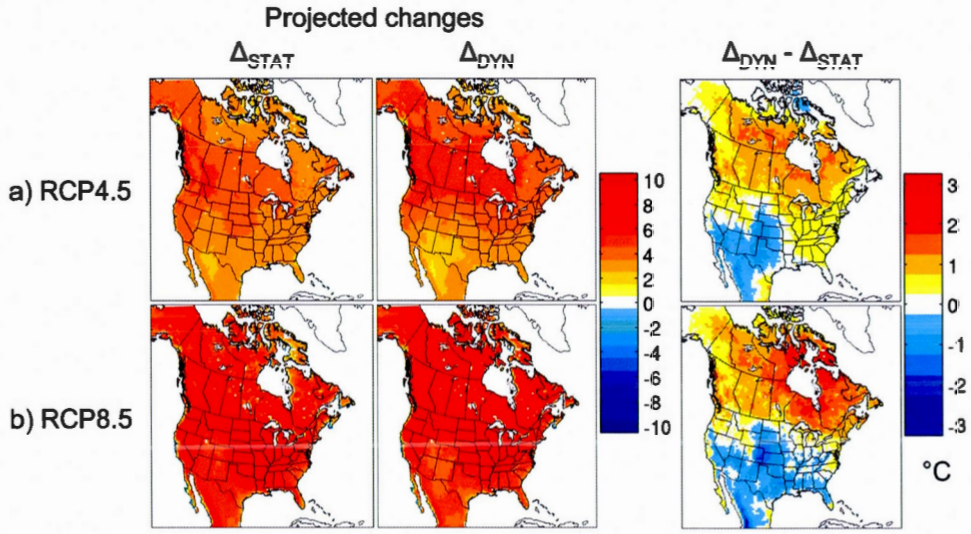

Figure 3.6 Summer (JJA) mean temperature (°C) for (a) projected change by 2071–2100 in STAT_RCP45 (1^{st} column) and DYN_RCP45 (2^{nd} column), and their differences (3^{rd} column), and (b) projected change by 2071–2100 in STAT_RCP85 (1^{st} column) and DYN_RCP85 (2^{nd} column), and their differences (3^{rd} column).

refore to an increase in sensible heat flux (figures not shown). This effect is stronger in DYN_RCP85 due to the larger increase in maximum LAI for the northern regions, compared to DYN_RCP45. In more southerly regions, there is a warming attenuation in DYN_RCP45 and DYN_RCP85, with respect to STAT_RCP45 and STAT_RCP85, respectively, due to hydrological feedbacks related to an increase in latent heat flux (figure not shown).

The difference in projections between static and dynamic vegetation simulations over eastern US for the 2071–2100 period varies with the RCP scenario. In DYN_RCP45, vegetation dynamics amplifies climate warming due to an amplification of sensible heat flux increase, compared to STAT_RCP45. On the other hand, in DYN_RCP85, vegetation dynamics attenuates climate warming through a general attenuation of projected increase in sensible heat flux. For this region, results thus suggest that the contribution

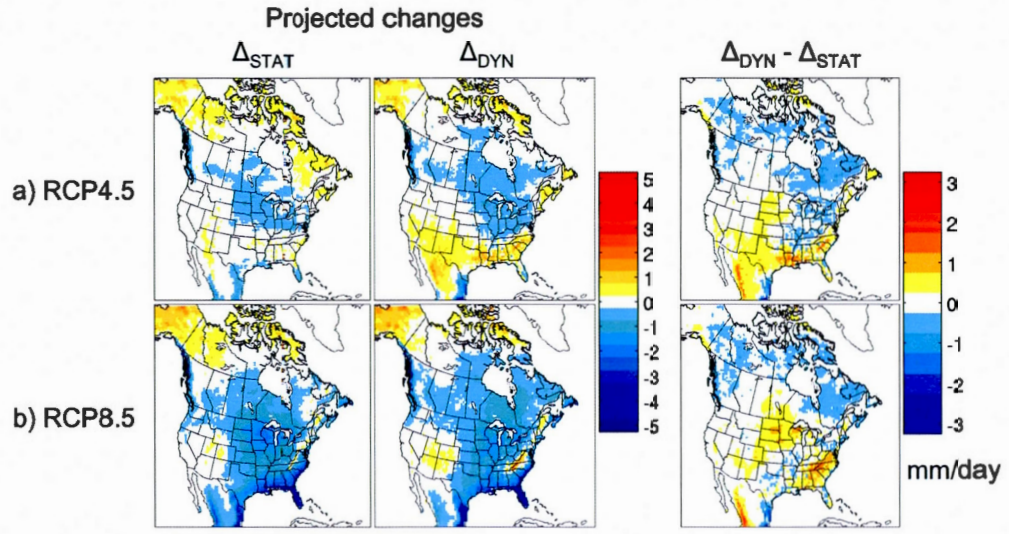

Figure 3.7 Summer (JJA) precipitation (mm/day) for (a) projected change by 2071–2100 in STAT_RCP45 (1^{st} column) and DYN_RCP45 (2^{nd} column), and their differences (3^{rd} column), and (b) projected change by 2071–2100 in STAT_RCP85 (1^{st} column) and DYN_RCP85 (2^{nd} column), and their differences (3^{rd} column).

of the biosphere to climate warming depends on the extent of the warming itself.

The impact of vegetation dynamics on precipitation is less obvious than on temperature. Nevertheless, Fig. 3.7 shows a notable decrease in precipitation in both RCP8.5 scenario simulations, particularly along the Gulf coast. This decrease is slightly attenuated in DYN_RCP85 over the southern regions.

Figure 3.7 shows a decrease in precipitation for the future 2071–2100 period over most parts of North America in DYN_RCP85 and over northeastern North America in DYN_RCP45. The trends in maximum LAI in these regions however increases as can be seen in Fig. 3.4. This suggests that the water use efficiency (WUE; Drake *et al.*, 1997) of vegetation increases due to rising CO_2 concentrations in the atmosphere. Indeed, with increased CO_2 concentrations, vegetation can reduce the time during which the stomata are open, thus maintaining productivity while minimizing water loss.

Over south-eastern US, the projected increase in temperatures and decrease in precipitation for the 2071–2100 period in DYN_RCP85 are probably the cause of the decreasing trend in NPP shown in 3.5e. As mentioned earlier, the threshold temperature for optimum photosynthesis is 34°C in the case of needleleaf evergreen trees, which cover most of this region. During the future 2071–2100 period, this threshold temperature is often exceeded in summer in DYN_RCP85. Unfavorable temperature and precipitation conditions (Fig. 3.7) could lead to additional stress, which further reduces photosynthesis. In this region, the CO_2 fertilization effect does not compensate for the heat and water stress in DYN_RCP85, as it does in DYN_RCP45, in the future 2071–2100 period. This is reflected in the maximum LAI and the total vegetation biomass as well, as seen in Fig. 3.4 c-d.

3.3.4 Evolution of biosphere-atmosphere correlations

The correlations between the annual maximum LAI and mean spring/summer (MAM-JJA) temperature, and annual precipitation, for the current 1971–2000 and the future 2071–2100 periods are shown in Figs. 3.8 and 3.9. In the case of DYN_RCP45 and DYN_RCP85, the maximum LAI is the direct result of the temperature mainly in spring and summer and the precipitation throughout the year.

In STAT_RCP45 and STAT_RCP85, temperature determines the length of the growing season, while precipitation does not affect the biosphere (Garnaud *et al.*, 2014b). However, since the maximum LAI is prescribed in these two simulations, the correlations between maximum LAI and temperature and precipitation (Fig. 3.8a and Fig. 3.9a) are nearly non-existant.

During the 1971–2000 period in both DYN_RCP45 and DYN_RCP85 simulations, the correlations between maximum LAI and temperature (Fig. 3.8b) are negative over southernmost parts of North America. Two feedbacks between LAI and temperature - the thermal and hydrological - act in these regions, leading to negative correlations between the two variables, as was shown in Garnaud *et al.* (2014b). Vegetation is subject to

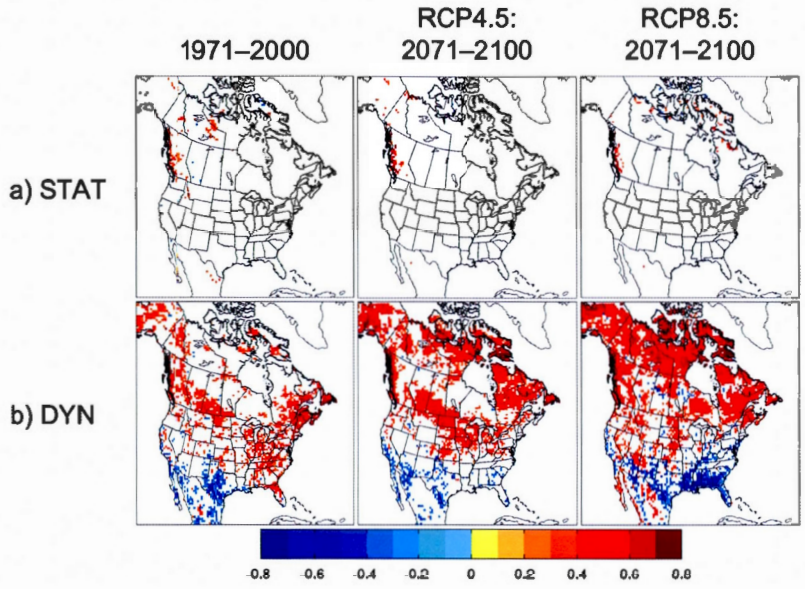

Figure 3.8 Spatial plots of the correlations between the annual maximum LAI and mean spring/summer (MAMJJA) temperature for the current 1971–2000 and future 2071–2100 periods for (a) STAT_RCP45 and STAT_RCP85 and (b) DYN_RCP45 and DYN_RCP85. Regions where correlations are not significant are shown in white; significance is calculated using the Student's t-test at 10% significance level

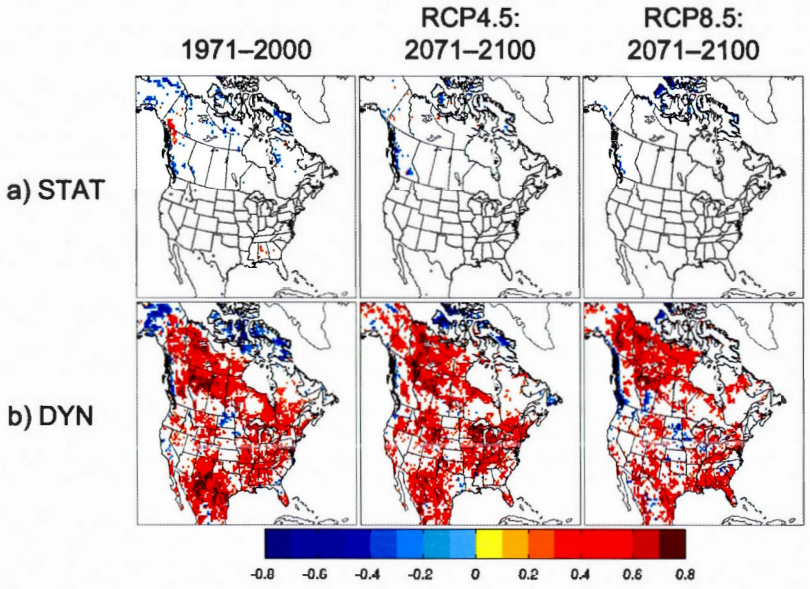

Figure 3.9 Spatial plots of the correlations between the annual maximum LAI and mean annual precipitation for the current 1971–2000 and future 2071–2100 periods for (a) STAT_RCP45 and STAT_RCP85 and (b) DYN_RCP45 and DYN_RCP85. Regions where correlations are not significant are shown in white; significance is calculated using the Student's t-test at 10% significance level

heat stress due to the thermal feedback between the biosphere and temperature, which consequently decreases vegetation productivity. The hydrological feedback is associated with an increase in LAI, leading to a decrease of sensible heat flux through an increase in latent heat flux, thus cooling the surface. The correlations are mostly positive in the mid to high latitudes, where vegetation benefits from warmer temperatures due to the lengthening of the growing season. This positive effect increases in the 2071–2100 period, particularly in the high latitudes, due to the large projected increase in temperatures.

For the 1971–2000 period, the correlations between the maximum LAI and precipitation are very strong with mainly positive values (Fig. 3.9b) for DYN_RCP45/DYN_RCP85. This is related to a positive LAI-precipitation feedback loop, with a positive precipitation anomaly boosting plant productivity and LAI, which leads to increased evapotranspira-

tion and possibly to increased amount of local rainfall. However, the strong maximum LAI-precipitation correlations are projected to decrease slightly in DYN_RCP85 : the average positive correlations in the 1971–2000 period is 0.47 and 0.45 in the 2071–2100 period. This is probably due to increasing atmospheric CO_2 concentrations and decreasing annual precipitation (data not shown), similarly to summer precipitation, both enhancing vegetation water-user efficiency.

In southeastern US in DYN_RCP85, the maximum LAI and precipitation are strongly and positively correlated (Fig. 3.9b) during the 2071–2100 period. In this region, one-year lagged correlations (Delire *et al.*, 2011; Garnaud *et al.*, 2014b) between these two variables (figures not shown), with precipitation leading maximum LAI and similarly maximum LAI leading precipitation, are generally found positive. This suggests that the long-term memory of both the atmosphere and the biosphere contribute to the decrease in maximum LAI in this region, due to the projected decrease in precipitation (Fig. 3.7b). To add on, the maximum LAI-temperature correlation is strongly negative (Fig. 3.8b), due to heat stress affecting the biosphere, hence the projected negative trends in NPP (Fig. 3.5e) in this region for the 2071–2100 period.

3.4 Summary and Conclusions

Projected changes to climate and biosphere characteristics and their interactions over North America in future 2071–2100 period with respect to current 1971–2000 period are studied. In particular, changes to vegetation in terms of phenology and productivity, and their role in modulating increasing GHG-mediated warming are investigated. This is achieved through four transient climate change simulations of CRCM5, which performs dynamical downscaling of the second generation Canadian Earth System Model (CanESM2) simulated data, for RCP4.5 and RCP8.5 radiation forcing scenarios. For each RCP scenario, two CRCM5 simulations are performed - one with static vegetation and the other with dynamic vegetation (i.e. CTEM) - for the 1950–2100 period over North America.

The warmer temperatures in future climate, particularly for northern latitudes, result in earlier leaf onset and therefore to a longer growing season in the two dynamic vegetation simulations (DYN_RCP45 and DYN_RCP85). This causes an increase in vegetation productivity and biomass, strongest in DYN_RCP85, but the increase in productivity reaches a plateau by the end of the 21st century and the net primary productivity starts exhibiting a negative trend over eastern US by the end of the century in the DYN_RCP85 simulation. This suggests that, in this region, the beneficial effect of CO_2 fertilization is subdued by the continually rising temperatures causing heat and water stress to the biosphere. Over the rest of North America however, and particularly up until the middle of the 21st century, the negative temperature effect is more than counterbalanced by the positive effect of CO_2. Claesson and Nycander (2013) were lead to similar conclusions although their study was performed for selected geographical sites around the world.

Vegetation dynamics allows biosphere to respond to climate change through feedbacks and interactions, which in turn modulate climate change. Thus, in DYN_RCP45 and DYN_RCP85 simulations compared to STAT_RCP45 and STAT_RCP85, respectively, an albedo-mediated warming enhancement occurs in the northern regions, in line with other studies (Bonan *et al.*, 1992; Notaro *et al.*, 2006; Loranty *et al.*, 2014), due to the increase in maximum LAI over time in the dynamic vegetation simulations. In more southerly regions, however, vegetation dynamics leads to a warming attenuation due to hydrological feedbacks related to an increase in latent heat flux. The impact of vegetation dynamics on precipitation, however, is less obvious than on temperature.

Interestingly, summer precipitation decreases with time over most regions in DYN_RCP85 and over northeastern North America in DYN_RCP45. However, large parts of the continent show an increase in maximum LAI, particularly in DYN_RCP85. This suggests that vegetation enhances its water use efficiency with time due to rising CO_2 concentrations in the atmosphere, similarly to what was reported in Port *et al.* (2012). Indeed, with increased CO_2 concentrations, vegetation can reduce the time during which the stomata are open, thus maintaining productivity while minimizing water loss.

The projected changes in biosphere-atmosphere correlations show decreasing maximum LAI-precipitation correlations in the 2071–2100 period over low to mid latitudes in the two dynamic vegetation simulations, particularly in DYN_RCP85. This is due an enhancement of vegetation water-use efficiency.

Although this study shows that vegetation dynamics could significantly contribute to climate change depending on the region, its impact remains small compared to the atmospheric CO_2 forcing. However, the simulations performed here do not take into account competition between PFTs and as a result the fractional coverage of PFT does not change over time. As shown by Smith *et al.* (2011), competition is important to model vegetation shifts and changing tree line which can have non-negligible effects on temperature and precipitation through biophysical feedbacks, particularly in the context of a changing climate. Indeed, the simulation of competition amongst PFTs could result in a northward expansion of the tree cover in the high latitudes, which would further reduce the albedo and lead to additional warming (O'ishi and Abe-Ouchi, 2009; Port *et al.*, 2012; Loranty *et al.*, 2014).

Furthermore, the present study does not take land-use change, such as deforestation, afforestation and contraction of croplands, into account, which would likely impact the strength of the feedbacks investigated in our study. For example, Trail *et al.* (2013) show that reforestation of former cropland over south-eastern US would tend to warm the surface by an additional 0.5K by the year 2050.

Although biogeochemical feedbacks are not considered in this study, results suggest an increase in the terrestrial carbon sink due to future increases in LAI and biomass. It must be noted that the effects of nitrogen deposition (Holland *et al.*, 1997) and land use change, such as the abandonment of croplands over eastern US, both of which are not included in these simulations, would be expected to yield an additional carbon sink (Reay *et al.*, 2008; Arora and Boer, 2010).

CONCLUSION

The main scientific objective of this thesis was to study biosphere-climate interactions over North America in current and future climates. This was achieved using a regional climate model framework, given the limited observations over the region. Thus, the main tool used is the Canadian Regional Climate Model (CRCM5) with the Canadian Terrestrial Ecosystem Model (CTEM). The main findings from this research are summarized below, along with some of the limitations of the methodology and possible research lines to explore in the near future.

At the start of the research, no dynamic vegetation model was implemented in CRCM5. The dynamic vegetation model CTEM was implemented in CRCM5 to better represent biosphere-atmosphere interactions. Prior to implementing CTEM, a necessary step was to evaluate the performance of this component. The first part of the research presented in this thesis therefore focused on evaluating CLASS/CTEM in offline simulations. The offline simulations were driven with NCEP and ERA40 reanalysis data from 1958 to 2001 over North America and simulated quantities were compared with observation- and model-based estimates. Important differences between the two driving climate datasets, as well as the inconsistencies in the observed data, coming from different sources, used for model validation made the task of model assessment somewhat difficult. However, the simulations were able to provide broad insights into the behavior of the CTEM model. The model was able to reproduce the broad spatial patterns of LAI, woody biomass, NPP and GPP as well their meridional distributions. The simulated values of carbon use efficiency also compared reasonably well with observation-based estimates of DeLucia *et al.* (2007).

Some weaknesses, however, were noticed in simulated quantities. In particular, the simulated LAI was low compared to the ISLSCP II satellite based estimates, although

Gibelin *et al.* (2006) show that the LAI estimates in this product are higher than other satellite-based estimates, especially for the boreal forest. Also, the model did not capture the GPP of the productive needleleaf evergreen forests along the interior West Coast of the United States. This model limitation was also obvious in the comparisons of simulated woody biomass with their observation-based estimates. Despite its generally higher than observed woody biomass, the model was not able to simulate enough woody biomass along the United States West Coast as well as in the interior British Columbia. The simulations were also used to assess the land carbon sink over the North American domain. Despite very different gross fluxes, the model yielded fairly similar estimates of the net atmosphere-land CO_2 flux with the two forcing datasets. The simulated sink of 0.5 Pg C/yr during the 1980s and 1990s compared well with other model-based estimates but was lower than the inversion-based estimates. This was expected since the simulations did not include land use change and the effect of nitrogen deposition. The analysis of spatial distribution of trends in simulated carbon pools and fluxes showed that the simulated carbon sink was driven primarily by NPP enhancements over eastern United States and the resulting carbon sequestration in the woody biomass.

Given the encouraging results, CRCM5 simulations were performed with CTEM. The impact of dynamic vegetation on CRCM5-simulated climate over North America for the 1971–2010 period was investigated by comparing two simulations – CRCM5_STAT with static vegetation represented by the land surface scheme CLASS and CRCM5_DYN which models vegetation as a dynamic component through CTEM coupled with CLASS. Both simulations were driven by ERA-40/ERA-Interim reanalysis at the lateral boundaries. Comparison of simulated and observed spatial distribution of the biosphere state, i.e. LAI, suggests that CRCM5_DYN, particularly in summer, better captures the distribution of the biosphere, except over western Canada where it underestimates the LAI, similarly to the results from the offline simulations. Peng *et al.* (2014) suggest that another needleleaf evergreen PFT, better adapted to this region's climate, is probably required.

The differences in LAI between CRCM5_DYN and CRCM5_STAT lead to differences

in surface albedo, SHF and LHF between the two simulations over various regions, which are reflected in the simulated temperature and precipitation fields. Comparison of temperature and precipitation in both simulations to those observed indicates that introduction of dynamic vegetation improves the performance of CRCM5 in some regions, although it introduces new biases in other regions, which are related, at least partly, to the underestimation of LAI. Nonetheless, dynamic vegetation enhances biosphere-atmosphere interactions, which are reflected in the higher values of correlation between atmosphere and biosphere variables. Dynamic vegetation also introduces long-term memory in CRCM5, estimated via lagged correlations between precipitation/temperature and LAI. In CRCM5_DYN, improved biosphere-atmosphere interactions and long-term memory leads to better interannual variability, particularly noticeable in the biosphere and atmosphere states during anomalously wet and dry years.

Having investigated biosphere-climate interactions in current climate, the next scientific question that was addressed was how biosphere characteristics change in future climate and how they modulate climate change. Thus, projected changes to climate and biosphere characteristics and their interactions over North America in future 2071–2100 period with respect to current 1971–2000 period were studied using transient climate change experiments of CRCM5, driven by CanESM2 for RCP4.5 and RCP8.5. In particular, changes to vegetation in terms of phenology and productivity, and their role in modulating increasing GHG-mediated warming were investigated. Results show that vegetation responds to climate change through feedbacks and interactions, which in turn modulates climate change. In fact, the extension of the growing season in future climate in dynamic vegetation simulations, due to increasing temperatures, leads to greater vegetation productivity and biomass. In turn, vegetation dynamics induces an albedo-mediated warming enhancement in the northern latitudes and a warming attenuation due to hydrological feedbacks in more southern regions. The projected increase in summer LAI, despite a significant decrease in summer precipitation, suggests that vegetation enhances its water use efficiency, which is also noted in the projected LAI-precipitation correlations. However, vegetation productivity projections indicate weake-

ning trends by the end of the 21st century. This suggests that the negative effects of increased temperature and decreased precipitation on vegetation will override the effect of CO_2 fertilization on the biosphere.

In summary, this study, for the first time, provided useful insights related to the added value of dynamic vegetation in a regional climate model, and more specifically in CRCM5, as well as the nature and variability of biosphere-atmosphere interactions over North America in current and future climate. It opens up multiple avenues that require further study to improve our current understanding of biosphere-climate interactions, which would enhance the quality of climate projections.

Limitations and Future Work

One of the limitations of this research is that competition amongst PFTs is not simulated in the version of CTEM that was used here. Since the competition sub-module in CTEM (Arora and Boer, 2006) will soon be functional in the coupled CRCM5/CLASS/CTEM framework, research would have to be undertaken with the new version of CTEM in order to evaluate its performance in current climate with respect to observations and to assess projected changes to biosphere-climate interactions in future. Indeed, competition between PFTs has been shown to have a probable impact on the amplitude of climate change, as vegetation shifts and changing tree line can have non-negligible effects on temperature and precipitation through biophysical feedbacks, particularly in the context of a changing climate (O'ishi and Abe-Ouchi, 2009; Smith *et al.*, 2011; Port *et al.*, 2012). Thus, simulations using the new version of CTEM (including competition) would allow a more complete understanding of the interactions between a fully dynamic biosphere and the atmosphere. In addition, it would be interesting to compare these simulations to those from the present research in order to assess the impact of changing fractional areas of PFTs on climate compared to fixed fractional areas.

In addition, the simulation of fire was not used in this research. However, Wotton *et al.* (2010) suggest that fire occurrence in the Canadian boreal forest could increase by 75%

to 140% by the end of the century. Warmer temperatures lead to longer fire season, more lightning activity and drier fuels that would contribute to fire occurrence and spread. Therefore, there is a potential for positive feedback as boreal ecosystems contain large proportions of the world's terrestrial carbon. Thus, simulating forest fires might prove crucial to a better estimation of projected changes in the terrestrial carbon sink.

Although CTEM simulates leaf and stem fall as well as root mortality, all of which contribute to the litter carbon pool and ultimately to the soil organic matter, CLASS does not take this information into account. However, soil composition has been shown to have a significant impact on the thermal and moisture regimes of soils, which then can modify energy and moisture partitioning at the surface (Paquin and Sushama, 2014). Thus, this inconsistency would also have to be addressed.

Due to limited computer resources and time, the number of simulations that could be performed and analysed were limited. Now that a tool is available to study biosphere-atmosphere interactions, several interesting experiments could be performed. For instance, it would also be useful to distinguish the impact of rising temperatures from the impact of rising CO_2 on the biosphere in climate change simulations, both factors strongly influencing the biosphere, and its evolution in time and space, and the resulting feedbacks to the atmosphere. Two more CRCM5 simulations with CTEM would have to be performed, corresponding to RCP4.5 and RCP8.5, with fixed current atmospheric CO_2 concentrations affecting the biosphere only. These two simulations could then be compared to DYN_RCP45 and DYN_RCP85 (from Chapter III), respectively. This would enhance our understanding of the sensitivity of the biosphere to the evolution of different environmental conditions.

It would also be interesting to run the coupled model CRCM5/CLASS/CTEM at different resolutions in order to test the sensitivity of the simulated biosphere-atmosphere interactions and feedbacks to model resolution and to identify the added value of using a high-resolution RCM (vs. a GCM). Moreover, in this study, the projected changes to biosphere and biosphere-atmosphere interactions are based on a single RCM driven by a

single GCM. Given the various uncertainties associated with RCMs, such as structural and boundary forcing uncertainties, it is important to extend this study to a multimodel ensemble. Furthermore, since technologies evolve rapidly, ongoing validation of the model with newly produced observation datasets would also be required.

REFERENCES

Alcaraz-Segura, D., Chuvieco, E., Epstein, H., Kasischke, E. and Trishchenko, A. (2010). Debating the greening vs. browning of the North American boreal forest : differences between satellite datasets. *Global Change Biology*, *16*(2), 760–770. http://dx.doi.org/DOI:10.1111/j.1365-2486.2009.01956.x

Arora, V. K. (2003). Simulating energy and carbon fluxes over winter wheat using coupled land surface and terrestrial ecosystem models. *Agricultural and Forest Meteorology*, *118*(1-2), 21–47. http://dx.doi.org/DOI:10.1016/S0168-1923(03)00073-X

Arora, V. K. and Boer, G. J. (2003). A representation of variable root distribution in dynamic vegetation models. *Earth Interactions*, *7*(6).

Arora, V. K. and Boer, G. J. (2005). A parameterization of leaf phenology for the terrestrial ecosystem component of climate models. *Global Change Biology*, *11*(39-59). http://dx.doi.org/DOI:10.1111/j.1365-2486.2004.00890.x

Arora, V. K. and Boer, G. J. (2006). Simulating competition and coexistence between plant functional types in a dynamic vegetation model. *Earth Interactions*, *10*.

Arora, V. K. and Boer, G. J. (2010). Uncertainties in the 20th century carbon budget associated with land use change. *Global Change Biology*, *16*, 3327–3348. http://dx.doi.org/10.1111/j.1365-2486.2010.02202.x

Arora, V. K., Boer, G. J., Christian, J., Curry, C., Denman, K., Zahariev, K., Flato, G., Scinocca, J., Merryfield, W. and Lee, W. (2009). The effect of terrestrial photosynthesis down-regulation on the 20th century carbon budget simulated with the CCCma Earth System Model. *Journal of Climatology*, *22*(6066-6088). http://dx.doi.org/10.1175/2009JCL13037.1

Beer, C., Reichstein, M., Tomelleri, E., Ciais, P., Carvalhais, M. J. N., Rödenbeck, C., Arain, M., Baldocchi, D., Bonan, G., Bondeau, A., Cescatti, A., Lasslop, G., Lomas, M., Luyssaert, S., Margolis, H., Oleson, K., Roupsard, O., Veenendaal, E., Viovy, N., Williams, C., Woodward, F. and Papale, D. (2010). Terrestrial gross carbon dioxide uptake : Global distribution and covariation with climate. *Science*, *329*, 834–838. http://dx.doi.org/10.1126/science.1184984

Belair, S., Mailhot, J., Girard, C. and Vaillancourt, P. (2005). Boundary layer and shallow cumulus clouds in a medium-range forecast of a large-scale weather system. *Monthly Weather Review*, *133*, 1938–1960.

Benoit, R., Cote, J. and Mailhot, J. (1989). Inclusion of a TKE boundary layer parameterization in the Canadian regional finite-element model. *Monthly Weather Review, 117*, 1726–1750.

Betts, A., Ball, J., Beljaars, A., Miller, M. and Viterbo, P. (1996). The land surface-atmosphere interaction : a review based on observational and global modeling perpectives. *Journal of Geophysical Research, 101*, 7209–7225.

Bonan, G. (2008). *Ecological Climatology concepts and applications, 2nd edition.* Cambridge University Press.

Bonan, G., Levis, S., Sitch, S., Vertenstein, M. and Oleson, K. (2003). A dynamic global vegetation model for use with climate models : concepts and description of simulated dynamics. *Global Change Biology, 9*, 1543–1566.

Bonan, G., Pollard, D. and Thompson, S. (1992). Effects of boreal forest vegetation on global climate. *Nature, 359*, 716–718.

Box, E. (1996). Plant functional types and climate at a global scale. *Journal of Vegetation Science, 7*(309-320). http://dx.doi.org/10.2307/3236274

Brovkin, V. (2002). Climate-vegetation interaction. *Journal de Physique, 12*, 57–82.

Champeaux, J., Masson, V. and Chauvin, F. (2005). ECOCLIMAP : a global database of land surface parameters at 1km resolution. *Meteorological Applications, 12*(29-32). http://dx.doi.org/10.1017/S1350482705001519

Choudhury, B. (2000). Carbon use efficiency, and net primary productivity of terrestrial vegetation. *Advances in Space Research, 26*(7), 1105–1108. http://dx.doi.org/10.1016/S0273-1177(99)01126-6

Claesson, J. and Nycander, J. (2013). Combined effect of global warming and increased CO2-concentration on vegetation growth in water-limited conditions. *Ecological Modelling, 256*, 23–30.

Collatz, G., Ball, J., Grivet, C. and Berry, J. (1991). Physiological and environmental regulation of stomatal conductance, photosynthesis and transpiration : A model that includes a laminar boundary layer. *Agricultural and Forest Meteorology, 54*, 107–136. http://dx.doi.org/10.1016/0168-1923(91)90002-8

Collatz, G., Ribas-Carbo, M. and Berry, J. (1992). Coupled photosynthesis-stomatal conductance model for leaves of C4 plants. *Functional Plant Biology, 19*(5), 519–538. http://dx.doi.org/10.1071/PP9920519

Côté, J., Gravel, S., Methot, A., Patoine, A., Roch, M. and et al. (1998). The Operational CMC-MRB Global Environmental Multiscale (GEM) Model. Part I : design considerations and formulation. *Monthly Weather Review, 126*, 1373–1395.

Cox, P. (2001). Description of the TRIFFID Dynamic Global Vegetation Model. *Hadley Center technical note*, *24*, 16.

Cox, P., Betts, R., Bunton, C., Essery, R., Rowntree, P. and Smith, J. (1999). The impact of new land surface physics on the GCM simulation of climate and climate sensitivity. *Climate Dynamics*, *15*, 183–203.

Cox, P., Betts, R., Jones, C., Spall, S. and Totterdell, I. (2000). Acceleration of global warming due to carbon-cycle feedbacks in a coupled climate model. *Nature (Letters to Nature)*, *408*, 184–187.

Cramer, W., Bondeau, A., Woodward, F., Prentice, I., Betts, R., Brovkin, V., Cox, P., Fisher, V., Foley, J., Friend, A., Kucharik, C., Lomas, M., Ramankutty, N., Sitch, S., Smith, B., White, A. and Young-Molling, C. (2001). Global response of terrestrial ecosystem structure and function to CO2 and climate change : results from six dynamic global vegetation models. *Global Change Biology*, *7*(4), 357–373.

Crevoisier, C., Sweeney, C., Gloor, M., Sarmiento, J. and Tans, P. (2010). Regional US carbon sinks from the three-dimensional atmospheric CO2 sampling. *PNAS*, *107*(43), 18348–18353. `http://dx.doi.org/10.1073/pnas.0900062107`

Dee, D., Uppala, S., Simmons, A. and et al. (2001). The ERA-Interim reanalysis : configuration and performance of the data assimilation system. *Quarterly Journal of the Royal Meteorological Society*, *137*, 553–597. `http://dx.doi.org/doi:10.1002/qj.828`

Delage, Y. (1997). Parameterising sub-grid scale vertical transport in atmospheric models under statically stable conditions. *Boundary-Layer Meteorology*, *82*, 23–48.

Delage, Y. and Girard, C. (1992). Stability functions correct at the free convection limit and consistent for both the surface and Ekman layers. *Boundary-Layer Meteorology*, *58*, 19–31.

Delire, C., Foley, J. and Thompson, S. (2004). Long-term variability in a coupled atmosphere-biosphere model. *Journal of Climate*, *17*, 3947–3959.

Delire, C., Noblet-Ducoudre, N. D., Sima, A. and Gouirand, I. (2011). Vegetation dynamics enhancing long-term climate variability confirmed by two models. *Journal of Climate*, *24*(9), 2238–2257.

DeLucia, E., Drake, J., Thomas, R. and Gonzalez-Melers, M. (2007). Forest carbon use efficiency : is respiration a constant fraction of gross primary production ? *Global Change Biology*, *13*, 1157–1167. `http://dx.doi.org/10.1111/j.1365-2486.2007.01365.x`

den Hoof, C. V., Hanert, E. and Vidale, P. (2011). Simulating dynamic crop growth with an adapted land surface model- JULES-SUCROS : Model development and validation. *Agricultural and Forest Meteorology*, *151*, 137–153. `http://dx.doi.org/10.1016/j.agrformet.2010.09.011`

Denman, K. and et al. (2007). Couplings between changes in the climate system and biogeochemistry. Dans S. S. et al. (dir.). *Climate Change 2007 : The physical Science Basis. Contributions of working group I to the fourth Assessment report of the Intergovernmental Panel on Climate Change.*, 499–587. Cambridge University Press.

Dong, J., Kaufmann, R., Myneni, R., Tucker, C., Kauppi, P., Liski, J., Buermann, W., Alexeyev, V. and Hughes, M. (2003). Remote sensing estimates of boreal and temperate forest woody biomass : carbon pools, sources, and sinks. *Remote Sensing of Environment, 84*(3), 393–410.

Drake, B., Gonzalez-Meler, M. and Long, S. (1997). More efficient plants : a consequence of rising atmospheric CO2. *Annual Review of Plant Physiology and Plant Annual Review of Plant Physiology and Plant Molecular Biology, 48*, 609–639.

Dubreuil, V., Debortoli, N., Funatsu, B., Venelec, V. and Durieux, L. (2012). Impact of land-cover change in the Southern Amazonia climate : a case study for the region of Alta Floresta, Mato Grosso, Brazil. *Environmental Monitoring and Assessment, 184*, 877–891.

Farquhar, G., von Caemmerer, S. and Berry, J. (1980). A biochemical model of photosynthetic CO2 assimilation in leaves of C3 species. *Planta, 149*, 78–90.

Fischer, E., Seneviratne, S., Luthi, D. and Schar, C. (2007). Contribution of land-atmosphere coupling to recent European summer heat waves. *Geophysical Research Letters, 34*(L06707).

Foley, J., Costa, M., Delire, C., Ramankutty, N. and Snyder, P. (2003). Green surprise? How terrestrial ecosystems could affect earth's climate. *Frontiers in Ecology and the Environment, 1*(1), 38–44.

Foley, J., Prentice, I., Ramankutty, N., Levis, S., Pollard, D. and andA Haxeltine, S. S. (1996). An integrated biosphere model of land surface processes, terrestrial carbon balance, and vegetation dynamics. *Global Biogeochemical Cycles, 10*(4), 603–628.

Frantz, J. and Bugbee, B. (2005). Acclimation of plant populations to shade : Photosynthesis, respiration, and carbon use efficiency. *Journal of the American Society for Horticultural Science, 130*(6), 918–927.

Friedlingstein, P., Fung, I., Holland, E., John, J., Brasseur, G., Erickson, D. and Schimel, D. (1995). On the contribution of the biospheric CO2 fertilisation to the missing sink. *Global Biogeochemical Cycles, 9*, 541–556.

Friend, A., Stevens, A., Knox, R. and Cannell, M. (1995). A process-based terrestrial biosphere model of ecosystem dynamics (Hybrid v3.0). *Ecological Modelling, 95*, 249–287.

Garcia-Carreras, L. and Parker, D. (2011). How does local tropical deforestation affect rainfall? *Geophysical Research Letters, 38.*

Garnaud, C., Sushama, L. and Arora, V. (2014a). The effect of driving climate data on the simulated terrestrial carbon pools and fluxes. *International Journal of Climatology*, *34*, 1098–1110. http://dx.doi.org/10.1002/joc.3748

Garnaud, C., Sushama, L. and Verseghy, D. (2014b). Impact of interactive vegetation phenology on the Canadian RCM simulated climate over North America. *Climate Dynamics (accepted, under revision)*.

Garrigues, S., Lacaze, R., Baret, F., Morisette, J., Weiss, M., Nickeson, J., Fernandes, R., Plummer, S., Shabanov, N., Myneni, R., Knyazikhin, Y. and Yang, W. (2008). Validation and intercomparison of global leaf area index products derived from remote sensing data. *Journal of Geophysical Research*, *113*. http://dx.doi.org/10.1029/2007JG000635

Gibelin, A.-L., Calvet, J.-C., Roujean, J.-L., Jarlan, L. and Los, S. (2006). Ability of the land surface model ISBA-A-gs to simulate leaf area index at the global scale : Comparison with satellites products. *Journal of Geophysical Research*, *111*. http://dx.doi.org/10.1029/2005JD006691

Gobron, N., Pinty, B., Mélin, F., Taberner, M., Verstraete, M., Belward, A., Lavergne, T. and Widlowski, J.-L. (2005). The state of vegetation in Europe following the 2003 drought. *International Journal of Remote Sensing*, *26*(9), 2013–2020. http://dx.doi.org/10.1080/01431160412331330293

Hall, F., de Colstoun, E. B., Collatz, G., Landis, D., Dirmeyer, P., Betts, A., Huffman, G., Bounoua, L. and Meeson, B. (2006). The ISLSCP Initiative II global data sets : Surface boundary conditions and atmospheric forcings for land-atmosphere studies. *Journal of Geophysical Research*, *111*. http://dx.doi.org/10.1029/2006JD007366

Hansen, J. and Sato, M. (2001). Trends of measured climate forcing agents. *PNAS*, *98*, 14778–14783.

Hansen, J. and Sato, M. (2004). Greenhouse gas growth rates. *PNAS*, *101*, 16109–16114.

Hicke, J., Asner, G., Randerson, J., Tucker, C., Los, S., Birdey, R., Jenkins, J. and Field, C. (2002). Trends in North American net primary productivity derived from satellite observations, 1982-1998. *Global Biogeochemical Cycles*, *16*(2). http://dx.doi.org/10.1029/2001GB001550

Hickler, T., Smith, B., Prentice, I., Mjofors, K., Miller, P., Arneth, A. and Sykes, M. (2008). CO2 fertilization in temperate forest FACE experiments not representative of boreal and tropical forests. *Global Change Biology*, *14*, 1531–1542.

Holland, E., Braswell, B., Lamarque, J.-F., Townsend, A., Sulzman, J., Müller, J.-F., Dentener, F., Brasseur, G., Levy, H.-I., Penner, J. and Roelofs, G. (1997). Variations in the predicted spatial distribution of atmospheric nitrogen deposition and their impact on carbon uptake by terrestrial ecosystems. *Journal of Geophysical Research*, *102*(D13), 15849–15866. http://dx.doi.org/10.1029/96JD03164

Hopkinson, R., McKenney, D., Milewska, E., Hutchinson, M., Papadopol, P. and Vincent, L. (2011). Impact of aligning climatological day on gridding daily maximum-minimum temperature and precipitation over Canada. *Journal of Applied Meteorology and Climatology*, *50*(8), 1654–1665.

Hughes, J., Vlades, P. and Betts, R. (2006). Dynamics of a global-scale vegetation model. *Ecological Modelling*, *198*, 452–462.

Jiang, Y., Zhuang, Q., Schaphoff, S., Sitch, S., Sokolov, A., Kicklighter, D. and Melillo, J. (2012). Uncertainty analysis of vegetation distribution in the northern high latitudes during the 21st century with a dynamic vegetation model. *Ecology and Evolution*, *2*(3), 593–614.

Kalnay, E., Kanamitsu, M., Kistler, R. and Coauthors (1996). The NCEP/NCAR 40-year reanalysis project. *Bulletin of the American Meteorological Society*, *77*, 437–470.

Keeling, C., Bacastow, R., Bainbridge, A., Ekdahl, C., Guenther, P. and Waterman, L. (1976). Atmospheric carbon dioxide variations at Mauna Loa Observatory, Hawaii. *Tellus*, *28*, 538–551. `http://dx.doi.org/10.1111/j.2153-3490.1976.tb00701.x`

Kendall, M. (1975). *Rank Correlation Methods*. London : Charless Griffin.

Khaliq, M., Ouarda, T., Gachon, P., Sushama, L. and St-Hilaire, A. (2009). Identification of hydrological trends in the presence of serial and cross correlations : A review of selected methods and their application to annual flow regimes of Canadian rivers. *Journal of Hydrology*, *368*, 117–130. `http://dx.doi.org/10.1016/j.jhydrol.2009.01.035`

Knorr, W., Prentice, I., House, J. and Holland, E. (2005). Long-term sensitivity of soil carbon turnover to warming. *Nature*, *433*, 298–301.

Kuo, H. (1965). On formation and intensification of tropical cyclones through latent heat release by cumulus convection. *Journal of Atmospheric Science*, *22*, 40–63.

Laprise, R. (1992). The Euler equation of motion with hydrostatic pressure as independent coordinate. *Monthly Weather Review*, *120*(1), 197–207.

Laprise, R. (2008). Regional climate modeling. *Journal of Computational Physics*, *227*(7), 3641–3666.

Leuning, R. (1995). A critical appraisal of a combined stomatal-photosynthesis model for C3 plants. *Plant, Cell and Environment*, *18*, 339–355.

Li, J. and Barker, H. (2005). A radiation algorithm with correlated-k distribution. Part I : local thermal equilibrium. *Journal of Atmospheric Science*, *62*, 286–309.

Li, R. and Arora, V. (2011). Effect of mosaic representation of vegetation in land surface schemes on simulated energy and carbon balances. *Biogeosciences Discussions*, *8*, 5849–5879. `http://dx.doi.org/10.5194/bgd-8-5849-2011`

Liu, Z., Notaro, M. and Kutzbach, J. (2006). Assessing global vegetation-climate feedbacks from observations. *Journal of climate*, *19*, 787–814.

Loranty, M., Berner, L., Goetz, S., Jin, Y. and Randerson, J. (2014). Vegetation controls on northern high latitude snow-albedo feedback : observatioins and CMIP5 model simulations. *Global Change Biology*, *20*, 594–606.

Los, S., Collatz, G., Malmstrom, C., Pollack, N., DeFries, R., Bounoua, L., Parris, M., Tucker, C. and Dazlich, D. (2000). A global 9-year biophysical land-surface data set from NOAA AVHRR data. *Journal of Hydrometeorology*, *1*, 183–199.

Manabe, S. (1969). Climate and the ocean circulation : 1, the atmopsheric circulation and the hydrology of the Earth's surface. *Monthly Weather Review*, *97*, 739–805.

Martynov, A., Laprise, R., Sushama, L., Winger, K., Separovic, L. and Dugas, B. (2013). Reanalysis-driven climate simulation over CORDEX North America domain using the Canadian Regional Climate Model, version 5 : model performance evaluation. *Climate Dynamics*, *41*, 2973–3005.

Maurer, E., Wood, A., Adam, J., Lettenmaier, D. and Nijssen, B. (2002). A long-term hydrologically-based data set of land surface fluxes and states for the conterminous United States. *Journal of Climate*, *15*, 3237–3251.

McFarlane, N. (1987). The effect of orographically excited gravity-wave drag on the circulation of the lower stratosphere and troposphere. *Journal of Atmospheric Science*, *44*, 1175–1800.

Mitchell, T. and Jones, P. (2005). An improved method of constructing a database of monthly climate observations and associated high-resolution grids. *International Journal of Climatology*, *25*, 693–712. `http://dx.doi.org/10.1002/joc.1181`

Myneni, R., Dong, J., Tucker, C., Kaufmann, R., Kauppi, P., Liski, J., Zhou, L., Alexeyev, V. and Hughes, M. (2001). A large carbon sink in the woody biomass of Northern forests. *Proceedings of National Academy of Science*, *98*(26), 14784–14789. `http://dx.doi.org/10.1073/pnas.261555198`

Nemani, R., Keeling, C., Hashimoto, H., Jolly, W., Piper, S., Myneni, C. T. R. and Running, S. (2003). Climate-driven increases in global terrestrial net primary production from 1982 to 1999. *Science*, *300*, 1560–1563. `http://dx.doi.org/10.1126/science.1082750`

Nobre, C., Sellers, P. and Shukla, J. (1991). Amazonian deforestation and regional climate change. *Journal of Climate*, *4*, 957–988.

Notaro, M., Liu, Z. and Williams, J. (2006). Observed vegetation-climate feedbacks in the United States. *Journal of Climate*, *19*, 763–786.

Notaro, M., Vavrus, S. and Liu, Z. (2007). Global vegetation and climate change due to future increases in CO2 as projected by a fully coupled model with dynamic vegetation. *Journal of Climate*, *20*, 70–90.

O'ishi, R. and Abe-Ouchi, A. (2009). Influence of dynamic vegetation on climate change arising from increased CO2. *Climate Dynamics*, *33*, 645–663.

Pacala, S., Hurtt, G., Baker, D., Peylin, P., Houghton, R., Birdsey, R., Heath, L., Sundquist, E., Stallard, R., Ciais, P., Moorcroft, P., Caspersen, J., Shevliakova, E., Moore, B., Kohlmaier, G., Holland, E., Gloor, M., Harmon, M., Fan, S., Sarmiento, J., Goodale, C., Schimel, D. and Field, C. (2001). Consistent land- and atmosphere-based U.S. carbon sink estimates. *Science*, *292*(5525), 2316–2320.

Paquin, J.-P. and Sushama, L. (2014). On the Arctic near-surface permafrost and climate sensitivities to soil and snow model formulations in climate models. *Climate Dynamics*. `http://dx.doi.org/10.1007/s00382-014-2185-6`

Peng, C. (2000). From static biogeographical model to dynamic global vegetation model : a global perspective on modelling vegetation dynamics. *Ecological Modelling*, *135*, 33–54.

Peng, Y., Arora, V., Kurz, W., Hember, R., Hawkins, B., Fyfe, J. and Werner, A. (2014). Climate and atmospheric drivers of historical terrestrial carbon uptake in the province of British Columbia, Canada. *Biogeosciences*, *11*, 635–649.

Pielke, R., Avissar, R. S., Raupach, M., Dolman, A., Zeng, X. and Denning, A. (1998). Interactions between the atmosphere and terrestrial ecosystems : influence on weather and climate. *Global Change Biology*, *4*, 461–475.

Pinto, E., Shin, Y., Cowling, S. and Jones, C. (2009). Past, present and future vegetation-cloud feedbacks in the Amazon Basin. *Climate Dynamics*, *32*(6), 741–751.

Pitman, A. (2003). Review : The evolution of, and revolution in, land surface schemes designed for climate models. *International Journal of Climatology*, *23*, 479–510.

Poitras, V., Sushama, L., Seglenieks, F., Khaliq, M. and Soulis, E. (2011). Projected changes to streamflows characteristics over Western Canada as simulated by the Canadian RCM. *Journal of Hydrometeorology*, *12*(6), 1395–1413. `http://dx.doi.org/10.1175/JHM-D-10-05002.1`

Port, U., Brovkin, V. and Claussen, M. (2012). The influence of vegetation dynamics on anthropogenic climate change. *Earth System Dynamics*, *3*, 233–243.

Prentice, I., Cramer, W., Harrison, S., Leemans, R., Monserud, R. and Solomon, A. (1992). A global biome model based on plant physiology and dominance, soil properties and climate. *Journal of biogeography*, *19*(2), 117–134.

Quillet, A., Peng, C. and Garneau, M. (2010). Toward dynamic global vegetation models for simulating vegetation-climate interactions and feedbacks : recent developments, limitations and future challenges. *Environmental reviews*, *18*, 333–353.

Reay, D., Dentener, F., Smith, P., Grace, J. and Feely, R. (2008). Global nitrogen deposition and carbon sinks. *Nature Geoscience*, *1*, 430–437.

Richardson, A., Keenan, T., Migliavacca, M., Ryu, Y., Sonnentag, O. and Toomey, M. (2013). Climate change, phenology, phenological control of vegetation feedbacks to the climate system. *Agricultural and Forest Meteorology*, *169*, 156–173.

Rummukainen, M. (2010). State-of-the-art with regional climate models. *WIREs Climate Change*, *1*(1), 82–96.

Schulze, E., Leuning, R. and Kelliher, F. (1995). Environmental regulation of surface conductance for evaporation from vegetation. *Vegetatio*, *121*, 79–87.

Sen, P. (1968). Estimates of the regression coefficient based on Kendall's tau. *Journal of the American Statistical Association*, *63*, 1379–1389.

Separovic, L., Alexandru, A., Laprise, R., Martynov, A., Sushama, L., Winger, K., Tete, K. and Valin, M. (2013). Present climate and climate change over North America as simulated by the fifth-generation Canadian regional climate model. *Climate Dynamics*. http://dx.doi.org/10.1007/s00382-013-1737-5

Sietse, O. (2010). *ISLSCP II FASIR-adjusted NDVI Biophysical Parameter Fields, 1982-1998*. Technical report, In Hall FG, Collatz G, Meeson B, Los S, Brown de Colstoun E, Landis D (eds.). ISLSCP Initiative II Collection data set available online [http ://daac.ornl.gov/] from Oak Ridge National Laboratory Distributed Active Archive Center, Oak Ridge, Tennessee, U.S.A

Simmons, A., Jones, P., da Costa Bechtold, V., Beljaars, A., Kallberg, P., Saarinen, S., Uppala, S., Viterbo, P. and Wedi (2004). Comparison of trends and low-frequency variability in CRU, ERA-40, and NCEP/NCAR analyses of surface air temperature. *Journal of Geophysical Research*, *109*. http://dx.doi.org/10.1029/2004JD005306

Sitch, S., Huntingford, C., Gedney, N., Levy, P., Lomas, M., Piao, S., Betts, R., Ciais, P., Cox, P., Friedlingstein, P., Jones, C., Prentice, I. and Woodward, F. (2008). Evaluation of the terrestrial carbon cycle, future plant geography and climate-carbon cycle feedbacks using five Dynamic Global Vegetation Models (DGVMs). *Global Change Biology*, *14*, 2015–2039.

Sitch, S., SMith, B., Prentice, I., Arneth, A., Bondeau, A., Cramer, W., Kaplans, J., Levis, S., Lucht, W., Sykes, M., Thonicke, K. and Venevsky, S. (2003). Evaluation of ecosystem dynamics, plant geography and terrestrial carbon cycling in the LPJ dynamic global vegetation model. *Global Change Biology*, *9*, 161–185.

Smith, B., Prentice, I. and Sykes, M. (2001). Representation of vegetation dynamics in the modelling of European ecosystems : Comparison of two contrasting approaches. *Global Ecology and Biogeography, 10*, 621–637.

Smith, B., Samuelsson, P., Wramneby, A. and Rummukainen, M. (2011). A model of the coupled dynamics of climate, vegetation and terrestrial ecosystem biogeochemistry for regional applications. *Tellus, 63A*, 87–106. `http://dx.doi.org/10.1111/j.1600-0870.2010.00477.x`

Snyder, P., Foley, J., Hitchman, M. and Delire, C. (2004). Analysing the effects of complete tropical forest removal on the regional climate using a detailed three-dimensional energy budget : An application to Africa. *Journal of Geophysical Research, 109*(D21102).

Snyder, P. and Liess, S. (2013). The simulated atmopsheric response to expansion of the arctic boreal forest biome. *Climate Dynamics*. `http://dx.doi.org/10.1007/s00382-013-1746-4`

Stephenson, N. (1990). Climatic control of vegetation distribution : the role of the water balance. *The American Naturalist, 135*, 649–670. `http://dx.doi.org/10.2307/2462028`

Sundqvist, H., Berge, E. and Kristjansson, J. (1989). Condensation and cloud parameterization studies with a mesoscale numerical weather prediction model. *Monthly Weather Review, 117*, 1641–1657.

Sushama, L., Laprise, R., Caya, D., Frigon, A. and Slivitzky, M. (2006). Canadian RCM projected climate-change signal and its sensitivity to model errors. *International Journal of Climatology, 26*, 2141–2159.

Taylor, K., Stouffer, R. and Meehl, G. (2009). *A Summary of the CMIP5 Experiment Design*. Technical report, http ://www-pcmdi.llnl.gov/.

Taylor, K., Stouffer, R. and Meehl, G. (2012). An overview of CMIP5 and the experiment design. *Bulletin of the American Meteorological Society, 93*, 485–498. `http://dx.doi.org/10.1175/BAMS-D-11-00094.1`

Taylor, K., Williamson, D. and Zwiers, F. (2000). *The Sea Surface Temperature and Sea-ice Concentration Boundary Conditions for AMIP II Simulations*. Lawrence Livermore National Laboratory, (program for climate model diagnosis and intercomparison éd.).

Thompson, S., Govindasamy, B., Mirin, A., Caldeira, K., Delire, C., Milovich, J., Wickett, M. and Erickson, D. (2004). Quantifying the effects of CO2-fertilized vegetation on future global climate and carbon dynamics. *Geophysical Research Letters, 31*(L23211).

Thoning, K., Tans, P. and Komhyr, W. (1989). Atmospheric carbon dioxide at Mauna Loa Observatory 2. Analysis of the NOAA GMCC data, 1974-1985. *Journal of Geophysical Research, 94*, 8549–8565. http://dx.doi.org/10.1029/JD094iD06p08549

Trail, M., Tsimpidi, A., Liu, P., Tsigaridis, K., Hu, Y., Nenes, A., Stone, B. and Russell, A. (2013). Potential impact of land use change on future regional climate in the southeastern U.S. : Reforestation and crop. *Journal of Geophysical Research : Atmospheres, 118*(11), 577–588.

Uppala, S., Kallberg, P., Simmons, A. and Coauthors (2005). The ERA-40 re-analysis. *Quarterly Journal of the Royal Meteorological Society, 131*, 2961–3012. http://dx.doi.org/10.1256/qj.04.176

Verseghy, D. (1991). CLASS - A Canadian land surface scheme for GCMs, I. Soil model. *International Journal of Climatology, 11*, 111–133. http://dx.doi.org/10.1002/joc.3370110202

Verseghy, D. (2011). *CLASS - The Canadian land surface scheme (version 3.5). Technical Documentation (version 1).* Technical report, Environment Canada, Climate Research Division, Science and Technology Branch.

Verseghy, D., McFarlane, N. and Lazare, M. (1993). CLASS - A Canadian land surface scheme for GCMs, II. Vegetation model and coupled runs. *International Journal of Climatology, 13*, 347–370. http://dx.doi.org/10.1002/joc.3370130402

Walter, H. and Box, E. (1976). Global classification of natural terrestrial ecosystems. *Vegetatio, 32*, 75–81.

Wang, A., Price, D. and Arora, V. (2006). Estimating changes in global vegetation cover (1850-2100) for use in climate models. *Global Biogeochemical Cycles, 20.* http://dx.doi.org/10.1029/2005GB002514

Wang, F., Notaro, M., Liu, Z. and Chen, G. (2014). Observed local and remote influences of vegetation on the atmosphere across North America using a model-validated statistical technique that first excludes oceanic forcings. *Journal of climate, 27*, 362–382.

Webb, R., Rosenzweig, C. and Levine, E. (1991). *A global data set of soil particle size properties.* Technical report 4286, NASA Technical Memorandum.

Willmott, C. and Matsuura, K. (1995). Smart interpolation of annually averaged air temperature in the United States. *Journal of Applied Meteorology, 34*, 2577–2586.

Woodward, F. (1987). *Climate and plant distribution.* Cambridge, UK : Cambridge University Press.

Wotton, B., Nock, C. and Flannigan, M. (2010). Forest fire occurence and climate change in Canada. *International Journal of Wildland Fire, 19*, 253–271.

Wramneby, A., Smith, B. and Samuelsson, P. (2010). Hot spots of vegetation-climate feedbacks under future greenhouse forcing in Europe. *Journal of Geophysical Research, 115.*

Yeh, K.-S., Cote, J., Gravel, S., Methot, A., Patoine, A. and et al. (2002). The CMC-MRB global environmental multiscale (GEM) model. Part III : nonhydrostatic formulation. *Monthly Weather Review, 130,* 339–356.

Zadra, A., Roch, M., Laroche, S. and Charron, M. (2003). The subgrid scale orographic blocking parametrization of the GEM model. *Atmosphere-Ocean, 41,* 155–170.

Zhao, M., Heinsch, F., Nemani, R. and Running, S. (2005). Improvements of the MODIS terrestrial gross and net primary production global data set. *Remote Sensing of Environment, 95,* 164–176.

Zhao, X., Tan, K., Zhao, S. and Fang, J. (2011). Changing climate affects vegetation growth in the arid region. *Journal of Arid Environments, 75,* 946–952.